Modelling the Impact of Subsonic Aviation on the Composition of the Atmosphere

PROEFSCHRIFT

ter verkrijging van de graad van doctor aan de
Technische Universiteit Eindhoven, op gezag van de
Rector Magnificus, prof.dr. R.A. van Santen, voor een
commissie aangewezen door het College voor
Promoties in het openbaar te verdedigen
op woensdag 21 november 2001 om 16.00 uur

door

Ernst Willem Meijer

geboren te Rotterdam

Dit proefschrift is goedgekeurd door de promotoren:

prof.dr. H. Kelder
en
prof.dr. I.S.A. Isaksen

Copromotor:
dr. P.F.J. van Velthoven

Contents

Voorwoord

De afgelopen jaren heb ik onderzoek gedaan naar de effecten van vliegverkeer op de samenstelling van de atmosfeer. Als afgestudeerd natuurkundige was dit promotieonderzoek voor mij aangenaam concreet en tastbaar. Het bleek ook een onderwerp waar je met je familie en vriendenkring over kon praten. Als ik uitlegde dat de uitstoot van vliegverkeer ozonvorming tot gevolg had, moest ik daar wel gelijk aan toevoegen dat dit niets met de ozonlaag te maken had, maar dat ozon ook een broeikasgas was. Niettemin was het duidelijk een onderwerp dat de mensen om me heen aansprak. Hiervóór was ik afgestudeerd op een natuurkundig model voor magnetisme, waarbij ik de bepaling van de temperatuur waarbij materie magnetisch wordt, nauwkeuriger en efficiënter probeerde te maken. Een model dat bovendien een zeer beperkte beschrijving van de werkelijkheid geeft. Het zal duidelijk zijn dat die kamergeleerdheid minder geschikt was voor een praatje met de buren.

Ik mocht mijn promotieonderzoek dan wel heel concreet vinden, toen ik een leuke kaft voor dit proefschrift wilde verzinnen, bleek het onderwerp toch moeilijker aanschouwelijk te maken dan ik dacht. Uiteindelijk heb ik ervoor gekozen om een ander effect van vliegverkeer af te beelden, namelijk de zogenaamde condenssporen. Deze vliegtuigstrepen hebben net als de ozonvorming door vliegverkeer netto een opwarmend effect op het klimaat. In zekere zin is de afbeelding op de kaft toch wel van toepassing op mijn onderzoek. Door de condensatie van uitgestoten waterdamp, wordt duidelijk dat vliegtuigen een duidelijke uitlaatpluim hebben. De processen die in zulke pluimen plaatsvinden, maakten deel uit van het onderzoek in dit proefschrift. De foto zelf heeft nog een andere relatie met mijn onderzoek: ik heb hem gemaakt op het strand van Nice, waar ik was voor een conferentie waar ik een presentatie hield over de effecten van vliegverkeer. Overigens ben ik dank verschuldigd aan Pieter Valks, die zijn vrije tijd moest opofferen aan het scannen van het negatief en het vervolgens geduldig wegpoetsen van alle oneffenheden die als gevolg van mijn slordige negatiefbeheer waren opgetreden.

Alhoewel dit werk natuurlijk een wetenschappelijk karakter heeft, is de onderliggende vraag of het vanuit milieustandpunt gezien wel zo verstandig is om te vliegen. Het was daarom frappant dat ik voor mijn werk zo vaak moest vliegen. Ik geloof dat ik voordat ik bij het KNMI werkte zo'n 3 à 4 keer had gevlogen, terwijl ik in de afgelopen 5 jaar bij het KNMI 14 keer met het vliegtuig heb gereisd, waarvan 4 keer naar de Verenigde Staten. Dit schijnt nog een bescheiden frequentie te zijn in vergelijking met sommige andere onderzoekers, maar het geeft toch aan hoe moeilijk vliegverkeer is weg te denken uit de hedendaagse werkelijkheid. Het is een feit dat de wereld steeds kleiner wordt en dat mensen, alle moderne communicatiemiddelen ten

spijt, toch elkaar af en toe fysiek moeten ontmoeten om goed te kunnen samenwerken. Hoewel ik persoonlijk vind dat vliegen een van de meest oncomfortabele manieren van verplaatsen is, moet ik tegelijk bekennen dat het een luxe is om allerlei verre en zonnige vakantieoorden eenvoudig en goedkoop binnen handbereik te hebben.

Vliegen mag dan een handige of zelfs noodzakelijke manier van transport zijn, toch beïnvloedt het ook het klimaat op aarde. Het maatschappelijk besef dat ongebreidelde groei van de economie grote klimatologische consequenties kan hebben, neemt toe. Het feit dat een studie van het IPCC (Intergovernmental Panel on Climate Change) naar de effecten van vliegverkeer in opdracht van deze transportsector zelf is uitgevoerd, is daar een goed voorbeeld van. De huidige wereld draait echter op economische groei en er zijn daarom sterke en goed onderbouwde wetenschappelijke argumenten nodig om beleidsmakers ervan te overtuigen dat reductie van de uitstoot van broeikasgassen noodzakelijk is. Ik heb dan ook geprobeerd met dit onderzoek een kleine bijdrage te leveren door de geschatte effecten van vliegverkeer beter te onderbouwen.

Mijn naam staat op dit proefschrift, maar dit werk had nooit tot stand kunnen komen zonder de hulp en bijdragen van vele anderen. Een groot deel van mijn proefschrift is gebaseerd op het vergelijken van modelresultaten met metingen. Deze metingen zijn grotendeels uitgevoerd en gecoördineerd door de DLR (Deutsche Forschungsanstalt für Luft- und Raumfahrt), naar wiens medewerkers mijn dank uitgaat. I would like to express my acknowledgements to the people of the DLR, who performed and coordinated the measurement campaigns that provided a starting point for this thesis. In particular, I would like to thank Hans Schlager and Ulrich Schumann as coordinators of the POLINAT project, and Hartmut Höller and Heidi Huntrieser as coordinators of the EULINOX project. Since most chapters of this thesis consist of already published papers, I also thank all co-authors that have contributed to this work. Binnen het KNMI gaat mijn dank uit naar Peter van Velthoven, die als een spin in het AS web zit, en die altijd tijd wist te vinden om ook mijn stukje spinrag in de gaten te houden. Natuurlijk ben ik ook Hennie Kelder erkentelijk, vooral om zijn vermogen om de onderzoekers van zijn sectie de volledige vrijheid te geven en ze af te schermen van allerlei bestuurlijke rompslomp die een organisatie als het KNMI met zich meebrengt. De collega's binnen AS bedank ik voor de goede sfeer die hier altijd heerst. Over het KNMI als werkgever valt veel te zeggen, zowel positief als negatief. Voor mij is het KNMI een werkgever met bijzondere secundaire arbeidsvoorwaarden, aangezien het meetveld elke week het toneel vormt voor een potje voetbal tijdens lunchtijd, iets waar ik elke week weer naar uitkijk. Tot slot wil ik Ingrid bedanken, natuurlijk voor alles wat niets met mijn werk te maken heeft, maar zeker ook voor alle ruimte die je me toestond om mijn proefschrift op tijd af te ronden. Op het laatst was het nog een race tegen de klok, omdat de geboorte van ons eerste kindje elk moment kon gebeuren. Uiteindelijk was alles op tijd af, hoewel deze laatste zinnen pas verschenen nadat Maarten alweer de derde week van zijn leven bereikte.

Samenvatting

Het onderzoek dat in dit proefschrift beschreven wordt, richt zich op de effecten van de uitstoot van stikstofoxiden door vliegverkeer. Deze uitstoot wordt veroorzaakt door de hitte die vrijkomt in de straalmotoren, waardoor zuurstofmoleculen worden ontbonden en reageren met stikstofmoleculen. Stikstofoxiden (NO_x=NO+NO_2) veroorzaken via chemische omzettingen onder invloed van zonlicht ozon (O_3), wat een gas is met zeer gevarieerde eigenschappen. In de stratosfeer absorbeert ozon schadelijk ultraviolet zonlicht en beschermt zo het leven op aarde, terwijl geringe verhogingen op leefniveau, de zogenaamde zomersmog, schadelijk zijn voor de gezondheid van mensen, dieren en gewassen. Ozonvorming ten gevolge van vliegverkeer is echter niet aan deze eigenschappen gerelateerd, maar aan mogelijke klimaatveranderingen. Ozon is namelijk ook een sterk broeikasgas, vooral op een hoogte van 8-12 km, waar de meeste uitstoot door vliegtuigen plaatsvindt.

Verschillende modelberekeningen in het recente verleden geven aan dat de concentraties van stikstofoxiden in de belangrijkste vliegcorridors met 20 tot 70% zijn toegenomen door vliegverkeer. Hoewel die toename aanzienlijk is, is de berekende toename van ozon geringer, nl. zo'n 2 to 10%. Mogelijke klimaatveranderingen worden doorgaans uitgedrukt in stralingsforcering: de verandering van de infrarode straling die aan de bovenkant van de atmosfeer wordt uitgezonden.[1] De toename van ozon ten gevolge van het vliegverkeer heeft naar schatting een stralingsforcering van 0.015 W/m^2, wat relatief weinig is in verhouding tot de geschatte stralingsforcering van 2.4 W/m^2, ten gevolge van het totaal aan menselijke activiteiten. Echter, vliegverkeer neemt snel toe, gemiddeld met zo'n 5% per jaar, zodat ook de bijbehorende klimaateffecten snel kunnen toenemen.

De bovengenoemde schattingen zijn gebaseerd op de uitkomsten van verschillende chemie-transportmodellen, die berekeningen maken van de uitstoot van verschillende chemische componenten zoals NO_x en koolmonoxide (CO), de chemische omzettingen in de atmosfeer en de verplaatsingen van die stoffen door de wind, turbulentie,

---

[1] Het inkomende zonlicht warmt de aarde op. De aarde staat deze warmte weer af door infrarode straling uit te zenden, waarvan een deel door broeikasgassen, zoals CO_2 en ozon, wordt geabsorbeerd. Hierdoor warmt de atmosfeer op, die op zijn beurt ook weer infrarode straling uitzendt. Daarbij stelt zich een stralingsevenwicht in, wat zeggen wil dat de aarde en de atmosfeer die temperatuur aannemen, waarbij de hoeveelheid geabsorbeerd zonlicht gelijk is aan de hoeveelheid uitgezonden infrarode straling. Als de hoeveelheid broeikasgassen in de atmosfeer toeneemt, zal daarom de gemiddelde temperatuur bij het aardoppervlak gaan stijgen. Het berekenen van de stralingsforcering is dus een eenvoudige manier om een versterkt broeikaseffect te bepalen, zonder de precieze temperatuursveranderingen te berekenen.

e.d.. Die berekeningen omvatten echter veel verschillende atmosfeerprocessen en gaan gepaard met veel onzekerheden. Bovendien waren die modellen een paar jaar geleden nog nauwelijks getoetst aan de werkelijkheid, simpelweg door het gebrek aan geschikte metingen. Dit was de motivatie voor een speciale meetcampagne om de samenstelling van de lucht op de belangrijkste vliegroutes tussen Europa en de Verenigde Staten te meten. Het onderzoek in dit proefschrift richt zich op het vergelijken van die metingen met de modelresultaten van het chemie-transportmodel TM3. Het doel van die vergelijking was het verder onderbouwen van de eerder gerapporteerde effecten van vliegverkeer, maar ook het opsporen van de zwakke punten van het model om die, waar mogelijk, te verbeteren.

Het vergelijken van modelresultaten met metingen is echter niet eenvoudig. Een model zoals TM3 is een wiskundige representatie van de werkelijkheid en deelt de atmosfeer op in een rooster met bepaalde afmetingen. Voor elk roosterpunt worden vervolgens de gemiddelde concentraties van de chemisch actieve stoffen berekend. Helaas zijn die roosters, opgelegd door de huidige computercapaciteit, nog steeds relatief grof: een roosterpunt in TM3, bijv., representeert een atmosfeervolume van 400×400 km oppervlakte met een dikte van zo'n 1.5 km. Het zal duidelijk zijn dat metingen alleen al binnen zo'n volume variaties kunnen opleveren, die uiteraard niet door het model kunnen worden gereproduceerd.

Ondanks deze beperking blijken de modelberekingen redelijk goed met de gemeten stikstofoxide- en ozonconcentraties overeen te komen. De vergelijking met ozon is over het algemeen goed, maar metingen van de ozonconcentratie in de stratosfeer zijn in het algemeen iets door het model onderschat. Dit is een gevolg van het tamelijk grove rooster waarop gerekend wordt. In de stratosfeer neemt de ozonconcentratie namelijk snel toe met de hoogte. Deze toename kan door het model niet altijd goed gerepresenteerd worden, vooral niet in situaties waarin kleinschalige uitstulpingen van de stratosfeer (zogenaamde tropopauzevouwen) voorkomen. De vergelijking met stikstofoxide (NO) is het beste voor gemeten concentraties tot 150 pptv.[2] De meeste metingen leverden waarden in dat concentratiegebied op. De minder frequent gemeten concentraties van meer dan 500 pptv zijn minder goed door het model gereproduceerd. Dit is voor een deel begrijpelijk, omdat zulke concentraties afkomstig kunnen zijn van processen die zich op een te kleine schaal afspelen om door het model berekend te kunnen worden; te denken valt bijv. aan een uitlaatpluim van een net gepasseerd vliegtuig. Aan de andere kant zijn de berekende NO-concentraties altijd lager dan 200 pptv, in tegenstelling tot de metingen. Dit duidt erop dat niet alle processen goed door het model beschreven worden. Mogelijk zijn dat processen die geassocieerd worden met bliksem of convectie. Een bliksemontlading verhit de lucht tot wel 30.000 °C. Bij die hoge temperatuur wordt de lucht in het ontladingskanaal ontleed, waardoor NO_x wordt gevormd. Bliksem is dus een natuurlijke bron van NO_x. Mondiaal over een jaar gezien is de NO_x-productie door bliksem naar schatting een orde groter dan de uitstoot van NO_x door vliegverkeer[3]. Echter, bliksem komt

---

[2]Met pptv (parts per trillion per volume) wordt de concentratie in een zogenaamde mengverhouding aangegeven: 1 pptv NO betekent dat 1 op de 1000 miljard luchtmoleculen een NO-molecuul is.

[3]ter vergelijking: de totale NO_x-productie door bliksem bedraagt ongeveer 5 Tg(N)/jaar (5000 miljoen kg stikstof/jaar), terwijl de totale uitstoot door vliegverkeer 0.55 Tg(N)/jaar bedraagt

vooral voor in de tropen, terwijl vliegverkeer vooral op gematigde breedtes op het Noordelijk halfrond plaatsvindt. Convectie is een proces waarin snelle opwaartse bewegingen van lucht door instabiliteit worden veroorzaakt en gaat vaak gepaard met onweersbuien. Convectieve opwaartse bewegingen kunnen zo sterk zijn dat vervuilingen dichtbij het aardoppervlak (waaronder NO_x met concentraties van veel meer dan 1000 pptv) in 10 minuten naar 10 km hoogte gebracht kunnen worden. Hierdoor kan de NO_x-concentratie op 10 km hoogte dus lokaal sterk verhoogd worden.

Een goede vergelijking van modelberekeningen met gemeten concentraties alleen is niet voldoende om de berekende schattingen van de effecten van vliegverkeer te onderbouwen. Het moet ook nog aannemelijk gemaakt worden dat de in het model berekende bijdragen van vliegverkeer aan de totale concentraties kloppen. Om dat te kunnen onderzoeken is het model uitgebreid met de mogelijkheid om chemische stoffen te 'labelen'. Met deze labeltechniek kunnen bijdragen van de verschillende NO_x-bronnen (vliegverkeer, bliksem, oppervlaktebronnen) aan de berekende O_3- en NO-concentraties worden bepaald. Verschillende metingen zijn zo uitgevoerd dat de waargenomen concentratieverschillen duidelijke aanwijzingen vormen dat deze verschillen door vliegverkeer zijn veroorzaakt. Zo zijn er bijvoorbeeld meetvluchten uitgevoerd op verschillende hoogten, waarbij een duidelijke toename in de NO-concentratie samenviel met de kruisvluchthoogte van het vliegverkeer. Een ander voorbeeld is een meetvlucht van Ierland naar de Kanarische Eilanden, waarbij een plotselinge sterke afname van de NO-concentratie is waargenomen, toen het meetvliegtuig het gebied met de belangrijkste vliegroutes verliet. Het model reproduceert die concentratieverschillen goed en laat bovendien m.b.v. de labeltechniek zien dat de verhoogde NO-concentraties inderdaad van vliegverkeer afkomstig waren. Het vliegverkeer draagt in die gevallen voor gemiddeld 50% bij aan de totale NO-concentratie, maar die bijdrage kan oplopen tot 75%. Bovendien bevestigen trajectorieënberekeningen[4] dat de lucht waarin deze hoge NO-concentraties zijn gemeten de voorgaande dagen nauwelijks was blootgesteld aan andere NO_x-bronnen. Deze feiten bij elkaar genomen geven aan dat het model niet de juiste totale NO-concentraties zou berekenen, als de vliegtuigbron van NO_x afwezig of onjuist zou zijn. Er kan dus gesteld worden dat de metingen de berekende bijdragen van vliegverkeer aan de totale NO-concentratie bevestigen. Helaas is het niet mogelijk gebleken de berekende bijdragen aan de ozonconcentratie te bevestigen met metingen. De variaties in de gemeten ozonconcentraties worden voornamelijk bepaald door de relatieve positie van de meting t.o.v. de tropopauze, omdat rond de tropopauze de ozonconcentratie sterk stijgt bij toenemende hoogtes. De berekende bijdrage van vliegverkeer aan ozon is veel kleiner dan de natuurlijke variaties die ontstaan door de verschillende posities t.o.v. de tropopauze. Bovendien is de berekende relatieve bijdrage van vliegverkeer aan de ozonconcentratie te klein (ongeveer 10%) om bij de huidige mate van overeenkomst tussen modelresultaten en metingen goed te kunnen onderscheiden.

Zoals gezegd zou de beschrijving van de NO_x-productie door bliksem een zwak punt van het model kunnen zijn. Dit zou indirect kunnen leiden tot verkeerde schat-

---

[4]Aan de hand van de windvelden kan vanaf de positie van een meting tot enkele dagen worden teruggerekend waar de lucht vandaan kwam. Zo kan bepaald worden of de lucht zich alleen in de vliegtuigroutes heeft bevonden of ook voor een deel vanaf het continent is opgestegen. De door de lucht afgelegde banen worden trajectorieën genoemd.

tingen van de effecten van vliegverkeer. Dit komt met name doordat de ozonproductie niet lineair verandert bij een toename van de NO_x-concentratie. Bekend is dat bliksem een grote NO_x-bron is, maar de onzekerheidsmarge is erg groot, nl. 2 à 20 Tg(N)/jaar. In de zomer van 1998 is daarom een speciale meetcampagne gestart om in en rondom onweersbuien te meten. Vergelijking van modelresultaten met de metingen liet overduidelijk zien dat de toenmalige modelbeschrijving van de NO_x-productie door bliksem onvoldoende was: het model onderschatte in alle gevallen de gemeten NO-concentratie en gaf nergens een belangrijke bijdrage aan de NO-concentratie door bliksem. Teneinde een nieuwe modelbeschrijving van de NO_x-productie door bliksem te ontwikkelen, is gezocht naar een meteorologische grootheid waarmee bliksem kan worden voorspeld. Dit is gedaan door het vergelijken van verschillende meteorologische grootheden uit het Europese weermodel met waargenomen blikseminslagen. Hieruit is gebleken dat neerslag die optreedt bij convectie de beste indicator is. Het aantal blikseminslagen is evenredig met die neerslag. Gegevens van convectieve neerslag maken het dus mogelijk om de positie en de intensiteit van bliksem te voorspellen. De verticale verdeling van de door bliksem geproduceerde NO_x is echter niet goed te bepalen. Daarom werd het model getest met de nieuwe bliksemindicator en met verschillende keuzes voor de verticale verdeling. Daaruit is gebleken dat de overeenkomst met metingen het beste is met een verticale verdeling die de herverdeling van de door bliksem geproduceerde NO_x door de convectie voorschrijft. Met deze nieuwe beschrijving van de NO_x-productie door bliksem is de overeenkomst met metingen van de NO-concentratie sterk verbeterd voor zowel situaties in en rond onweersbuien als situaties waar de lucht recent (tot enkele dagen geleden) was blootgesteld aan bliksem. De onnauwkeurigheid van de totale bronsterkte van bliksem kan niet teruggebracht worden, aangezien de metingen een beperkt gebied en tijdspanne bestrijken, nl. West-Europa gedurende de zomer van 1998.

Tenslotte is er ook onderzoek gedaan naar de mogelijke effecten van de processen die in de uitlaatpluimen van vliegtuigen plaatsvinden. Zoals gezegd delen modellen de atmosfeer in een rooster op. Per rooster wordt voor elke tijdstap in het model de totale uitstoot die in dat atmosfeervolume en tijdsinterval plaatsvindt, opgeteld bij de gemiddelde NO_x-concentratie. Dit betekent dat impliciet aangenomen wordt dat die uitstoot direct volledig gemengd is met de achtergrondconcentratie. De waarnemingen van vliegtuigsporen geven echter aan dat in werkelijkheid de uitstoot enige tijd blijft bestaan als een aparte pluim. In zo'n pluim is de NO_x-concentratie vele malen groter en omdat de atmosferische chemie niet-lineair is, ontstaan door deze modelaanpak fouten: in een pluim zal in eerste instantie ozon worden afgebroken, terwijl er in de achtergrondsituatie juist ozon gevormd zal worden. Ook de vorming van zogenaamde reservoirstoffen, zoals salpeterzuur, zal in zo'n vliegtuigpluim veel efficiënter zijn. Om die reden is een vliegtuigpluimmodel ontwikkeld dat deze processen beschrijft. Door pluimeffecten in het mondiale chemie-transportmodel in rekening te brengen, nemen de berekende schattingen van de bijdragen van vliegverkeer aan de NO_x-concentratie met 25%-45% af. De precieze afname is afhankelijk van het seizoen. Het effect op de bijdrage aan de ozonconcentratie is complexer: voor de maand juli neemt de bijdrage lokaal toe met maximaal 8%, maar in het algemeen neemt de bijdrage juist af met zo'n 10%. Er zijn echter nog geen geschikte metingen om de resultaten van het vliegtuigpluimmodel te testen, zodat deze uitkomsten als voorlopig moeten worden beschouwd.

Er is met het onderzoek dat in dit proefschrift beschreven wordt, een flinke stap vooruitgezet met betrekking tot de berekening van de effecten van vliegverkeer. Het is gebleken dat het chemie-transportmodel in het algemeen goed in staat is metingen van ozon- en stikstofoxideconcentraties in de belangrijkste vliegcorridors te reproduceren. Bovendien onderbouwen de metingen de berekende bijdragen van vliegverkeer aan de stikstofoxideconcentraties. Zo'n onderbouwing van eerder gemaakte schattingen is niet alleen belangrijk vanuit wetenschappelijk oogpunt, maar draagt ook bij aan de bruikbaarheid voor politieke besluitvorming. Verder is de beschrijving van NO_x-productie door bliksem aantoonbaar verbeterd, hetgeen bijdraagt aan de betrouwbaarheid van modelberekeningen met betrekking tot de effecten van vliegverkeer. Wat de mogelijke effecten van vliegtuigpluimen waren, was tot voor kort slechts een open vraag. Hierop is nu een antwoord gegeven. Dit antwoord moet echter nog wel aan de hand van metingen getoetst worden.

1

Introduction and overview

The work, described in this thesis, focuses on the impact of subsonic aviation on atmospheric nitrogen oxides and ozone, with respect to global climate change. This chapter starts with a short description of the relation between atmospheric nitrogen oxides and ozone, and gives a historical overview of studies on the effects of aviation on atmospheric ozone. A short overview of the estimated climate effects of aviation is given. Thereafter some background is given on the chemistry and transport processes in the atmosphere, and is concluded by a description of the motivation of this research.

1.1 Ozone and nitrogen oxides

Nitrogen oxides form a natural part of the composition of the atmosphere. Due to human activities the atmospheric burden of nitrogen oxides is increasing since prein-dustrial times. There is some concern over the consequences of acidification, because nitrogen oxides are converted to nitric acid, which is washed out to the surface [*Galloway*, 1984]. However, the main reason for the interest in nitrogen oxides stems from their influence on atmospheric ozone, which is an important trace gas with contrasting properties. These properties manifest themselves at different altitudes. Also the way that nitrogen oxides influence the ozone concentration varies with altitude.

In the stratosphere, where the majority of atmospheric ozone resides (about 90%), ozone plays a vital beneficial role by protecting the Earth from biologically harmful ultraviolet sunlight. *Chapman* [1930] discovered that ozone in the stratosphere is formed by the photodissociation of molecular oxygen. Later, when measurements became more refined, it appeared that ozone abundances were remarkably smaller than predicted by Chapman's reaction cycles. This resulted in the discovery of the role of nitrogen oxides in stratospheric chemistry. Also the role other constituents such as halogen compounds and water vapour, became apparent. Nitrogen oxides act as catalytic destructors of ozone in stratospheric chemistry [*Crutzen*, 1970].

Near the Earth's surface relatively small increases cause toxic levels of the ozone concentration for humans, animal life, and vegetation [i.e. *EPA*, 1984; *WHO*, 1984]. Downward transport of ozone from the stratosphere constitutes a source of ozone in the troposphere, but ozone is also produced locally in the troposphere. Tropospheric ozone production consists of sunlight-driven chemical reaction cycles involving nitro-

gen oxides, hydrocarbons, and carbon monoxide, as was first suggested in studies of the 'Los Angeles' smog, the classical example of summer smog [e.g. *Haagen-Smit and Fox*, 1954]. In these reactions cycles nitrogen oxides act as catalytic producers of ozone. Paradoxically, ozone plays also a key role in the removal of many trace pollutants, that are responsible for ozone increases, such as carbon monoxide, hydrocarbons, and sulphuric compounds [i.e. *Finlayson-Pitts and Pitts*, 1986; *Seinfeld and Pandis*, 1998; and *Warneck*, 1988].

Finally, ozone acts as a greenhouse gas with highest efficiency in the cold upper troposphere and lowermost stratosphere [*Lacis et al.*, 1990]. In this region increases of nitrogen oxides enhance the photochemical production of ozone, similarly as in the smog formation mechanism near the surface. So nitrogen oxides emissions of subsonic aviation in the tropopause region can enhance the ozone production locally with possible climate effects. This is the focus of this thesis.

1.2   Effects of aviation on atmospheric ozone

The exhaust of an aircraft contains nitrogen oxides, formed in the hot engines by thermal decomposition of molecular oxygen and subsequent oxidation of molecular nitrogen. The first studies on the impact of aviation did not focus on possible climate effects, but on the potential harm that nitrogen oxides could impose on the ozone layer. This concern was initiated in the early 1970s by the proposal of developing a fleet of supersonic aircraft, because supersonic aircraft have cruise altitudes in the stratosphere (Concorde flies at 18 km) and could thus form a threat to the ozone layer. The outcome of these impact studies [*Johnston*, 1971; *Crutzen*, 1972; *CIAP*, 1975] contributed (to a certain extent) to the decision of not building this supersonic fleet.

These studies also drew the attention to the possible impact of NO_x emissions of subsonic aviation at lower altitudes. [e.g. *Hidalgo and Crutzen*, 1977; *Isaksen*,1980]. At subsonic cruise altitudes in the range of 8-12 km, nitrogen oxides can produce ozone. Although the emission of nitrogen oxides by subsonic aviation is small with respect to other anthropogenic sources, the possible climate effects of air traffic form an important research topic for several reasons. As already said, increased ozone concentrations will have strongest effect on the radiative forcing at subsonic cruise altitudes [*Lacis et al.*, 1990]. Secondly, aircraft directly inject nitrogen oxides in the tropopause region, where ambient concentrations of nitrogen oxides are low. Also, the chemical lifetime of nitrogen oxides in that region is about 5-10 days, whereas the majority of anthropogenic nitrogen oxide emissions occur at low altitudes with corresponding short lifetimes of less than 1 day [*Jacob et al.*, 1996]. Therefore, nitrogen oxide emissions are more efficient in producing ozone near the tropopause than near the Earth's surface. Furthermore, subsonic aviation has an estimated annual growth rate of 5%-6% [IATA, 1995], so that the effects of aircraft emissions are expected to become larger in the future.

In the early 1990s interest in the environmental impact of subsonic aviation has renewed and many studies have been performed since. Some early studies consisted of two-dimensional model calculations [e.g. *Beck et al.*, 1992; *Hauglustaine et al.*, 1994], but nowadays it is generally recognised that three-dimensional models are required to

perform such studies [*Friedl et al.*, 1997; *van Velthoven et al.*, 1997]. This is due to the fact that the concentration of nitrogen oxides shows large variations in the east-west direction, combined with the fact that the ozone production responds non-linearly to these variations. Several three-dimensional model calculations [e.g.*Brasseur et al.*, 1996; *Stevenson et al.*, 1997; *Wauben et al.*, 1997] predicted large increases of the nitrogen oxides concentrations of about 20%-70% with smaller increases of ozone of about 2%-10%. These increases are located at 8-12 km altitude at northern midlatitudes, and depend on season. The majority of these studies were performed in the framework of the EU project AERONOX [*Schumann*, 1995; 1997]. In the late 1990s several international assessments were made [*Brasseur et al.*, 1998; IPCC, 1999] that gave these predicted aircraft-induced increases of nitrogen oxides and ozone a firmer basis.

1.3   Climate effects of aviation

The assessments also addressed the possible climate changes from aviation. The climate response to changes of trace gas concentrations is usually expressed in terms of radiative forcing, defined as the net radiative flux change at tropopause level (W/m^2). The changes in ozone due to aircraft emissions, as calculated by different models, result in a radiative forcing of 0.023 W/m^2 (0.013-0.046 W/m^2) [*IPCC*, 1999]. *Brasseur et al.*, [1998] report a very similar radiative forcing range of 0.015-0.05 W/m^2. Aviation also has other possible effects on the climate. These include global warming effects due to the emissions of carbon dioxide (CO_2), water vapour, and soot particles, the formation of contrails, and possibly the enhancement of cirrus cloud formation. Cooling effects originate from sulphate aerosol formation and the reduction of the lifetime of atmospheric methane. The reduced lifetime of methane is a result of emitted nitrogen oxides. Best estimates of the corresponding radiative forcings are presented in Figure 1.1, taken from IPCC [1999] for present day (1992) and future (2050) aviation. The estimated present-day total radiative forcing of aviation is 0.05 W/m^2, which is small with respect to the estimated total present man-made radiative forcing of approx. 2.4 W/m^2 [IPCC, 2001].

1.4   Tropospheric ozone chemistry

In the troposphere and lowermost stratosphere ozone, O_3, is produced by the photolysis of nitrogen dioxide, NO_2, by solar radiation at wavelengths shorter than 420 nm. This reaction produces a ground-state oxygen atom, $O(^3P)$, that reacts with molecular oxygen, O_2, under collision with a third molecule M (either an oxygen or nitrogen molecule)

$$NO_2 + h\nu \rightarrow NO + O(^3P) \tag{1.1}$$

$$O(^3P) + O_2 + M \rightarrow O_3 + M \tag{1.2}$$
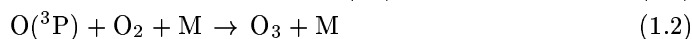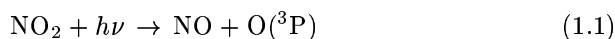
Ozone may then be destroyed by reaction with nitrogen oxide ,NO, to reform NO_2

$$O_3 + NO \rightarrow NO_2 + O_2 \tag{1.3}$$
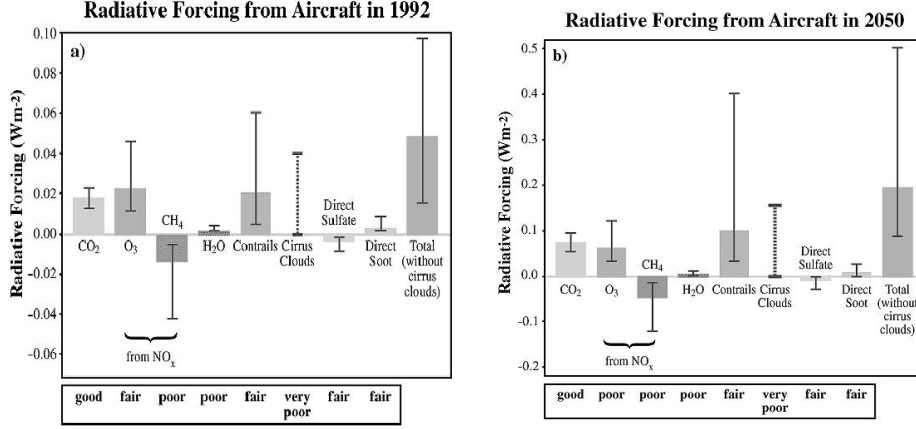
Figure 1.1: The annual global averages of the radiative forcings from subsonic aviation for 1992 and 2050, according to *IPCC* [1999].

These reactions constitute a null cycle with net zero ozone production: all this cycle does is transform NO into NO_2. It determines the ratio of the concentrations of NO and NO_2. With these reactions in equilibrium this ratio is given by the concentration of O_3, the temperature and the intensity of sunlight, the so-called photostationary state:

$$\frac{[NO]}{[NO_2]} = \frac{k_{1.2}[O_3]}{J_{NO_2}} \tag{1.4}$$

with $k_{1.2}$ the rate coefficient of reaction (1.2) and J_{NO_2} the photolysis rate of NO_2. Since NO and NO_2 are closely tied through these reactions, these species are often grouped together as active nitrogen NO_x (=NO+NO_2).

To actually produce ozone in the troposphere it takes an alternative reaction mechanism where reaction (1.3) that produces NO_2 and destroys ozone, is replaced by another reaction that produces NO_2 without the destruction of O_3. The produced NO_2 can be photolysed again to form O_3 by reactions (1.1) and (1.2). Such mechanisms require the hydroxyl radical, OH. Production of this radical starts with the photolysis of O_3 at wavelengths shorter than 315 nm, producing an exited oxygen atom, $O(^1D)$

$$O_3 + h\nu \rightarrow O(^1D) + O_2 \tag{1.5}$$

Most often $O(^1D)$ atoms collide with O_2 or N_2, which removes the excess energy and quenches $O(^1D)$ back to its ground state $O(^3P)$. Hereafter it forms O_3 again through reaction (1.2). However, a small fraction of $O(^1D)$ reacts with water vapour, H_2O, to generate the OH radical:

$$O(^1D) + H_2O \rightarrow 2\ OH \tag{1.6}$$

The OH radical is a key constituent because it reacts with virtually all trace gases, such as carbon monoxide CO, methane CH_4, or non-methane hydrocarbons, NMHC. Since OH is capable of reacting with virtually all pollutants, and hence responsible for the chemical removal of these pollutants, OH is sometimes called the "atmospheric

detergent". The simplest example consists of the oxidation of CO:

$$CO + OH \rightarrow CO_2 + H \qquad (1.7)$$

$$H + O_2 + M \rightarrow HO_2 + M \qquad (1.8)$$
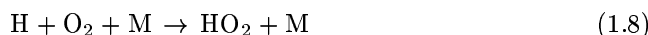
The less reactive hydroperoxy radical HO_2 reacts with NO

$$NO + HO_2 \rightarrow NO_2 + OH \qquad (1.9)$$

providing the alternative pathway for reaction (1.3), leading to net ozone production. This becomes apparent by calculating the net result of reactions (1.7), (1.8), (1.9), (1.1), and (1.2):

$$CO + 2\ O_2 + h\nu \rightarrow CO_2 + O_3 \qquad (1.10)$$
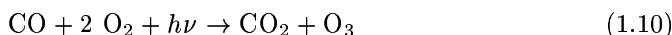
Note that neither NO_x or HO_x (=OH+HO_2) is lost in this reaction cycle. Like that of CO, also the oxidation of methane and NMHCs consists of NO_x and HO_x catalytic cycles. Only CO, methane, and the NMHCs are lost and are therefore often referred to as chemical fuel. Methane and CO are the most important chemical fuels because of their large abundances, even in the remote atmosphere. The cycle involving methane starts with the following reactions:

$$CH_4 + OH \rightarrow CH_3 + H_2O \qquad (1.11)$$

$$CH_3 + O_2 + M \rightarrow CH_3O_2 + M \qquad (1.12)$$

$$CH_3O_2 + NO \rightarrow CH_3O + NO_2 \qquad (1.13)$$

$$CH_3O + O_2 \rightarrow HCHO + HO_2; \qquad (1.14)$$
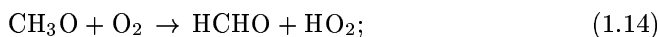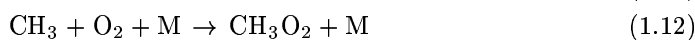
In these reactions CH_3 is called methyl, CH_3O_2 methylperoxy, CH_3O methyloxy, and HCHO formaldehyde (methanal). Reaction (1.13) provides another alternative pathway for reaction (1.3). Note that reaction (1.14) is also an alternative pathway by producing HO_2, which is available to react with NO (reaction (1.9)). The net result of these reactions (1.11), (1.12), (1.13), (1.14), together with reactions (1.9), (1.1), and (1.2) is

$$CH_4 + 4\ O_2 + h\nu \rightarrow HCHO + H_2O + 2O_3 \qquad (1.15)$$
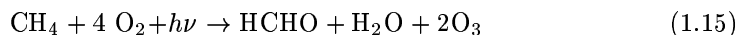
The produced formaldehyde will be oxidised further starting with photolysis or reaction with OH, leading to more ozone production,

$$HCHO + h\nu \rightarrow H + HCO \qquad (1.16)$$

$$HCHO + h\nu \rightarrow H_2 + CO \qquad (1.17)$$

$$HCHO + OH \rightarrow HCO + H_2O \qquad (1.18)$$

$$H + O_2 \rightarrow HO_2 \qquad (1.19)$$

$$HCO + O_2 \rightarrow HO_2 + CO \qquad (1.20)$$
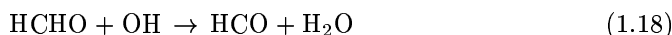
with the intermediate product formyl, HCO. CO is further oxidised as described above. Non-methane hydrocarbons are oxidised in a very similar way as methane, forming higher aldehydes (or ketones), that have similar fates as formaldehyde. All hydrocarbon oxidation-chains end with the formation of CO_2 from CO. Note that

the oxidation of formaldehyde (and also that of aldehydes and ketones) do not only contribute to the ozone production, but that also are an additional source of HO_x. *Ehhalt and Rohrer* [1995] estimated that about 0.6 molecules HO_x per molecule CH_4 are produced via the oxidation of formaldehyde under summer conditions at upper tropospheric midlatitudes.

Since NO_x acts as a catalyst in the formation of ozone, these reaction chains are limited by the conversion of NO_x to other nitrogen species. In the tropopause region the most important loss term is the formation of nitric acid, HNO_3:

$$NO_2 + OH + M \rightarrow HNO_3 + M \tag{1.21}$$
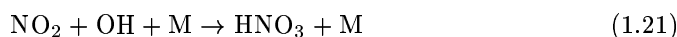
Other reactions that remove NO_x are:

$$NO_2 + HO_2 + M \rightarrow HO_2NO_2 + M \tag{1.22}$$
$$NO_2 + CH_3COO_2 \rightarrow CH_3COO_2NO_2 \tag{1.23}$$

forming peroxynitric acid, HO_2NO_2 and peroxyacetyl nitrate, $CH_3COO_2NO_2$ (PAN). Note that these reactions also remove the other catalyst HO_x. Other reactions that remove HO_x are:

$$OH + HO_2 \rightarrow H_2O + O_2 \tag{1.24}$$
$$HO_2 + HO_2 \rightarrow H_2O_2 + O_2 \tag{1.25}$$
$$HO_2NO_2 + OH \rightarrow H_2O + 2\,NO_2 \tag{1.26}$$
$$HO_2 + CH_3O_2 \rightarrow CH_3OOH + O_2 \tag{1.27}$$
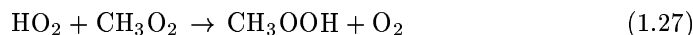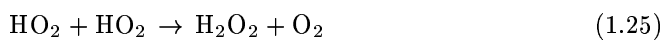
Products of these reactions are water vapour, hydrogen peroxide, H_2O_2, and methyl-hydroperoxide, CH_3OOH. The species HNO_3, HO_2NO_2, H_2O_2, and CH_3OOH are highly soluble in water and will partly be removed from the atmosphere by precipitation, providing a final sink for NO_x and HO_x. Reactions (1.24) and (1.26) form final sinks for HO_x. If not removed by precipitation, NO_x and HO_x can be regained from these species by photolysis or reaction with OH. Since these species have long lifetimes, they are often referred to as "reservoir" species. After formation, such species can be transported to other regions of the globe, and enhance the ozone production after reactions 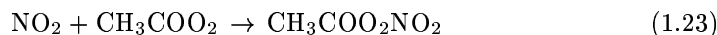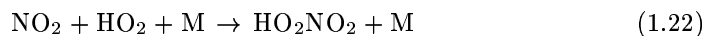that release the NO_x and HO_x. Especially PAN is regarded as an important reservoir species, because it is very stable at low temperatures, but decomposes rapidly at typical surface temperatures. Therefore it can enhance the ozone production at remote regions.

In the upper troposphere ozone production is largely controlled by the NO_x concentration. In 'low NO_x situations' the net production of ozone per NO_x molecule is very efficient, but with increasing NO_x concentrations the net ozone production stabilises and at 'high' NO_x concentrations the ozone production will even decrease again. These two regimes result from the dual role of NO_x in tropospheric chemistry, as pointed out above. On the one hand NO_x drives the ozone production, mainly via reaction (1.21). On the other hand NO_x promotes the removal of HO_x via reactions (1.21)-(1.27). With respect to HO_x removal, reactions (1.21),(1.22), and (1.26) are the most important pathways [*Wennberg*, 1998] in the tropopause region. The turnover point for the upper troposphere is expected to be at mixing ratios of several hundreds
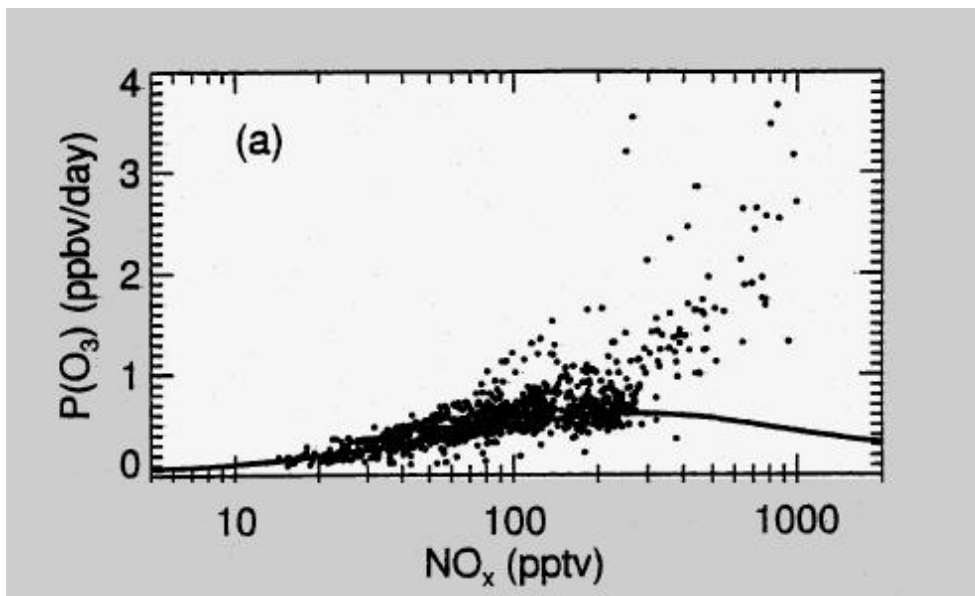
Figure 1.2: Observed ozone production rates, taken from *Jaeglé et al.* [1999]. The straight line corresponds to model-calculated values for median tropospheric background conditions during SONEX 1997.

of pptv NO_x. However, conditions in the upper troposphere can vary enormously. For instance, there are large variations in the background ozone concentrations. Also, lightning can produce sudden injections of NO_x. Furthermore, upward transport can also bring up boundary-layer pollutants, providing additional chemical fuel and HO_x sources. That our understanding on the upper-tropospheric ozone production still gives room for surprises, is illustrated by Figure 1.2, taken from *Jaeglé et al.* [1999], showing the calculated and observed daily mean ozone production $P(O_3)$ as a function of the NO_x concentration for upper tropospheric conditions at northern mid-latitudes, during the SONEX campaign (1997). The observed ozone production was constructed from very complete measurements of trace gases and ambient conditions, while the calculated production is constructed from median background conditions during the campaign. It clearly shows that the calculated ozone production has a turnover point around 300 pptv NO_x, but that this is in disagreement with the observed production numbers. Further discussion on the differences can be found in *Jaeglé et al.* [1999].

Nighttime chemistry also needs some consideration. During nighttime all NO_x is converted to NO_2 due to the absence of sunlight. NO_2 then reacts with ozone, forming the highly reactive nitrate radical, NO_3. During daylight this reaction pathway is unimportant, because NO_3 will be photolysed within seconds, but during the night it forms an equilibrium with dinitrogen pentoxide, N_2O_5.

$$NO_2 + O_3 \rightarrow NO_3 + O_2 \tag{1.28}$$
$$NO_3 + NO_2 + M \leftrightarrow N_2O_5 + M \tag{1.29}$$
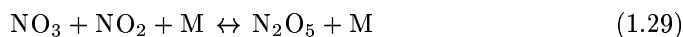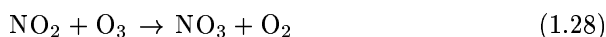
Obviously, these reactions are especially important during the polar night. The formation of N_2O_5 is important because of its heterogeneous reactions on sulphate aerosol and water droplets, forming HNO_3 (indices (g) and (a) denote gaseous and aqueous phase):

$$N_2O_5(g) + H_2O(a) \rightarrow HNO_3(g) \tag{1.30}$$
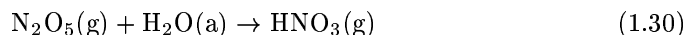
Note that reaction (1.28) also destroys ozone. During the day ozone is destroyed by reactions with OH and HO2

$$O_3 + OH \rightarrow HO_2 + O_2 \tag{1.31}$$

$$O_3 + HO_2 \rightarrow OH + 2\ O_2 \tag{1.32}$$

These reactions together with reaction (1.6) compete with the ozone-producing oxidation cycles of CO, CH_4, and NMHCs. Usually there is net ozone production. For instance, during the SONEX 1997 campaign the average ozone production was 0.57 ppbv/day, while the ozone destruction was 0.13 ppbv/day [*Jaeglé et al.*, 1999].

1.5   Global sources of nitrogen oxides

In order to assess the impact of subsonic aviation, all sources of atmospheric NO_x need to be quantified. In the framework of the AERONOX *Lee et al* [1997] have compiled an inventory with estimates of the different sources of nitrogen oxides for the year 1992. Table 1.1 gives a summary of the different sources with their uncertainty range and principal location. The different sources are categorised as: fossil fuel combustion (except aviation), biomass burning, soil microbial production, lightning, stratospheric decomposition of nitrous oxide, ammonia oxidation, and aircraft. The aircraft emissions were taken from the ANCAT 2/EC data, compiled by *Gardner et al.* [1997]. Originally a higher number (0.84 Tg[N]yr^{-1}) was reported, but it was adjusted afterwards to the current number [*Nüsser and Schmitt*, 1996].

Nitrogen oxides take part in the global nitrogen cycle, of which a schematic view is depicted in Figure 1.3. It is clarifying to regard the different sources in Table 1.1 from the perspective of this cycle. Molecular nitrogen in the atmosphere is the principal source of all nitrogen species. Although it is the most abundant gas in the atmosphere, only few processes are able to convert atmospheric nitrogen to other nitrogen species. The production of nitrogen oxides can occur directly from molecular nitrogen at high temperatures, or indirectly by the fixation of molecular nitrogen by microorganisms in soil.

Most of the nitrogen oxides in the atmosphere are produced thermally, commonly referred to as the Zeldovich mechanism. Between molecular and atomic oxygen an equilibrium exists that only allows significant atomic oxygen concentrations at high temperatures ($> \sim 2000$ K). At these high temperatures molecular nitrogen reacts with atomic oxygen, forming nitrogen oxide. Thermal NO_x production occurs in all fossil fuel combustion processes, including those in aircraft engines. It also occurs during biomass burning and in air that is heated by lightning discharges. Biomass and fossil fuel both contain nitrogen constituents that are converted to NO_x when burnt or combusted.

Table 1.1: Summary of "best" source estimates, uncertainties, and emission locations for 1992 (adopted from *Lee et al.*[1997]).

Source	Emission $(Tg[N]yr^{-1})$	Uncertainty range $(Tg[N]yr^{-1})$	Principal location of emissions
Fossil fuel combustion	22	13-31	Northern hemisphere midlatitude continental surface
Biomass burning	7.9	3-15	Tropical continental surface
Soil microbial production	7.0	4-12	Non-polar continental surface
Lightning	5.0	2-20	Tropical continent troposphere
Stratospheric decomposition of N_2O	0.64	0.4-1	Stratosphere
Ammonia oxidation	0.9	0.6	Tropical continental surface
Aircraft[a]	0.55	-	Northern hemisphere, latitudes 30°N-60°N

[a]From *Gardner et al.*, [1997]. The original number was 0.84 $Tg[N]yr^{-1}$, but it has been reduced afterwards because of double counting of aircraft movements.

Only a few soil microorganisms are capable of fixating atmospheric N_2 into biological useful nitrogen compounds. After fixation of N_2 microbial oxidation of NH_3 (nitrification) and the microbial reduction of nitrate NO_3^- (denitrification) produce NO. These processes also produce nitrous oxide N_2O that is stable in the troposphere but decomposes in the stratosphere by reaction with atomic oxygen and photolysis. Although naturally occurring, these processes are regarded as mainly human-made, because agriculture has increased the amounts of microorganisms that are capable of nitrogen fixation (most vegetables have a symbiotic relation with such microorganisms). Furthermore, the use of fertilisers intensifies the processes of nitrification and denitrification.

The oxidation of ammonia NH_3 is another source that produces NO_x. This source can be regarded as an anthropogenic source, since the emissions of ammonia are predominantly caused by human activities. Animal waste is the most important contributor.

Lightning is the most important natural source of atmospheric NO_x (Table 1.1). This source demands extra consideration, since it has a very inhomogeneous spatial and temporal distribution. Furthermore, lightning is the only source apart from aviation that directly injects NO_x in the troposphere. Since chemistry responds nonlinearly to increases in the NO_x concentrations, model calculations of the impact of aviation are very sensitive to the lightning source. [*Berntsen and Isaksen*, 1999]. Although the details of cloud electrification are still not fully understood [e.g. *Saunders*,
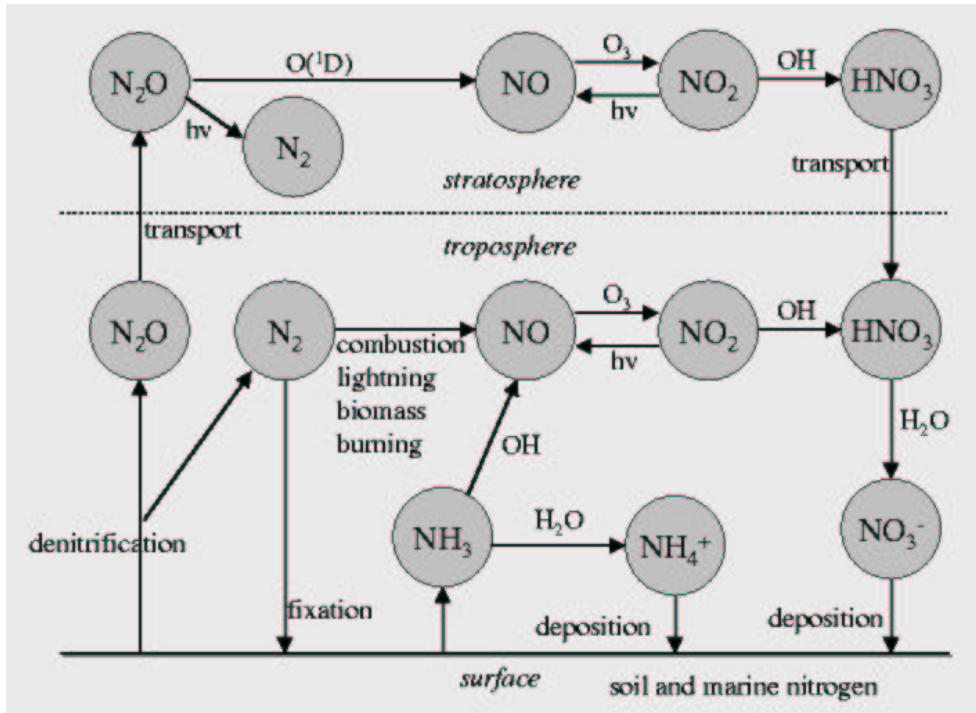
Figure 1.3: The global nitrogen cycle from the point of view of the formation of NO_x.

1994], ice particles, supercooled droplets, and graupel are generally believed to play a major role in the process of charge separation. One mechanism consists of polarisation of falling particles, which receive negative charge by colliding with smaller cloud particles that are carried upward in the strong thunderstormcloud updrafts. Other mechanisms arise from the thermoelectric effect in ice. This effect is the result of the fact that concentrations of dissociated ions have a strong temperature dependence, and that positive hydrogen ions are much more mobile than negative ones. The mechanisms itself are rather complicated and involve processes of heat transfer between rising and falling cloud particles. Whatever the exact mechanisms, once a typical thundercloud is electrified, its charge distribution resembles a positive dipole, with a net negative charge in the lower part of the cloud and a net positive charge in the upper part [e.g. *Williams*, 1985]. Figure 1.4 gives a schematic view of an electrified cloud. The negative charge near the cloud base induces a positive charge on the ground below. When the electrical field reaches a threshold, or breakdown potential, a lightning discharge occurs. The discharge can occur within the cloud (intracloud flash, IC), between the cloud and the ground (cloud-to-ground flash, CG), or occasionally between clouds (intercloud flash), or upward to the ionosphere (sprites). The last two types are not considered to be important for the global NO_x production of lightning. A typical discharge starts in the cloud with a local breakdown that initi-
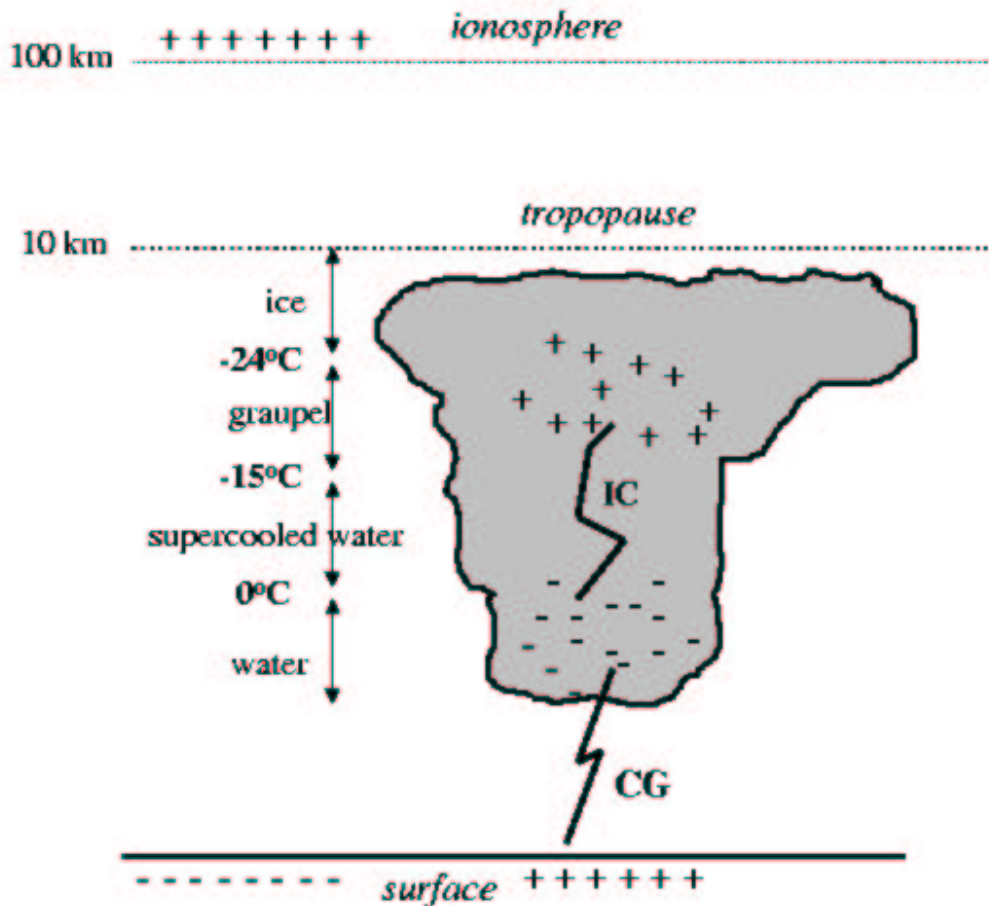
Figure 1.4: Schematic view of a thunderstorm with the charge distribution, the location of cloud particles, and the possible discharges (intracloud (IC) and cloud-to-ground (CG)) within the main charge centres.

ates a stepleader, a propagating discharge, and is highly branched. As this stepleader comes close to the ground (for a CG) or to another charge-centre in the cloud (for IC), another propagating discharge in opposite direction (from the ground or the opposite charge-centre) occurs. When the two leaders meet, a large current propagates through the created charged channel, known as the return stroke. This return stroke could reach another charge-centre in the cloud en initiate a subsequent stroke, called a dart leader, followed by a subsequent return stroke. So a lightning flash consists of a number of strokes, but for NO_x production only the return strokes are believed to be important, because they heat the air in the channel to possibly 30.000 K, after which NO_x is produced thermally until the air has cooled to approx. 2000 K.

1.6   Transport of trace gases

Once released in the atmosphere, nitrogen oxides, and other pollutants are subject to atmospheric transport and mixing processes. The time scales of the different transport processes must be larger or comparable to that of the atmospheric lifetime of the considered species for them to be relevant. For instance, CO_2 has a lifetime of over 100 years, which exceeds the time-scale of all atmospheric motions by far and is therefore a well-mixed gas. The OH radical, on the other side, has a lifetime of the order of a second, which is too short to be transported over significant distances.

Most nitrogen oxides and other pollutants are emitted near the Earth's surface in the planetary boundary layer (PBL); the part of the atmosphere that is strongly influenced by interaction with the surface. Here the thermodynamic structure is largely determined by turbulent motions, caused by surface friction and surface heating. These motions determine the depth of this layer. In the free atmosphere above, these turbulent motions can generally be ignored and the synoptic-scale motions show generally only slow vertical displacements. This confines tracers with lifetimes of the order of a day, such as NO_x and most hydrocarbons to the boundary layer, except under special conditions, such as frontal uplifting and deep convection.

Of particular importance for the vertical redistribution of boundary layer pollutants is convection, a process with strong vertical motions that can arise in an unstable atmosphere. Latent heat release accelerates upward motions in unstable areas. Convection causes efficient venting of the boundary layer, transporting boundary layer pollutants up to the tropopause region within hours, but sometimes even within several minutes [e.g. *Dickerson et al.*, 1987; *Pickering et al.* 1992]. Obviously these boundary layer pollutants have a strong effect on ozone chemistry, since they consist of NO_x, CO, and NMHCs. Some of the NMHCs are important HO_x precursors, such as acetone and methylhydroperoxide [*Singh et al.,,* 1995; *Chatfield and Crutzen*, 1984; *Müller and Brasseur*, 1999].

Frontal uplifting is often referred to as 'warm conveyor belt', which is one of the airflows in an extratropical cyclone [*Carlson*, 1980]. An extratropical cyclone consists of several coherent airflows that are associated with the warm and cold fronts. The most important flows are a warm conveyor belt with upward transport along the cold front, a cold conveyor belt with upward transport along the warm front, and a stratospheric intrusion into the cyclone. This process could take up air from the boundary layer in about a day [*Heijboer et al.*, 1996], which is at a relevant time-scale for most boundary layer pollutants.

Aircraft NO_x emissions themselves are directly injected in the tropopause region, but the mixing with the background air is not instantaneous. The emissions of an aircraft, mixed with ambient air, form a plume in the wake of an aircraft. Such a plume is first controlled by the jet dynamics, whereafter it follows the controlled motions of the trailing vortices of the aircraft, and breaks up into decaying turbulent motions. These stages last $\sim$ 100 s and thereafter the motions are controlled by atmospheric conditions. This last stage can last for several hours up to time of an order of a day [*Schumann et al.*, 1995b]. The atmosphere in the tropopause region is usually stably stratified with large bulk Richardson numbers. In these situations of weak turbulence the mixing of aircraft plumes follows the classical diffusion concepts approximately and can be described with the Gaussian plume theory [*Schumann et*

al., 1995b].

Once mixed with the background, emitted nitrogen oxides are subject to several atmospheric transport processes. The winds in this region are predominantly westerlies with annual mean windspeeds in the range of 10-30 m/s [*Peixoto and Oort*, 1992]. These speeds result in average global circulation times of about 15-30 days. Windspeeds are highest during winter. The lifetime of NO_x of about 5-10 days in this region is too short to allow transport around the globe, so NO_x emitted by aircraft will generally be located near to and eastward of the flight corridors. Ozone produced by aircraft NO_x emissions, with a lifetime of several months, will have a more zonally symmetric distribution.

Subsonic aviation emits nitrogen oxides partly in the stratosphere (about 20-40% [IPCC, 1999]) and partly in the troposphere. Exchange between these two atmospheric compartments is slow, hence aircraft emissions in the stratosphere will usually not be affected by other NO_x sources. Furthermore, the lifetime of NO_x is larger in the stratosphere than in the troposphere. At midlatitudes there are both upward and downward fluxes. However, the net transport is downward, from the stratosphere into the troposphere [*Siegmund et al.*, 1996], but is still not well quantified. Various processes lead to stratosphere-troposphere exchange: downward transport in tropopause folds and subsequent mixing, convective mixing in cut-off lows and cloud systems, radiative processes near the tropopause, and mixing by turbulence and waves near the tropopause [*Holton et al.*, 1995]. The relative importance of these different mechanisms is not yet known. Many of them occur during the lifecycles of extratropical cyclones.

1.7 Three-dimensional global chemistry transport models

The atmosphere can be regarded as an extremely complex reactive system in which numerous physical and chemical processes occur simultaneously. Our understanding of individual processes, does not imply understanding of the system as a whole. Therefore all relevant processes, the emissions and removal of pollutants, the different transport processes, and the chemical transformations in the atmosphere, need to be integrated in one mathematical model. Different problems require different model types. In order to calculate the impact of aircraft emissions we need a model that gives a three-dimensional description of the global atmosphere. Basically two types of such models are available: three-dimensional global chemistry transport models (CTMs) and global circulation models with chemistry (GCMs).

Of those two types, GCMs have the highest complexity. They solve the basic equations of motion, conservation of mass, and conservation of energy. Although these models are the most comprehensive and are, for instance able, to directly calculate the climate effects of aircraft-induced ozone increases, the high complexity requires a lot computer resources and implies a loss of flexibility. It is furthermore difficult to perform studies of a single process.

Therefore, chemistry transport models are very useful. CTMs use prescribed meteorological fields, which gives an obvious reduction in required computer resources and a gain in flexibility. Since CTMs use prescribed meteorological quantities, they

are often referred to as 'off-line' models. Another advantage of the off-line modelling approach is the possibility to use analysed meteorology, which gives the CTM a good description of the observed state of the atmosphere. This is especially useful for impact studies, since transport and removal processes of pollutants take place in the actual atmosphere. Thus it facilitates the comparison of measurements with tracer observations.

The starting point of three-dimensional chemistry transport models is the continuity equation for a chemical species i,

$$\frac{\partial c_i}{\partial t} + \nabla.(\mathbf{u}c_i) = R_i(\mathbf{c}) + E_i - S_i \tag{1.33}$$

with $c_i(\mathbf{x}, t)$ the concentration of i as a function of location $\mathbf{x}$ and time t, $\mathbf{u}(\mathbf{x},t)$ the wind vector, $R_i(\mathbf{c}(\mathbf{x}, t), \mathbf{x}, t)$ the net chemical production term, and $E_i(\mathbf{x}, t)$ and $S_i(\mathbf{x}, t)$ its sources and sinks, respectively. Since this equation requires to be solved numerically, the solutions is evaluated only at discrete times and locations (grid points). Equation (1.33) can be written in the so-called advective form

$$\frac{\partial \bar{c}_i}{\partial t} + \bar{\mathbf{u}}\nabla \bar{c}_i = \left(\frac{\partial \bar{c}_i}{\partial t}\right)_{\text{diff}} + \left(\frac{\partial \bar{c}_i}{\partial t}\right)_{\text{conv}} + R_i(\bar{\mathbf{c}}) + E_i - S_i \tag{1.34}$$

with $\bar{c}$ the grid-point mean concentration, $\bar{\mathbf{u}}$ the grid-point mean wind vector, and an additional diffusion and convection term. These additional transport terms arise from the discretisation and have to be parameterised, since not all atmospheric motions are resolved at a certain grid and time resolution.

The chemistry transport model used in this thesis is TM3. This model is adapted from the global tracer model TM2 [*Heimann*, 1995], and calculates the horizontal and vertical transport of tracers on the basis of 6-hourly output from the European Centre for Medium-Range Weather Forecasts (ECMWF) model. The chemistry, as well as the sources and the sinks, are fully decoupled from the transport part of the model, which results in a large flexibility (operator splitting). The model is applied to many different studies. For instance, the model has been used as a data-assimilation tool for observed total ozone columns [*Jeuken et al.*, 1999] or to study stratospheric chemistry problems [*Bregman et al.*, 2000]. For the work described in this thesis, the model was used at a resolution of 5° in longitude and 3.75° in latitude and 19 hybrid σ-pressure levels extending from the surface up to 10 hPa, with tropospheric chemistry. Details of the chemistry and other processes are given in the following chapters.

1.8   This thesis

The aim of the work for this thesis was to evaluate and improve the TM3 model with observations in order to enhance the credibility of the previously made estimations of the aircraft-induced NO_x and O_3 perturbations. The model TM3 was one of models that participated in the AERONOX project and the 1999 IPCC assessment. As already pointed out, these model calculations are of a high complexity and subject to many uncertainties. These include uncertainties in the emission data, and many uncertainties in the various chemical and physical processes, such as troposphere-stratosphere exchange, deep convection, heterogeneous chemistry, or even the closure

of the NO_y and HO_x budgets. None of the models involved in these studies were sufficiently tested with observations, simply because of a lack of suitable measurements. There were only few observations in the altitude range of subsonic aviation, but none of these were conducted in the North Atlantic flight corridor, the main flight corridor between the US and Europe. This implies an obvious constraint on the credibility of these model studies and was the motivation of the POLINAT experiment (Pollution from Aircraft Emissions in the North Atlantic flight corridor) [*Schlager et al.*, 1997; *Schumann et al.*, 2000] and the SONEX experiment (Subsonic Assessment Ozone and Nitrogen Oxide Experiment) [*Singh et al.*, 1999]. For these projects measurement campaigns were conducted with instrumental aircraft in and near the main flight corridors and provided excellent data to confront the models with.

Gaining confidence in the model and narrowing down the uncertainties in the estimates is important, not only from a scientific point of view, but certainly also from a policy makers point of view. The outcomes of assessments, such as IPCC [1999], will have a firmer basis, when they are supported by measurements. In this thesis the following scientific questions are addressed:

1. How well do the model calculations of the NO_x and O_3 concentrations in the main flight corridors agree with observations?

2. Can observations support model estimates of the calculated aircraft-induced perturbations of the NO_x and O_3 concentrations?

3. How much do the other NO_x sources contribute to the atmospheric composition of the main flight corridors?

4. Can the uncertainties in the spatial and temporal distributions of lightning, as well as in the global total of the lightning NO_x production, be reduced?

5. Do the small-scale processes, which are associated with single aircraft exhaust plumes, that cannot be resolved by a CTM, have an effect on the global distributions of NO_x and O_3?

In Chapter 2 the first three questions are addressed by comparing the model results of TM3 with the observations of the POLINAT and SONEX experiments. These comparisons were performed for different meteorological situations. Since emphasis is put on the NO_x contributions from aviation and other NO_x sources, a labelling technique was developed that partitioned the nitrogen oxides and ozone according to their source category. This labelling technique enabled us to consistently calculate the contributions from the different NO_x sources to the NO_x and ozone concentrations. The calculated contributions were qualitatively interpreted with the help trajectory analyses.

The fourth question is addressed in Chapter 3. The NO_x production by lightning imposes a large uncertainty on the model results, because of its uncertain, but probably large total contribution, and because of uncertainties concerning the spatial and temporal distribution of lightning. Since chemistry responds non-linearly to changes in the NO_x concentration, model shortcomings of the description of the lightning NO_x source could have a large effect on the calculated aircraft impact. Previously,

climatological lightning NO_x emissions were used in global CTMs, limiting the ability to simulate the observed state of the atmosphere and hampering the possibility to evaluate the model performance with observations. Since lightning is strongly linked to convection, it is possible to parameterise the NO_x production by lightning by searching for an empirical relation with a meteorological quantity that is linked to convection. This was the focus of the work presented in Chapter 3 that was done in the framework of the EULINOX (European Lightning Nitrogen Oxides) project [*Höller and Schumann*, 2001]. A new parameterisation for the production of NO_x by lightning was constructed, based on correlation of lightning observations with different meteorological fields of the ECMWF model. The model results with the new and old lightning parameterisation were compared with NO observations from the EULINOX campaign, as well from the SONEX and POLINAT campaigns.

Chapter 4 addressed the last question, which is a more fundamental question. Since CTMs have relatively coarse grids, they cannot describe the chemical and physical processes that occur in the wake of an aircraft. As pointed out above, the exhaust of an aircraft persists for several hours up to a day, slowly dispersing to the dimensions of a CTM's grid box. The chemistry responds non-linearly to the NO_x concentrations, resulting in differences between the chemistry in the plumes and the ambient air: the conversion of NO_x to reservoir species, such as HNO_3 is more efficient in the plumes. Also the production of ozone is strongly affected, starting with net destruction in the young exhaust, whereas there is a small net production of ozone in the ambient air. A plume exhaust model was developed to study these processes and to develop a parameterisation that accounts for the subgrid plume effects in a CTM.

These first two chapters are reviewed papers: Chapter 2 has been published in *Journal of Geophysical Research*, Vol. 105 in 2000 and Chapter 3 in *Physics and Chemistry of the Earth*, Vol. 26, 2001. Chapter 4 has been submitted to *Journal of Geophysical Research*, but a short paper on the effects of aircraft plumes has already been published in *Geophysical Research Letters*, Vol. 24, 1997, and is added as an appendix of Chapter 4.

2

Model calculations of the impact of NO$_x$ from air traffic, lightning, and surface emissions, compared with measurements

abstract

The impact of NO$_x$ from aircraft emissions, lightning, and surface contributions on atmospheric nitrogen oxides and ozone in the North Atlantic flight corridor has been investigated with the three-dimensional global chemistry transport model TM3 by partitioning the nitrogen oxides and ozone according to source category. The results have been compared with Pollution from Aircraft Emissions in the North Atlantic flight corridor (POLINAT 2) and Subsonic Assessment Ozone and Nitrogen Oxide Experiment (SONEX) airborne measurements in the North Atlantic flight corridor in 1997. Various cases have been investigated: measurements during a stagnant anticyclone and an almost cut-off low, both with expected high aircraft contributions, a southward bound flight with an expected strong flight corridor gradient and lightning contributions in the south, and a transatlantic flight with expected boundary layer pollution near the U.S. coast. The agreement between modelled results and measurements is reasonably good for NO and ozone. Also, the calculated impact of the three defined sources was consistent with the estimated exposure of the sampled air to these sources, obtained by specialised back trajectory model products. Model calculations indicate that aircraft contributes 55% to the mean NO$_x$ concentration and 10% to the O$_3$ concentration in the North Atlantic flight corridor in October 1997, whereas lightning and surface emissions add 15% and 25% to the NO$_x$ concentration and 20% and 30% to the O$_3$ concentration.

2.1   Introduction

Subsonic aviation perturbs the atmospheric composition at cruise altitudes of about 8 to 12 km altitude, mainly by the emission of NO$_x$ (NO and NO$_2$), which by photochemical conversions causes an increase in O$_3$ with possible climatic consequences. Global three-dimensional chemistry transport models are required to evaluate the impact of aircraft emissions [*Friedl et al.*, 1997; *Schumann*, 1995, 1997]. In the Impact of NO$_x$ Emissions from Aircraft upon the Atmosphere at Flight Altitudes 8-15 km (AERONOX) project [*Schumann*, 1995], calculations with different three-dimensional global chemistry transport models predicted a NO$_x$ perturbation of 20% -70% in the 8-12 km layer depending on season, causing a photochemically increased O$_3$ concentration of 2%-10%.

There are many uncertainties in the model results because these depend to a large degree on the emission data, the background concentrations, and on many aspects of the physics and chemistry of the atmosphere, such as troposphere-stratosphere exchange, deep convection, and heterogeneous chemistry. The Pollution from Aircraft Emissions in the North Atlantic flight corridor (POLINAT 2) and Subsonic Assessment Ozone and Nitrogen Oxide Experiment (SONEX) measurements produced data that is especially useful to test model predictions on the impact of aircraft on the atmospheric composition.

Lightning and surface emissions are the major sources of NO$_x$ in the atmosphere. Surface emissions add up to a total of about 31 Tg(N)yr^{-1} according to *Lee et al.* [1997], and lightning is generally believed to contribute in the range 2-10 Tg(N)yr^{-1} [e.g., *Levy and Moxim*, 1996; *Wang et al.*, 1998], whereas aircraft emissions only amount to 0.55 Tg(N)yr^{-1}. Clearly, it is expected that surface emissions and lightning have an impact on the atmospheric composition of the North Atlantic flight corridor. For this reason, it is necessary to calculate the impact of these sources as well, when investigating aircraft effects.

In this study, NO and O$_3$ measurements results of the POLINAT 2 and SONEX campaigns were compared with results of the three-dimensional chemistry transport model TM3. The model was enhanced by labelling NO$_x$ species according to their source (i.e., aircraft, lightning, and surface). Also, HNO$_3$ and O$_3$ are labelled accordingly. This is a different approach from the more common "difference" runs in which results of the full model are subtracted from the results without the source of interest. Our new approach has a few advantages: it avoids problems caused by the nonlinearly of chemical equations, and it gives insight in the combined effects of the different sources in a single calculation. Besides comparing the model results with measurements, specialised back trajectory calculations over the North Atlantic flight corridor that gives the exposure of air to convection, air traffic, and lightning are used to independently assess the contributions of the different sources.

Using these techniques, we were able to address the following relevant questions: 1. How well do the model calculations agree with the measurements of NO and O$_3$? 2. What is the impact of air traffic emissions on the O$_3$ and NO$_x$ concentrations in the region of the North Atlantic flight corridor? 3. Can the impact of air traffic emissions on the O$_3$ and NO$_x$ concentrations be detected? Furthermore, can a distinct north-south gradient in the NO$_x$ concentration, associated with the position of the North Atlantic flight corridor, be detected? 4. How does the impact of air traffic emissions

Table 2.1: NO$_x$ emissions

Source	(Tg[N] yr^{-1})
Microbial production	3.9
Industry and surface traffic	22.0
Biomass burning	5.3
Lightning	5
Aircraft	0.55

compare to that of surface contributions and to the lightning NO$_x$ production?

2.2 Model Description

The three-dimensional global chemistry transport model TM3 used in this study is an updated version of the CTMK model, previously used in POLINAT [*Wauben et al.*, 1997]. The model is adapted from the global tracer model TM2 [*Heimann*, 1995] and calculates the horizontal and vertical transport of tracers on the basis of 6-hourly output from the European Centre for Medium-Range Weather Forecasts (ECMWF) model [*Velders et al.*, 1994]. Analysed meteorological fields of wind, geopotential height, temperature, and humidity are used for this purpose. In this study, the model has been used at a resolution of 5° in longitude and 3.75° in latitude and 19 hybrid σ-pressure levels extending from the surface up to 10 hPa. Advection is calculated with the slopes scheme of *Russell and Lerner* [1981]. The subscale convection fluxes are evaluated according to the scheme of *Tiedtke* [1989], and the boundary layer is parameterized according to *Louis* [1979].

TM3 contains a chemical scheme involving the NO$_x$, HO$_x$, O$_3$ chemistry with methane oxidation. It evaluates the daytime chemistry of 13 trace gases by using the temperature and relative humidity fields from the ECMWF analyses. Daytime averaged photolysis rates for O$_3$, NO$_2$, H$_2$O$_2$, HNO$_3$, CH$_3$OOH, and HCHO are used, which have been computed with the method described by *Brühl and Crutzen* [1989]. A total of 25 chemical reactions are considered together with dry deposition for O$_3$, NO$_2$, H$_2$O$_2$, HNO$_3$, CH$_3$OOH, and NO, and wet deposition for H$_2$O$_2$, HNO$_3$, and CH$_3$OOH. Climatological precipitation data are used for the parameterisation of the wet deposition. Nighttime chemistry is described, besides deposition, with a parameterised reaction in which O$_3$ and NO$_x$ are converted into HNO$_3$ and accounts for the heterogeneous conversion of N$_2$O$_5$ into HNO$_3$ [*Dentener and Crutzen*, 1993]. Since the chemical scheme cannot adequately describe stratospheric chemistry, a zonally and monthly mean ozone climatology [*Fortuin and Langematz*, 1995] is prescribed above 50 hPa. Also, the destruction of CH$_4$ in the stratosphere through reactions with O(^{1}D) and Cl is prescribed from monthly mean rates from the Cambridge stratospheric chemistry transport model [*Law and Pyle*, 1993; *Velders*, 1995].

In Table 2.1 the NO$_x$ emissions per source category are given. The aircraft emissions are taken from the Abatement of Nuisances Caused by Air Transport (ANCAT 2) emission inventory [*Gardner et al.*, 1997]. Lightning is parameterised according to *Price and Rind* [1992], using the convective cloudtop heights with additional scaling

Table 2.2: CO emissions

Source	(Tg yr^{-1})
Anthropogenic	373
Soils	166
Oceans	162
Biomass burning	716

to the subgrid mass fluxes. The vertical distribution of lightning NO$_x$ is taken to be proportionate to air density. The efficiency over land is 10 times greater than over sea, following *Levy and Moxim* [1996]. The fraction of cloud-to-cloud over cloud-to-ground strokes is assumed 1/2.3 in the region between 40°S and 40°N and 1/1.3 toward the poles [*Gallardo et al.*, 1996]. The NO emission due to lightning is scaled to 5 Tg(N) yr^{-1} globally. Details on the other NO$_x$ emissions are given by *Lee et al.* [1997]. The stratospheric influx of NO$_x$ is parameterised by prescribing the HNO$_3$ concentration at 10 hPa, by using the ratio of HNO$_3$ to O$_3$ from the UARS data set, similar to *Murphy et al.* [1993]. The CO emissions are from *Müller* [1992] and are given in Table 2.2. Methane concentrations are prescribed at the surface according to *Fung et al.* [1991].

To calculate the impact of the various sources, NO$_x$ is partitioned according to three source categories, namely, NO$_x$ from air traffic, from lightning, and from surface contributions. The latter is the total of NO$_x$ emitted by soil microbial production, industry, surface traffic, and biomass burning. The stratospheric influx, which is treated as a HNO$_3$ source, is labelled as a fourth source category. The O$_3$ and HNO$_3$ concentrations are also explicitly split into four parts according to source category. The total concentrations of NO$_x$, O$_3$, and HNO$_3$ and the concentrations of the partitioned species are transported separately.

The NO$_x$ and HNO$_3$ partitioning changes by chemical conversions since reactions in which NO$_x$ is formed into HNO$_3$ and vice versa occur simultaneously. The new partitioning for a specific nitrogen constituent NO$_y$ after chemical conversions can be defined in the following manner:

$$f_{\mathrm{NO}_y,A}^{t+\Delta t} = \{f_{\mathrm{NO}_y,A}^{t}(\mathrm{NO}_y^{t+\Delta t} - \sum_{z\neq y} P_{\mathrm{NO}_z}^{t+\Delta t}) + \sum_{z\neq y} f_{\mathrm{NO}_z,A}^{t} P_{\mathrm{NO}_z}^{t+\Delta t}\}/\mathrm{NO}_y^{t+\Delta t} \qquad (2.1)$$

Here P is the production of NO$_y$ from another nitrogen species NO$_z$. So the first term on the right-hand side of the equation gives the fraction of source A that is lost by chemical conversion, which is proportional to the fraction of the nitrogen consistuent. The next terms are the production from the other nitrogen species, proportional to fractions of the other nitrogen consistuents.

The chemical production of O$_3$ in the troposphere is equivalent to the production of NO$_2$ from reactions other than that of O$_3$ + NO, that is the total of the reactions HO$_2$ + NO, RO$_2$ + NO, the photolysis of HNO$_3$, etc. These O$_3$ production terms are used to calculate the ozone formation from the different NO$_x$ sources:

$$f_{\mathrm{O}_3,A}^{t+\Delta t} = \{f_{\mathrm{O}_3,A}^{t}(\mathrm{O}_3^{t+\Delta t} - \sum_{y} P_{\mathrm{NO}_y}^{t+\Delta t}) + \sum_{y} f_{\mathrm{NO}_y,A}^{t} P_{\mathrm{NO}_y}^{t+\Delta t}\}/\mathrm{O}_3^{t+\Delta t} \qquad (2.2)$$

with P denoting the production of NO_2 from another nitrogen species NO_y.

2.3 Exposure Plots

The NASA Goddard and Ames theory teams [*Thompson et al.*, 2000] provided meteorological fields and specialised model products that permit identification of all of these sources in air masses sampled during SONEX and during the SONEX-coordinated POLINAT flights. The products were used in a forecast mode for flight planning. For postmission analysis, three products were selected for comparison with our model results. All images illustrated here are available on the SONEX website (telsci.arc.nasa.gov/~sonex /pages/model_products.html) or from the SONEX archive, which is available as a CD.

The products used are based on multiple back trajectories initiated at approximately flight altitude over a grid that covers the SONEX sampling region: 0°-80°W and 15°-70.5°N. Over a 1°x1° grid within that region, a parcel is initialised at each grid point. The model used is the NASA/Goddard Isentropic Trajectory model of *Sparling et al.* [1995]. The potential temperature surface used for the parcels typically corresponds to the mean sampling altitude of the flight, usually 330-345 K. The meteorological analyses used are those provided by the GEOS-STRAT version of the Goddard Data Assimilation Office (DAO) model. Parcels are initialised at 1200 UT for each flight day, unless otherwise specified, and are run back in time for a maximum of 5 days. Exposure to aircraft, convection, and lightning is determined as follows:

2.3.1 Aircraft Exposure

Parcel locations at 1-hour intervals are superimposed on a climatological map of aircraft positions. The map is based on the NASA 1992 emissions inventory of aircraft emissions [*Baughcum et al.*, 1996]. The emissions map was not used quantitatively. Instead, the emissions map was used to define whether air traffic was present in the specified air mass on an hour by hour basis. Positive responses were accumulated to give a maximum value of 120 hours. Note that this does not take into account the roughly diurnal pattern of most commercial flights, so the exposure times are likely to be overestimates. However, relative impact of air traffic should be indicated accurately.

2.3.2 Cloud Exposure

Two variations of this product are in the SONEX archive, one in which the parcels are linked to deep convection over land and ocean, and the other with linkage to land convection only. Deep convection that can advect surface NO_x into the parcels along the back trajectories is defined simply as a cloud brightness temperature 5° colder than the parcel temperature. This implies a thick cloud somewhat higher than the parcel. Potential vorticity (PV) is used to screen out potential stratospheric influences; that is, as the parcel travels, if stratospheric PV is encountered, no convective influence can occur at that time regardless of the cloud brightness temperatures. The C* products include tracking and weighting the number of days for which a parcel encountered

convective clouds at the appropriate potential temperature level. The maximum value, 5, denotes that during each of the 5 days of transit, deep convective clouds were encountered. The C* product is used in this study. The R* products record days from the most recent convective encounter; when a convective cloud is encountered, the trajectory is terminated based on the assumption that convection invalidates the isentropic assumption. This represents a lesser exposure than the cumulative impact and is similar to the treatment of lightning in the lightning exposure product.

2.3.3 Lightning Exposure

The satellite lightning product from the Optical Transient Detector (OTD) covers a given area for only a few minutes each day, so the National Lightning Detection Network (NLDN) and Long-Range Field (LRF) lightning products were captured each day during SONEX deployment. These networks are ground-based primarily over North America; with some drop-off in detection efficiency, they reach several thousand kilometres away from the continent. The reporting frequency is every minute or two. The standard lightning exposure product is based on maps in which lightning flashes were added for 6 hours; that is, four maps per day were archived. When a parcel encounters a grid box (1°x1°) with any detectable lightning flash, its trajectory is terminated. The lightning flash number is recorded in the grid corresponding to the initial parcel position. Not surprisingly, the regions sampled from Shannon showed relatively low lightning influences. Most of the lightning was in the Southeast of the United States, Caribbean, and Gulf of Mexico and its influences in 5 days' transit did rarely reach the eastern Atlantic.

2.4 Aircraft Measurements

The data used in this analysis were collected in situ with the DLR Falcon and the NASA DC-8 during POLINAT 2 and SONEX, respectively. On board the Falcon, NO was measured with NO/O$_3$ chemiluminescence, and O$_3$ was detected with a fast response UV photometer. Details on the instruments used have been given by *Schlager et al.* [1997] and *Ziereis et al.* [2000]. NO and O$_3$ on the DC-8 were measured using chemiluminescence technique as described by *Kondo et al.* [1997]. Overviews on the POLINAT 2 and SONEX missions have been provided by *Schumann et al.* [2000] and *Singh et al.* [1999].

2.5 Description of Selected Cases

From the combined SONEX and POLINAT 2 1997 campaign, four cases were selected for this study, namely, the transatlantic flight on October 15, 1997, a flight in an almost cut-off low on October 18, 1997, one in a stagnant anticyclone on October 23, 1997 and a southward bound flight from Shannon to Tenerife on October 20, 1997.
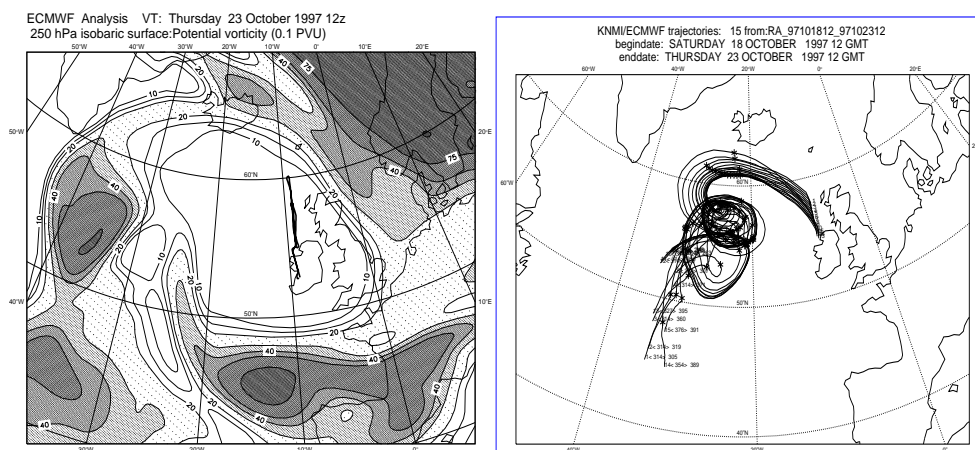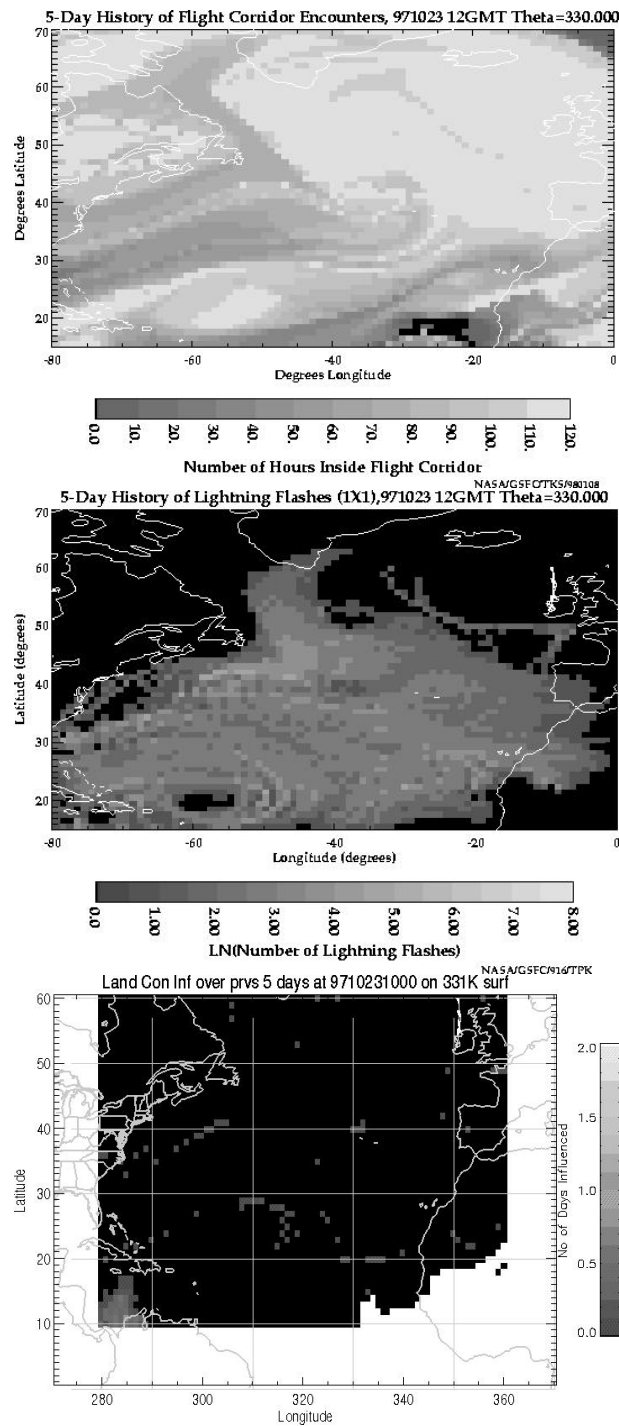
Figure 2.1: The ECMWF analysis of potential vorticity (0.1 PVU) on October 23 at 250 hPa with the flight pattern and 5-day backward trajectories ending above the Shannon area.

## 2.5.1 Stagnant Anticyclone: October 23, 1997

Figure 2.1 shows a map of the potential vorticity (0.1 PVU) at 250 hPa, calculated from the ECMWF analysis for October 23, 1997, with the flight pattern of the DLR Falcon. The map reveals a large ridge (high) over the Atlantic, centred at 18°W, 57°N, roughly covering the area from eastern England up to Iceland. The entire flight took place in the troposphere. Figure 2.1 also shows 5-day backward trajectories, all ending above the Shannon area where the aircraft took off. All trajectories perform more than 2 anticyclonal rotations, indicating the persistence of the stagnant blocking high. The blocking high encompasses the North Atlantic flight corridor, so a dominant aircraft NO signature is expected, since all trajectories stayed at cruise altitudes and were only exposed to aircraft emissions. The exposure plots for this case, depicted in Figure 2.2 confirm this. In the entire region of the blocking high, a maximal contribution of aircraft emissions is found, whereas lightning and convection over land influences are absent.

2.5.2 Almost Cut-off Low: October 18, 1997

Figure 2.3 depicts a map of the potential vorticity (0.1 PVU) at 250 hPa, calculated from the ECMWF analysis for October 18, 1997, with the flight pattern of the DLR Falcon and reveals an almost cut-off low east of Ireland and Spain, centred at 16°W, 45°N. Horizontal flight legs were performed at 376 hPa, 315 hPa, 262 hPa, and 217 hPa. The first two legs were in the troposphere, the third was in the tropopause, and the last was in the stratosphere. The 5-day backward trajectories, also shown in Figure 2.3, come from the south and have completed a half to a full cyclonic rotation in the low. This indicates that again a large aircraft contribution to the NO concentration can be expected without much influence of other sources, similar to the stagnant high case, although some of the trajectories originate from the U.S. boundary layer. The exposure maps from Figure 2.4 support the analysis from the potential vorticity and

Figure 2.2: The estimated exposure to aircraft, lightning, and convection of air in the North Atlantic flight corridor on October 23.
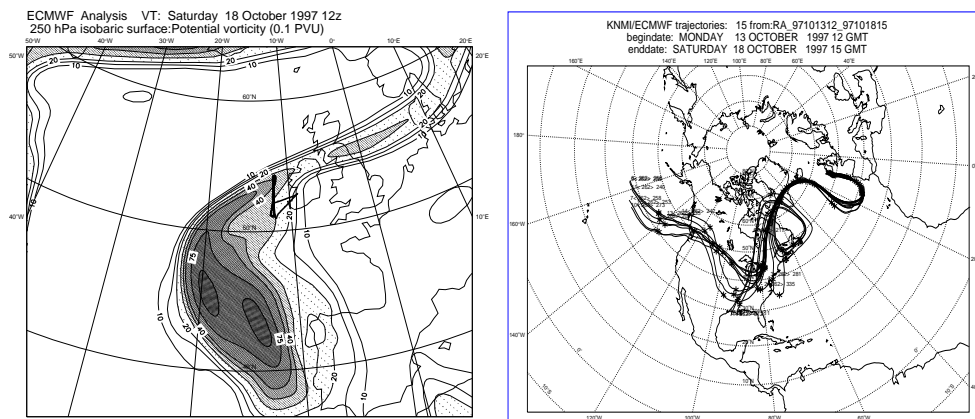
Figure 2.3: The ECMWF analysis of potential vorticity (0.1 PVU) on October 18 at 250 hPa with the flight pattern 5-day backward trajectories ending above the Shannon area.

the trajectories maps; both the exposure to lightning and convection is absent in the almost cut-off low, whereas aircraft exposure is maximal, except for the centre of the cyclone which contains stratospheric air, as can be seen from the potential vorticity map.

2.5.3 Southward Bound Flight: October 20, 1997

On October 20, 1997, the POLINAT aircraft made a flight from Shannon to Tenerife and back to examine if the boundary of the North Atlantic flight corridor in terms of the north-south gradient in the NO_x concentration can be detected. The SONEX aircraft flew a similar pattern, but did not stop at Tenerife. These flights are expected to have encountered lightning NO_x in the southern part of the flight. Figure 2.5 depicts the potential vorticity map at 250 hPa with the Falcon flight pattern. It reveals a complex system with an elongated upper level trough south of Ireland and another one in the Southwest. The Falcon's southbound leg was at high levels, while the northbound one took place lower in the troposphere, below the flight corridor. The trajectories indicate that the air had a wide variety of origins from the subtropical Atlantic and the United States. The exposure plots in Figure 2.6 reveal dominant aircraft contributions in the northern part of the flight pattern with a distinct decrease in the southern part. Lightning exposure is detected in the southern part and originated from the subtropical Atlantic, consistent with the trajectory analysis. There is no significant exposure to convection over land.

2.5.4 Transatlantic Flight: October 15, 1997

At October 15, 1997, the SONEX DC8 made a transatlantic crossing from Bangor to Shannon and sampled air with a wide variety of origins, as can be seen from Figure 2.7. In the first part of the flight over the East Coast of the United States, the DC8 encountered air that had been exposed to both lightning, convection over land,

Figure 2.4: The estimated exposure to aircraft, lightning, and convection of air in the North Atlantic flight corridor on October 18.
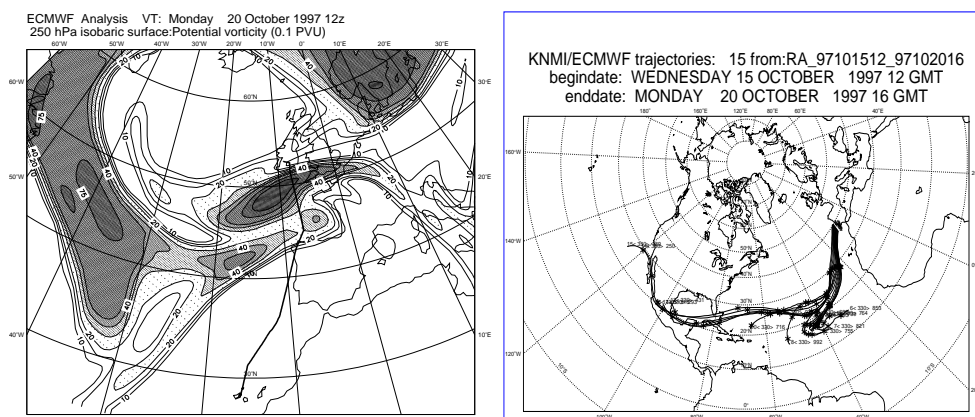
Figure 2.5: The ECMWF analysis of potential vorticity (0.1 PVU) on October 20 at 250 hPa with the flight pattern and 5-day backward trajectories ending above the Shannon area.
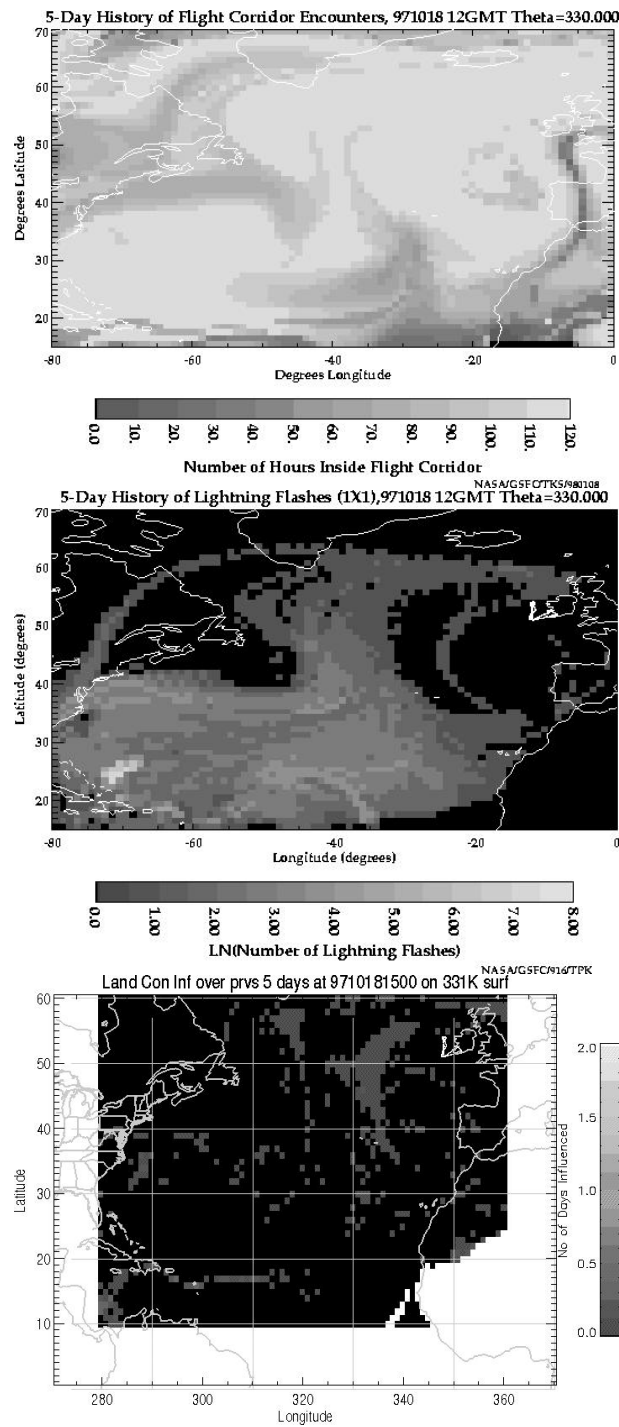
and aircraft emissions. Over the Atlantic Ocean the air was relatively clean with no influence by convection or lightning. The exposure to aircraft emissions remained large, but decreases considerably halfway the flight and increased again in the region of Shannon. This case seems to be atypical in the sense that exposure to aircraft seems to have been decreased in the North Atlantic flight corridor. Furthermore, this flight encountered a large classic tropopause fold.

2.6 Comparison of the Model Results with the Measurements

In this section the model results for NO and O_3 are compared with the measurements. The modelled values are linearly interpolated in space and time to the actual positions of the measurements. These figures contain, besides the total concentrations, the individual contributions of aircraft, lightning, and surface sources, as calculated by the model. The contribution from stratospheric sources is mainly as HNO_3 and only in negligible amounts of NO and is therefore not presented in these comparisons. The measurements are given as 1-min averages.

2.6.1 Results for NO

Figure 2.8 gives the model results for NO as a function of time, compared with the POLINAT measurements together with the flight levels for the stagnant anticyclone case (October 23, 1997). In this case, the measurements were taken at three distinct levels: the first within the main air traffic routes, followed by two subsequent levels below the corridor. The measurements clearly show the expected features: an accumulation of aircraft emissions, with large values of more than 0.1 ppbv in the first leg, dropping to about 0.05 ppbv in the second, and values smaller than 0.01 ppbv in the last leg. The model captures these features quite well. The model values are
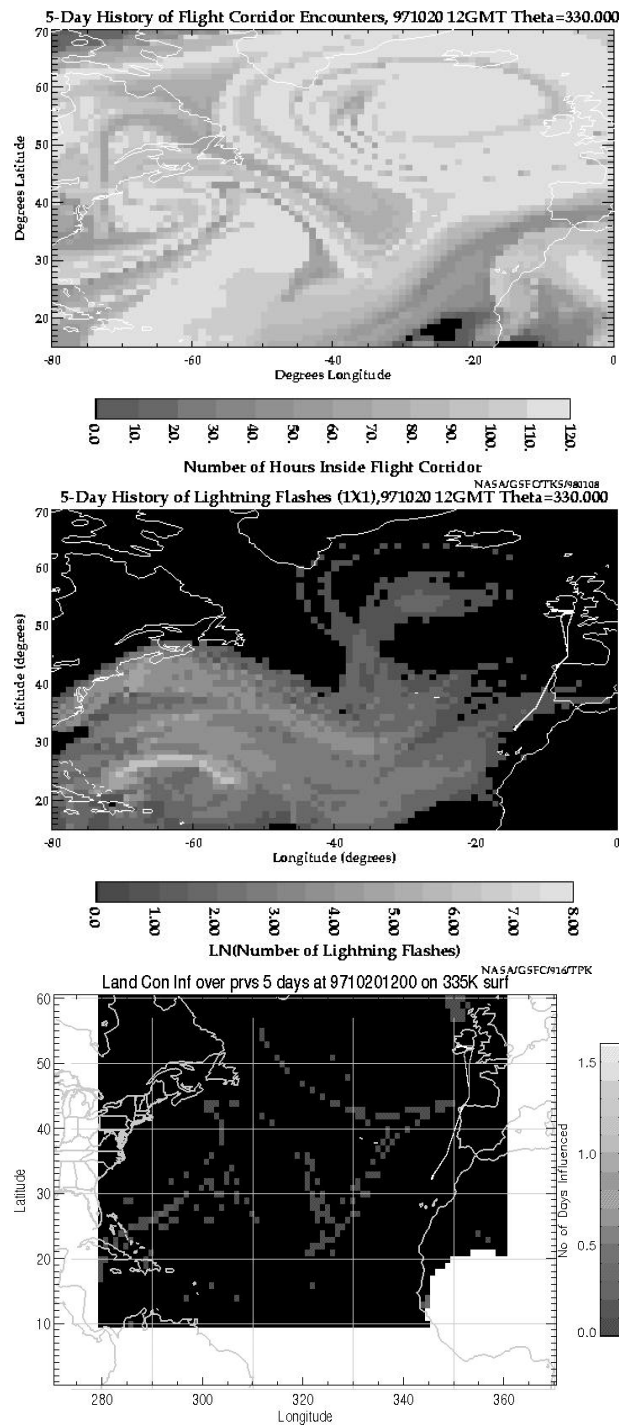
Figure 2.6: The estimated exposure to aircraft, lightning, and convection of air in the North Atlantic flight corridor on October 20.
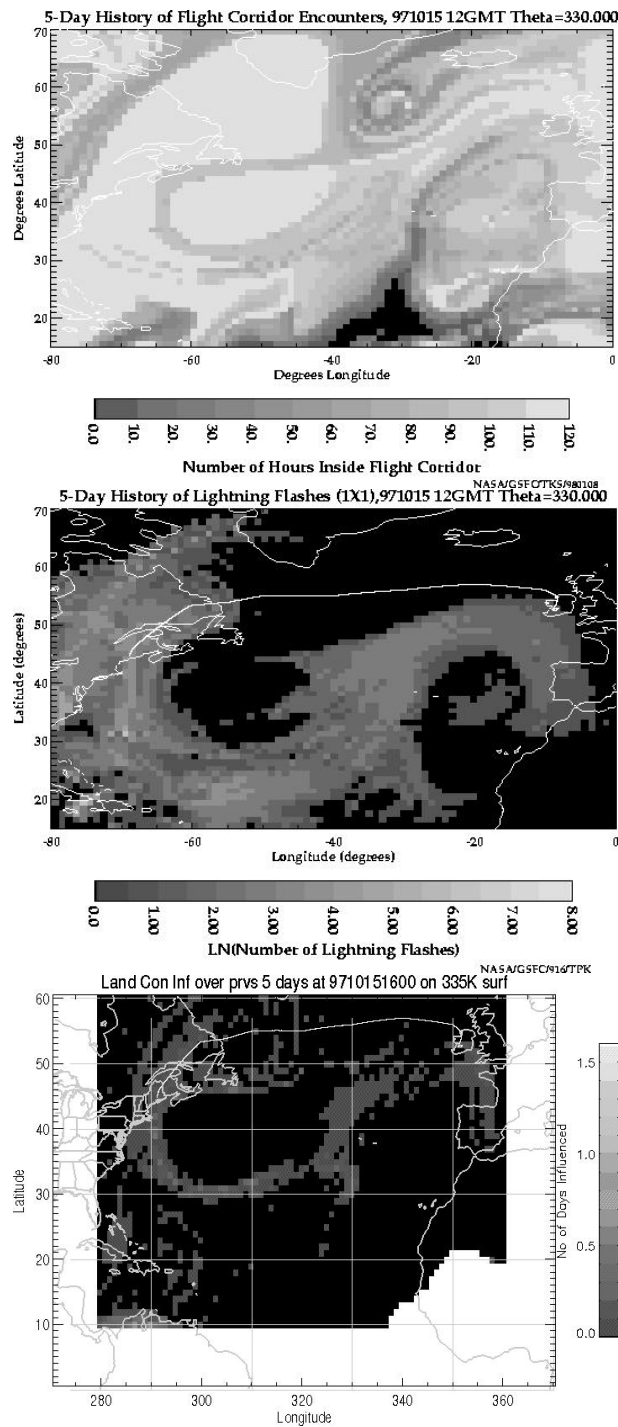
Figure 2.7: The estimated exposure to aircraft, lightning, and convection of air in the North Atlantic flight corridor on October 15.

POLINAT flight at 23–10–1997
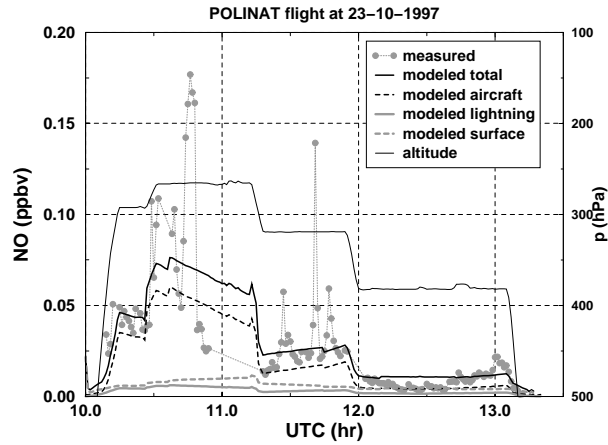
Figure 2.8: Time series of the measured NO concentrations and the total modelled concentrations with the contributions of aircraft, lightning, and surface sources for October 23. The flight level is also given and uses the right axis.

POLINAT flight at 18–10–1997
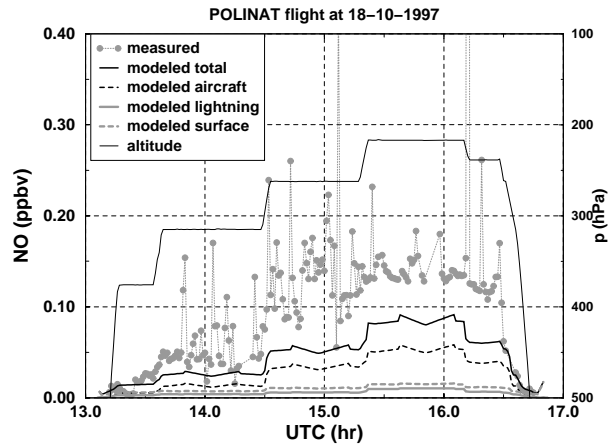
Figure 2.9: Time series of the measured NO concentrations and the total modelled concentrations with the contributions of aircraft, lightning and surface sources for October 18. The flight level is also given and uses the right axis.

obviously less spiky and decrease less steeply in the first leg, but the three distinct NO levels are recognisable. Also, the model results indicate that aircraft contributions dominate in the first leg with about 75% in the first two legs and have a much smaller contribution of about 40% in the last leg. The contributions of surface emissions and lightning are negligible.

Figure 2.9 gives the modelled total NO concentrations and the contributions of aircraft, lightning and the surface, compared with the POLINAT measurements for the almost cut-off low case (October 18, 1997). The flight levels are also depicted. The measurements show roughly three levels of NO concentrations, coinciding with

Figure 2.10: Time series of the measured NO concentrations and the total modelled concentrations with the contributions of aircraft, lightning, and surface sources for October 15. The flight level is also given and uses the right axis.

the different flight levels, although possible convection in the cut-off low may have smoothed the vertical gradients. The highest values were observed during the flight leg at 315 hPa. The modelled values also reflect the flight pattern of the Falcon, but the actual values are all smaller. The model underestimates the NO concentration somewhat in this case. The PV gradients in the filament, in which the measurements took place, are too strong to be represented by the model and cause a more diffused NO concentration field with smaller gradients. Aircraft emissions are the dominant contributor to the NO concentration throughout the flight, consistent with the exposure plots and the trajectory analysis.

Figure 2.10 shows the modelled NO concentrations and the SONEX measurements as function of longitude for the transatlantic flight on October 15, 1997. Only during the first part of the flight were relatively high values of over 0.1 ppbv measured, whereas during the remaining part of the flight background values of about 0.025 ppbv were measured. The very last part of the flight shows an increase of the NO concentration again. The model captures this profile of the NO concentration quite well. In the first part of the flight, aircraft emissions contribute about 50%, but also considerable amounts of NO are originating from lightning and surface emissions. In the remaining part of the flight, the NO concentration is almost entirely composed of surface emissions. This is mainly due to the flight altitude of the NASA DC-8, which was below the flight corridor to investigate the encountered tropopause fold. In the last part of the flight, aircraft contributions become larger again. The relatively high measured concentrations in the first part of the flight, and its subdivision among the various NO sources, are consistent with the exposure plots.

Figure 2.11 gives the modelled NO concentration as a function of latitude compared with the measurements and with the aircraft, lightning and surface contributions for the southward bound SONEX and POLINAT flights (October 20, 1997). The southward bound POLINAT flight started at a flight level within the flight cor-
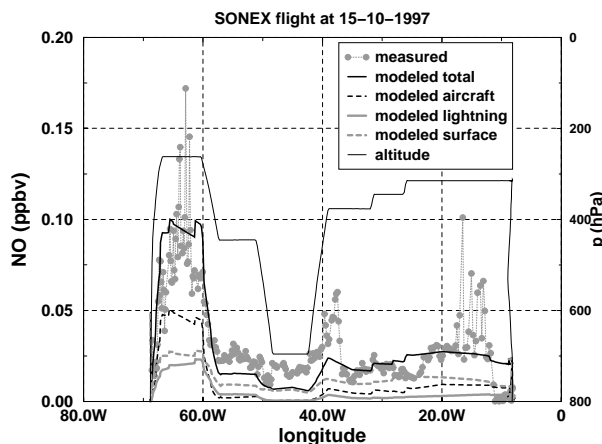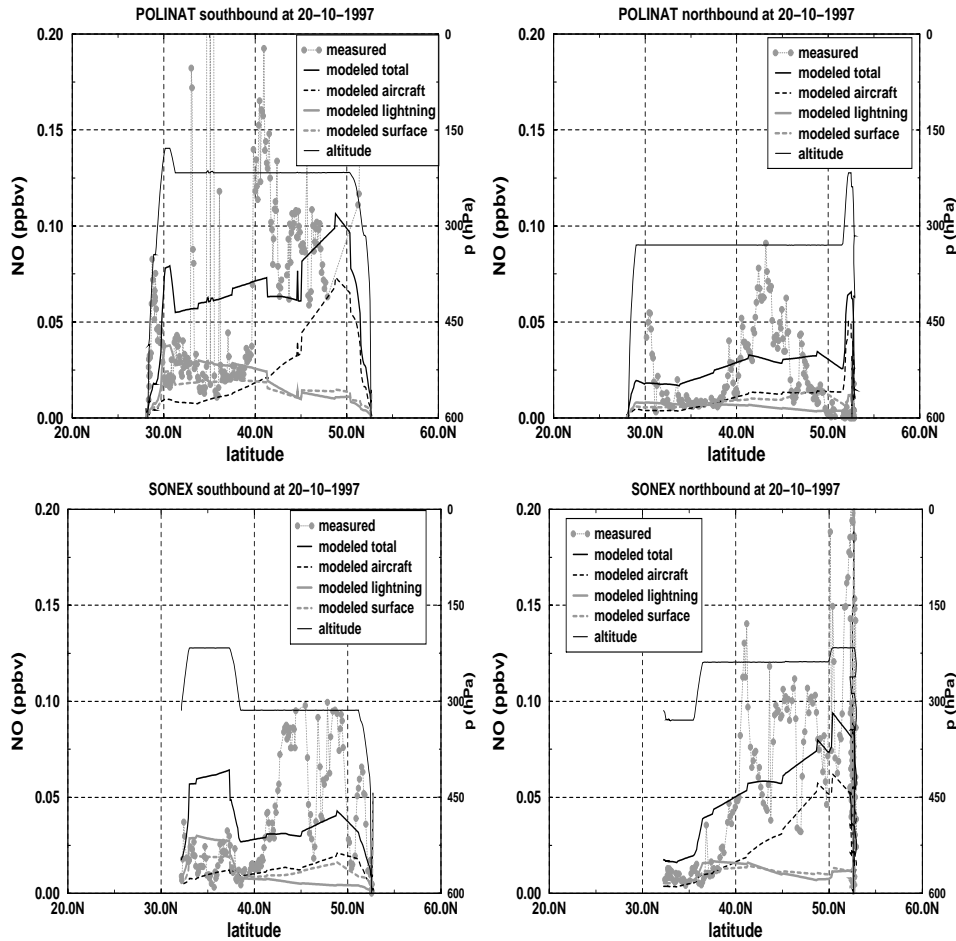
Figure 2.11: Time series of the measured NO concentrations and the total modelled concentrations with the contributions of aircraft, lightning, and surface sources for October 20. The flight level is also given and uses the right axis.

ridor and the SONEX flight at a lower level; the return flights were the other way around. The measurements during the southward bound flight of POLINAT show a distinct north-south gradient with a sudden drop in the NO concentration southward of 40°N. The NO spikes in the southern part of the flight are accidental encounters of the plume of the DC-8. Also, the measurements during the SONEX flight reveal a north-south gradient. The model results for POLINAT show a too smooth gradient that follows the measurements on an average. However, the relative contributions show a north-south gradient in the aircraft contribution and an opposite lightning contribution, which explains the smooth gradient in the total. The comparison with the SONEX measurements is worse. There is no gradient in the total concentration or in the aircraft contribution. The model also predicts a strong lightning contribution in the south, which leads to an overestimation of the NO concentration. However,

the modelled lightning contribution in the south is consistent with the analysis from the exposure plots. The measurements during the northward bound flight of SONEX gives the expected north-south gradient, which is followed by the model results, both in the total concentration and the aircraft contribution. There is still a small gradient in the lightning contribution visible. The measurements during the northward bound POLINAT flight do not reveal a distinct gradient; the model results follow the measurements on an average. Clear gradients in the model results are absent.

Figure 2.12 shows some other time series of NO. The POLINAT flight on September 21, 1997, took place from the Azores to Shannon. The entire flight was in the troposphere in a high. The majority of the flight took place in relatively clean air with NO concentrations below 0.025 ppbv. The measurements during the last part of the flight show a peak of NO that is captured by the model as a peak of aircraft emitted NO. The POLINAT flights of September 26 took place in a stagnant high over central Europe where again an accumulation of aircraft emissions is expected. The model results compare badly for the first flight and better for the second. The model results indicate the expected high aircraft contributions. The POLINAT flights on October 14, 1997, from Shannon to Tenerife and vice versa, is comparable to that of October 20, 1997 and reveal a weak north-south gradient with dominant aircraft contributions.

A comparison of all modelled and observed NO concentrations of the entire SONEX and POLINAT 1997 campaign is given in Figure 2.13. This scatterplot shows a reasonable agreement with a correlation coefficient of 0.66. Observed values higher than 0.3 ppbv are left out of the plot, but are included in the fit. The modelled values never exceeded 0.2 ppbv. The model does not capture the large variability of the observed data, probably due to its relatively coarse resolution.

2.6.2   Results for O_3

Figure 2.14 shows the modelled O_3 concentration compared with the measurements for different flights along with the potential vorticity and the contributions of surface emissions, aircraft emissions, and lightning. The remaining part of the O_3 concentration originates from the stratosphere and is the largest source. Generally, the model results resemble the measurements, but sometimes the resolution of the model is too coarse to follow steep gradients in tropopause folds that were present during the transatlantic flight (October 15, 1997), the southward bound SONEX flight (October 20, 1997), and the POLINAT flight on September 26, 1997. In those cases the model results attain stratospheric values but are smaller than measured. Tropospheric values show better agreement, although in some cases the model gives too high values in the vicinity of the tropopause. This is clear in the stagnant anticyclone case of October 23, where the SONEX measurements at the highest flight altitude give low tropospheric values. In the almost cut-off low case on October 18, large horizontal PV gradients were observed. The model results compare reasonably with the measurements, although the stratospheric values are too low.

The contributions by aircraft emission, surface emissions, and lightning are small compared to the total O_3 concentrations, and clear accumulations cannot be distinguished from the measurements and the modelled total concentrations alone. The contribution of surface emissions is in general the largest, followed by lightning. Even
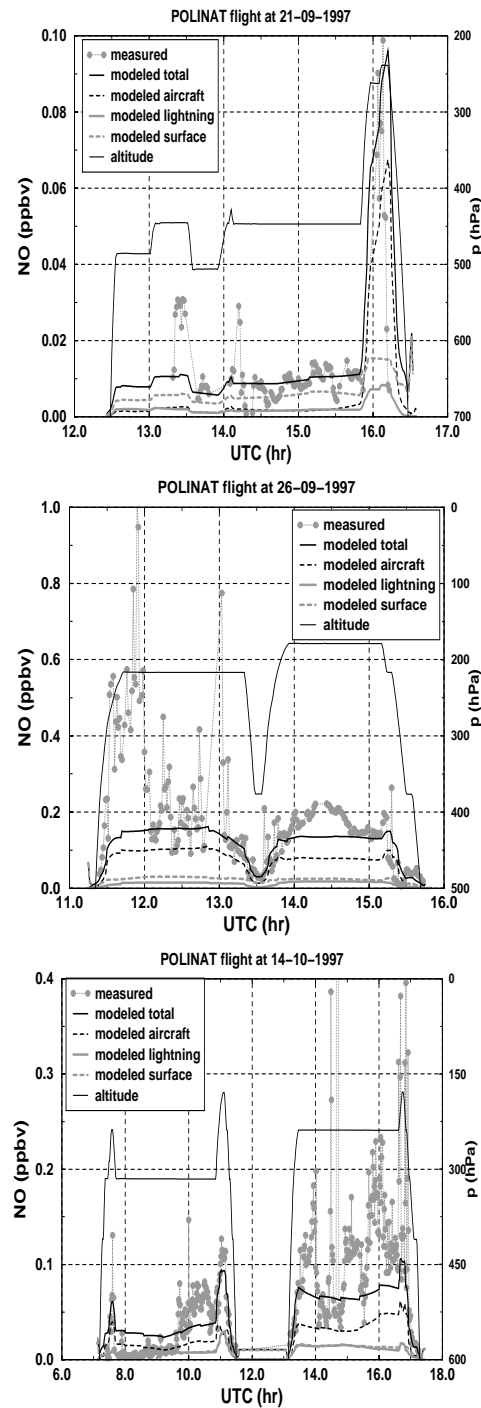
Figure 2.12: Time series of the measured NO concentrations and the total modelled concentrations with the contributions of aircraft, lightning, and surface sources for the POLINAT flights on September 21, September 26, and October 14.
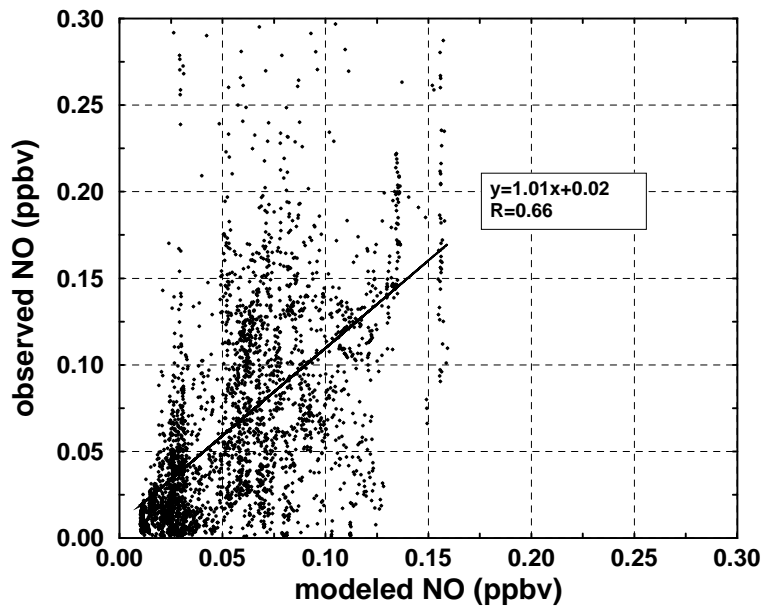
Figure 2.13: Scatterplot of modelled NO concentrations versus all NO measurements during the SONEX and POLINAT 1997 campaigns. The straight line is a linear regression.

in the cases with NO accumulations due to aircraft emissions (September 26, October 18, and October 23), the impact of aircraft emissions on the O$_3$ concentration remains small and is less than the contributions of the other two source categories.

A comparison of all modelled and observed O$_3$ concentrations of the entire SONEX and POLINAT 1997 campaign is given in Figure 2.15. This scatterplot shows a reasonable agreement with a correlation coefficient of 0.67. Most observed values higher than 150 ppbv indicate tropopause folds, which are not reproduced by the model. For this reason, a linear regression was made for values below 150 ppbv, which gave a correlation coefficient of 0.64.

2.7 Modelled NO$_x$ and O$_3$ Concentration Fields

Figures 2.16, 2.17, 2.18, and 2.19 depict the calculated NO$_x$ concentration fields with the contributions by surface emissions, aircraft, and lightning at 250 hPa at noon for the four selected cases. In the cases of the stagnant anticyclone (October 23, 1997) and the almost cut-off low (October 18, 1997) the accumulation of NO$_x$ in the two systems is clearly visible. The model also predicts the expected large contribution of aircraft emissions. Lightning and surface contributions are very small in the flight

Figure 2.14: Time series of the measured O_3 concentrations and the total modelled concentrations with the contributions of aircraft, lightning, and surface sources for different flights.
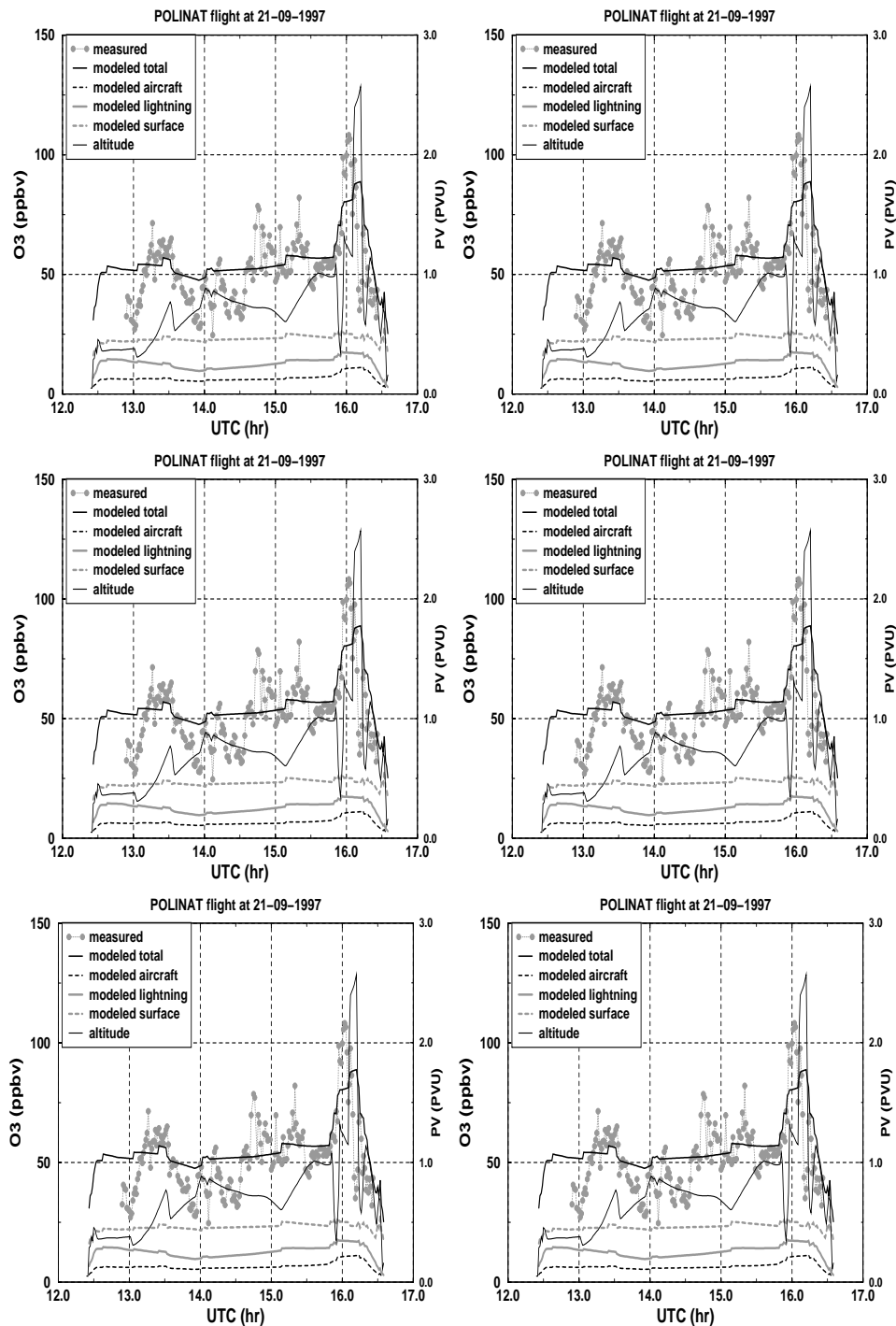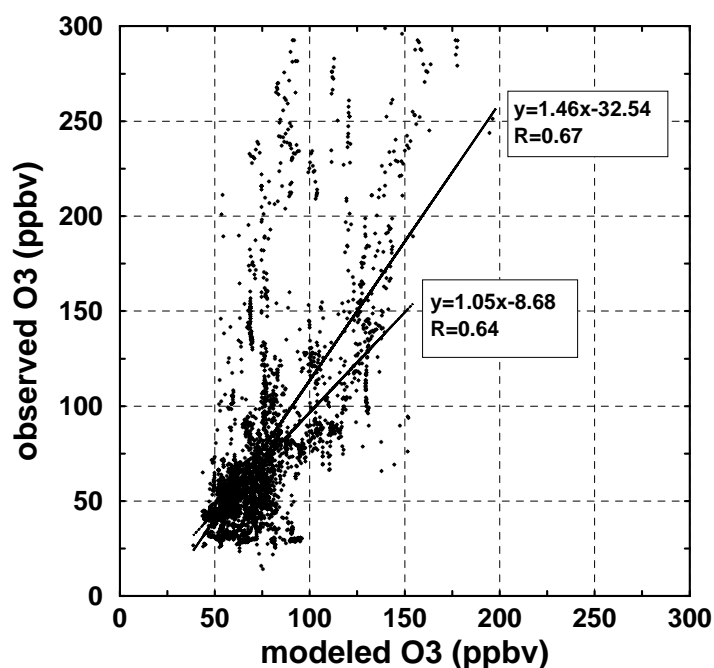
Figure 2.15: Scatterplot of modelled O$_3$ concentrations versus all O$_3$ measurements during the SONEX and POLINAT 1997 campaigns. The straight lines are linear regressions. The steepest line includes all data points, whereas the other line includes only values below 150 ppbv.

corridor for these cases. In the case of the southward bound flights on October 20 the NO$_x$ concentration field is more complex. The contribution of lightning is somewhat higher in this case than in the previous two and has shifted more to the north. The NO$_x$ concentration field of the transatlantic flight (October 15, 1997) reveals the patterns as measured with relative high concentrations over the east coast of the United States and lower concentrations in the flight corridor. Over the eastern U.S. coast a large plume exists with substantial contributions from aircraft, lightning, and surface emissions.

Figure 2.20 shows the calculated mean NO$_x$ concentration of the North Atlantic flight corridor for October 1997. The 250 hPa layer contains the centre of the North Atlantic flight corridor and has maximum relative contribution of air traffic that contributes 40%-60% to the mean NO$_x$. Maximum values of NO$_x$ coincide with a maximum contributions of aircraft of 60%. Lightning contributes 10%-20% to the mean NO$_x$ concentration and surface sources contribute 30%.

The north-south gradient of the NO$_x$ concentration determines the location of the North Atlantic flight corridor. Figure 2.21 shows this gradient along 8°W for the flights on October 18, 20, and 23, as calculated by TM3. In all cases the large peak
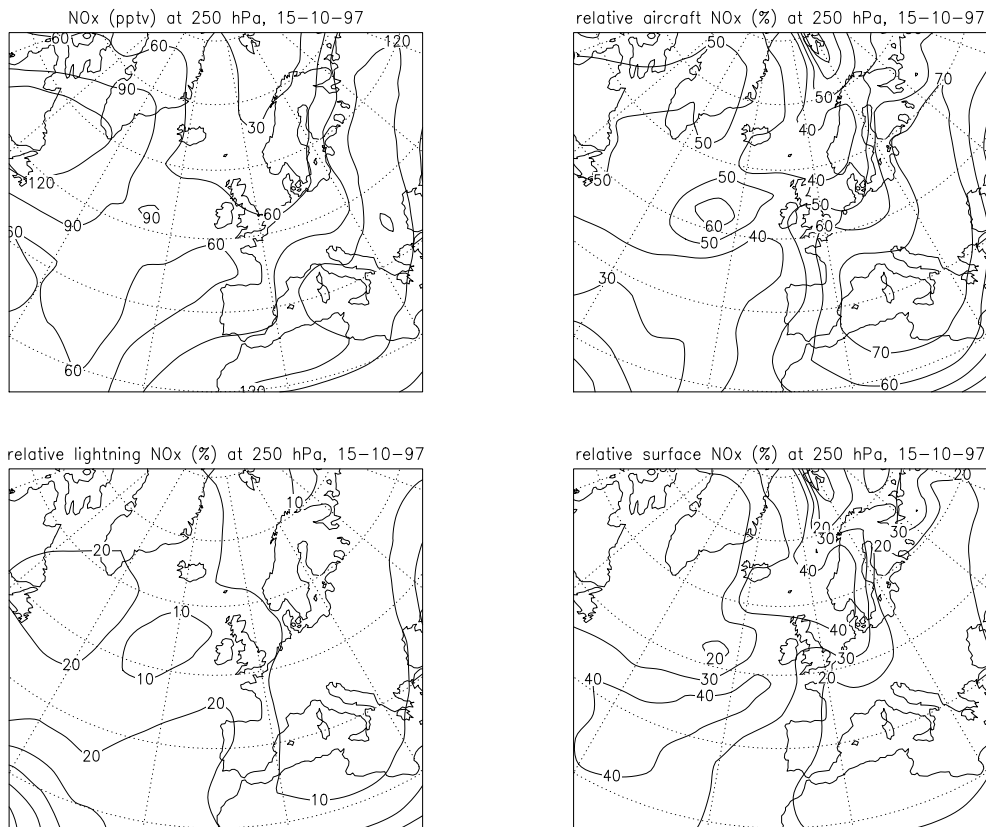
Figure 2.16: The calculated NO$_x$ (pptv) concentration field at 250 hPa on October 15 with the contributions of aircraft, lightning, and surface sources.

in the northern part of the plots consists mainly of aircraft emitted NO$_x$, whereas the peak in the tropics consists of lightning and surface contributions. The peaks on October 18 and 23 are located in the centres of the almost cut-off low and the stagnant high, respectively. The modelled gradient on 18 October is somewhat weaker since the accumulation of aircraft-emitted NO$_x$ occurred more in the south than normally. On October 20 the gradient is also weaker due to elevated lightning contributions in the south.

The comparison of the O$_3$ model results with the measurements already revealed convincingly that the calculated perturbations at flight altitudes by aircraft, lightning, or surface emissions cannot be distinguished. For this reason, Figure 2.22 shows the mean O$_3$ concentration field for the month of October 1997 instead of the actual concentration fields for the different cases. The contribution of air traffic to the O$_3$ concentration in the North Atlantic flight corridor is about 10%, whereas lighting and surface emissions are about 20%-30%, clearly exceeding the impact of air traffic. More to the South, lightning and surface contributions increase.

Table 2.3 gives the calculated relative contributions from aircraft, lightning, sur-

Figure 2.17: The calculated NO_x (pptv) concentration field at 250 hPa on October 18 with the contributions of aircraft, lightning, and surface sources.

face, and stratospheric sources to the monthly mean NO_x and O_3 concentrations for the months January, April, July, and October in the North Atlantic flight corridor. We added the results for the other months to show the seasonal cycle that appears in the results and to make comparison with other model results more convenient. The numbers result from calculating the mean concentrations for October in a box from 80°W-20°E and 40°N-70°N for three pressure layers (320 hPa, 250 hPa and, 190 hPa).

2.8 Discussion

The comparison of the model results with the measurements of O_3 and NO generally shows a reasonable agreement. However, the model does not resolve the large variability of the NO measurements and steep gradients of the O_3 concentration. Obviously, most of these discrepancies could be resolved by enhancing the resolution, but the current resolution is sufficient to analyse most of the SONEX and POLINAT flights, when combined with meteorological analysis.

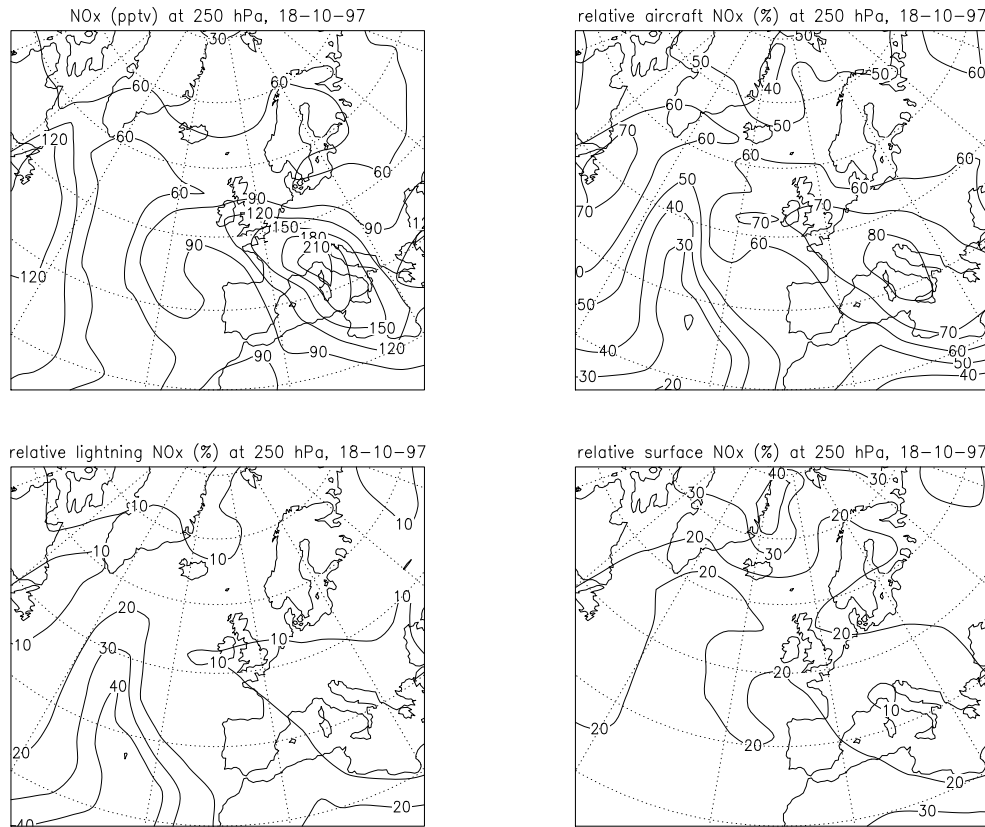The calculated impact of aircraft emissions on the NO concentration agrees well

Figure 2.18: The calculated NO$_x$ (pptv) concentration field at 250 hPa on October 20 with the contributions of aircraft, lightning, and surface sources.

with the conclusions that can be drawn from the exposure plots and the trajectory analyses. Since the meteorological input for the exposure plots and the trajectories plots are from different sources, the agreement between these products gives additional confidence in the analysis. Expected significant contributions from surface sources and lightning were occasionally found and were also consistent with the features on the exposure plots, but there were no cases were these sources were dominant. Events of fast upward transport can create large plumes with NO concentrations larger than 1 ppbv in the free troposphere [*Brunner et al.*, 1998]. Occasionally, these high NO concentrations were observed during some SONEX flights, but in this study modelled NO concentrations in the free troposphere never exceeded 0.2 ppbv. According to *Peters et al.* [1995], horizontal grid resolutions of 0.5° x 0.5° are required for an adequate modelling of these perturbations, so fast vertical transport of NO cannot be resolved by the model at its current resolution. The use of a chemical scheme with only methane oxidation is generally sufficient to describe free-tropospheric chemistry, but not for boundary layer chemistry or the chemistry during events of fast upward transport. The role of other nitrogen species, such as PAN, remains an open question.

NOx (pptv) at 250 hPa, 23-10-97

relative aircraft NOx (%) at 250 hPa, 23-10-97

relative lightning NOx (%) at 250 hPa, 23-10-97
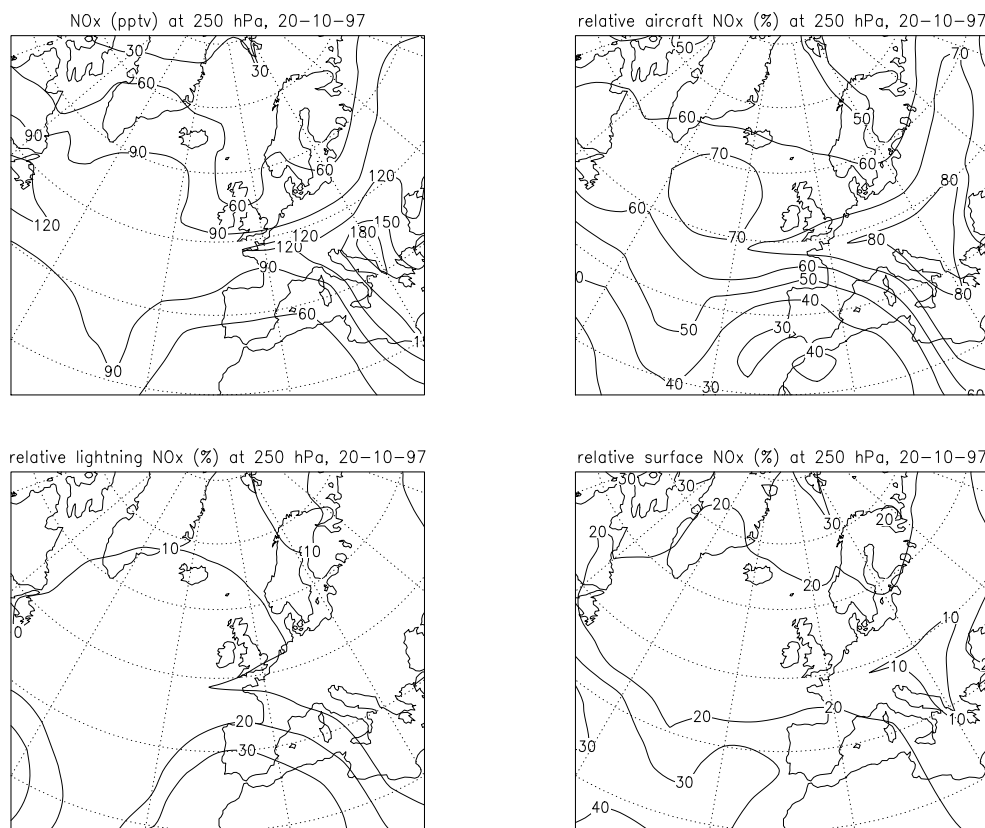
relative surface NOx (%) at 250 hPa, 23-10-97
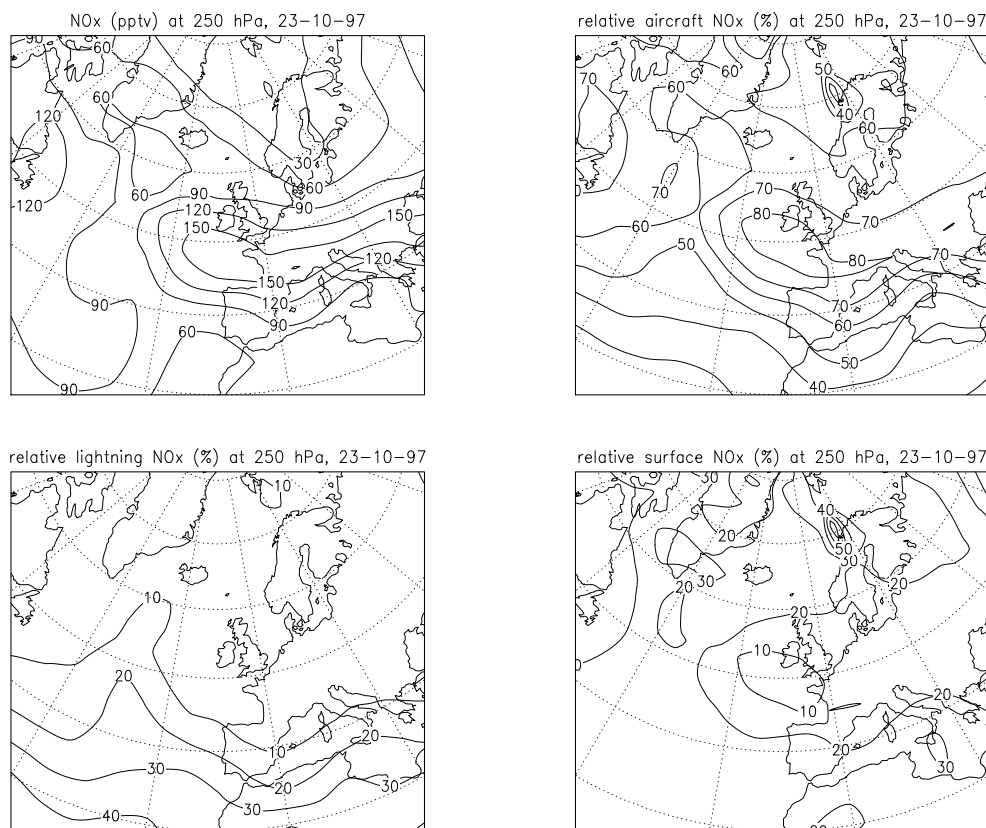
Figure 2.19: The calculated NO_x (pptv) concentration field at 250 hPa on October 23 with the contributions of aircraft, lightning, and surface sources.

We expect that the inclusion of a more detailed chemistry would result in higher surface NO contributions, since surface NO_x will easily be converted to other nitrogen species that can be converted back to NO_x after transport to the free troposphere. The impact of lightning is not sufficiently validated with the POLINAT and SONEX measurements, but our participation in the European lightning project EULINOX will provide us with useful data in the near future.

Previously, *Wauben et al.* [1997], calculated the impact of aircraft for January and July and compared the results with POLINAT 1 measurements. They found similar results. *Köhler et al.* [1997] used a general circulation method with simplified, linear chemistry and made rough qualitative comparisons on a climatological basis with measurements from STRATOZ III, POLINAT 1 and AASE II. They also made source attributions for January and July. We found similar results, although they found lower aircraft contributions and higher surface contributions for July. *Ehhalt et al.* [1992] compared results of STRATOZ III with results of a 2-D model with parameterised dynamics and concluded that the NO_x concentration was dominated by surface emissions and that 30% originates from aircraft. Our results for July give

Figure 2.20: The mean calculated NO$_x$ (pptv) concentration field at 250 hPa for October with the contributions of aircraft, lightning, and surface sources.

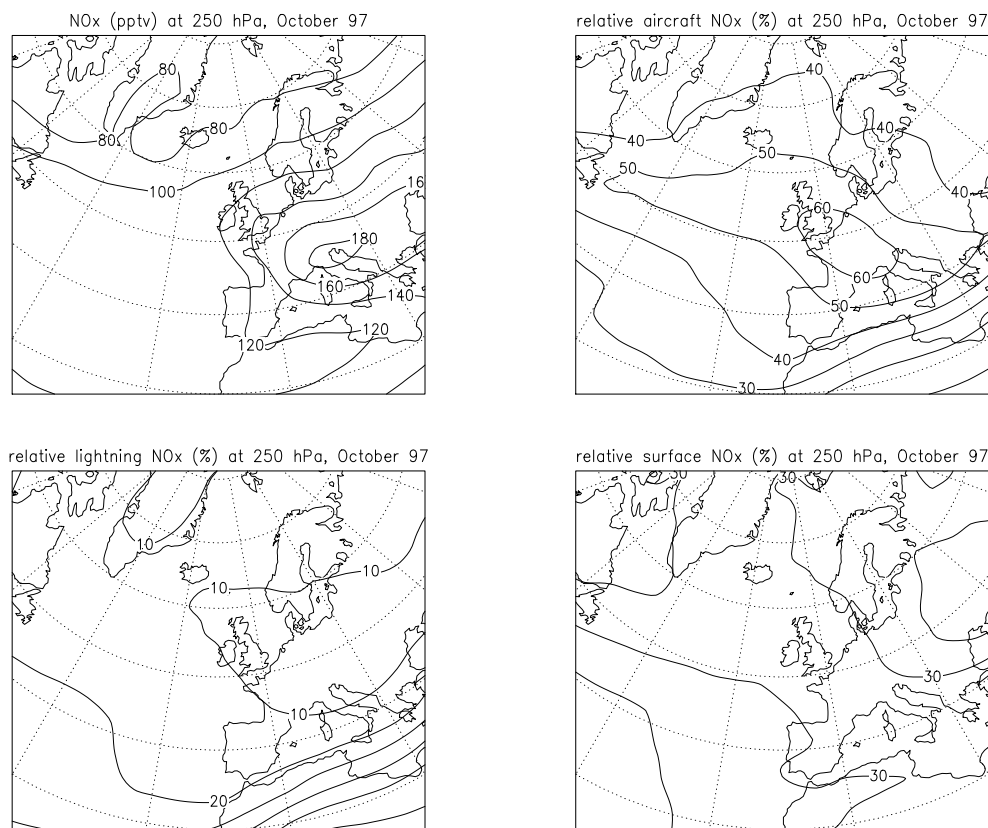**Table 2.3:** Calculated relative contributions to the total amounts of NO$_x$ and O$_3$ in the flight corridor for the months January, April, July, and October

	NO$_x$				O$_3$			
	Jan.	Apr.	Jul.	Oct.	Jan.	Apr.	Jul.	Oct.
Aircraft	68	50	36	48	5	6	9	10
Surface	27	29	35	27	16	16	27	30
Lightning	4	6	16	14	10	5	15	20
Stratosphere	1	15	13	11	69	73	49	40

Contributions are in percent.

slightly higher aircraft contributions of 36% and slightly lower surface contributions of 35%.

The calculated impact on the O$_3$ concentration is for all source categories small with respect to the total concentration and the natural variability that is observable from the measurements, so these calculated perturbations could not be validated with
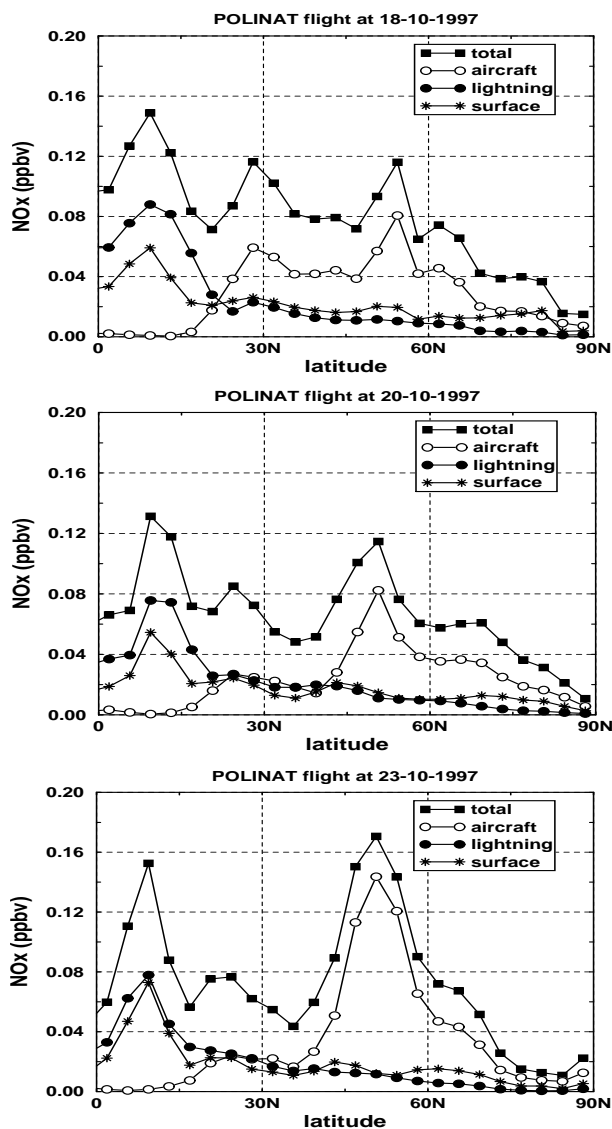
Figure 2.21: The calculated NO_x (pptv) concentration at 250 hPa as a function along $8°W$ of latitude with the contributions of aircraft, lightning, and surface sources for the flights on October 18, 20, and 23.

the measurements. The impact of the surface emissions is likely to be underestimated in this study, since the model chemistry lacks the oxidation of higher hydrocarbons that is needed for a proper description of O_3 production in the boundary layer. Also, the model probably underestimates upward transport somewhat.

The applied labelling technique in the model was essential to interpret the measurements. Especially, the impact of surface emissions is difficult to achieve without

O3 (ppbv) at 250 hPa, October 1997

relative aircraft O3 (%) at 250 hPa, October 1997

relative lightning O3 (%) at 250 hPa, October 1997

relative surface O3 (%) at 250 hPa, October 1997
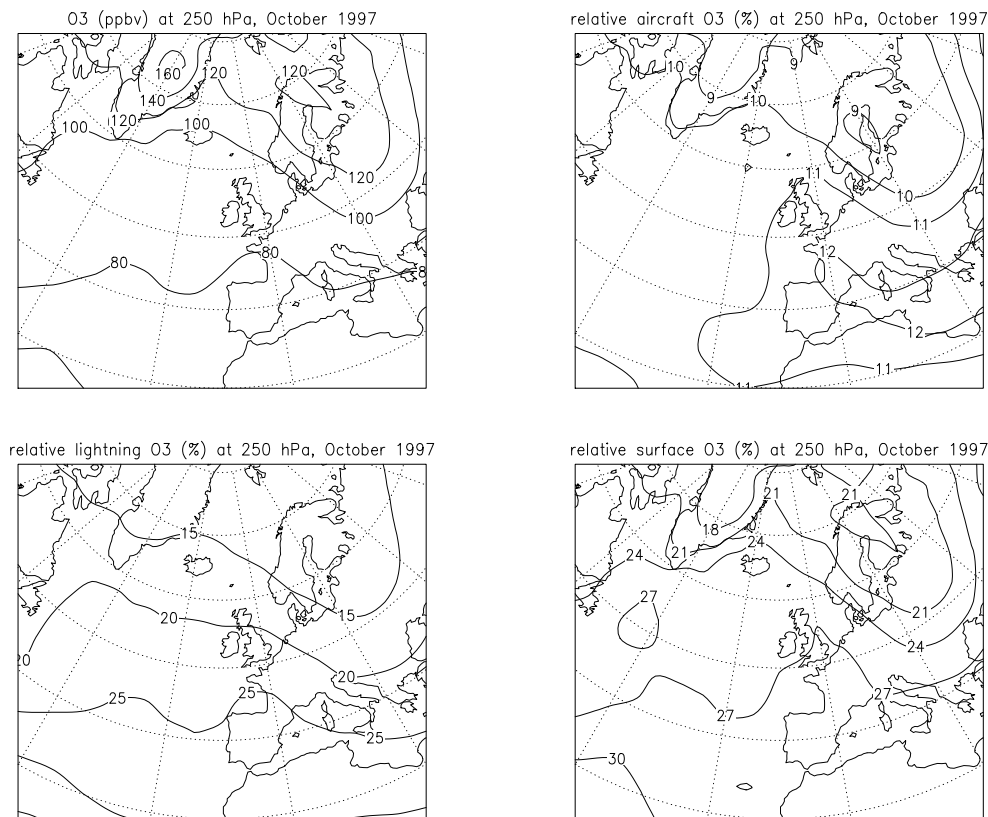
Figure 2.22: The mean calculated O$_3$ (ppbv) concentration field at 250 hPa for October with the contributions of aircraft, lightning, and surface sources.

this technique, since this very large source cannot be left out of the model without causing non-linear changes to the contributions by other sources. Taking out a source to calculate its impact on the O$_3$ concentration will change the net O$_3$ production rates and will give different results, due to the nonlinearity of the chemistry. The labelling technique calculates the impact of all sources separately, given the current O$_3$ production rates that are a result of all sources combined. The sum of the calculated perturbations is equivalent to the total perturbation. It is therefore a more consistent way to evaluate the contributions of the different sources.

2.9   Conclusions

We have investigated the impact of air traffic, lightning, and surface emissions on the composition of the atmosphere at flight altitudes with the global chemistry transport model TM3 with O$_3$, NO$_x$, and HNO$_3$ partitioned into species per source category and have compared the model results to the measurements of the POLINAT 2 and SONEX campaigns. By selecting the anticyclone and the almost cut-off low case, we

investigated two cases with expected dominant aircraft contributions. The difference of the composition of the atmosphere in and outside the North Atlantic flight corridor was investigated with the transatlantic flight and southward bound flight.

1. The NO and O_3 concentrations compares reasonably well with the measurements, although O_3 is generally a bit underestimated in the stratosphere, and the large variability of NO measurements is not reproduced by the model. The observed versus modelled NO and O_3 have correlation coefficients of 0.66 and 0.67. The agreement is, however, sufficient to describe the impact of aircraft emissions in the selected cases in this study.

2. Model calculations for October 1997 indicate that air traffic emissions in the North Atlantic flight corridor contribute about 50% to the NO_x concentration and 10% to the O_3 concentration and are clearly the dominant source of NO_x.

3. There is ample evidence that the impact of air traffic on the NO concentration at cruise altitudes can be detected. Measurements find elevated NO concentrations due to aircraft at the expected locations and are consistent with the model results and the exposure plots. The impact on the O_3 concentration did not appear to be detectable. The model reveals a distinct north-south gradient in the NO_x concentration for all the cases and is supported by the measurements during the southward bound flights, but the model gradient is generally less steep.

4. Model calculations for October 1997 indicate that surface sources and lightning emissions give minor contributions of 15%-25% to the NO_x concentration. Although the contributions of surface sources and lightning to the NO_x concentrations are small, the corresponding ozone perturbations are quite significant. Lightning contributes 20% to the O_3 concentration in the corridor region, and surface emissions contribute 30%, and are more important than aircraft emissions in this respect. The descriptions of these sources by the model were not validated sufficiently, due to the lack of cases where these sources were dominant. Hence these numbers should be regarded as tentative estimates. It is clearly important to direct further research into lightning NO_x and upward transport of boundary layer air.

The applied labelling technique in this study proved to be a powerful tool to investigate the impact of different source categories and how to interpret the measurements. The large impact of surface emissions on the O_3 concentration in the flight corridor, which is an important finding, could not be calculated without this method. Furthermore, the results of the labelling technique were consistent with the findings in the measurements and the expected effects, based on the meteorological situations.

3

Improvement and evaluation of the parameterisation of nitrogen oxide production by lightning

abstract

In order to describe the production of nitrogen oxides (NO_x) by lightning in chemistry-transport models the spatial and temporal distribution of this NO_x source needs to be specified. Various meteorological model parameters can be used as a proxy for specifying this distribution. In order to determine the most suitable parameter as a proxy for lightning, we have correlated different meteorological quantities from the ECMWF model, such as convective precipitation and cloud top height, with ground-based lightning observations made during the EULINOX project. Convective precipitation gave the best correlation for summer conditions over Europe. Using the established relationship between convective precipitation and lightning intensity, we have tested different vertical distributions of the NO_x lightning source in the global chemistry-transport model TM3. The model simulated NO fields have been compared with the NO observations made during the 1998 EULINOX and the 1997 POLINAT/SONEX campaigns. We found that a prescribed lightning NO_x profile gave the best agreement with the observations. The observations covered various conditions: typical background situations, inside thunderstorms, and the outflow of thunderstorms of various ages. The model underestimated the NO concentrations in cases of fresh lightning NO_x, likely due to its insufficient spatial and temporal resolution, but under most other circumstances the new parameterisation performed reasonably well, and is a clear improvement over the previously used parameterisation based on cloud top heights.

3.1 Introduction

Ozone is an important greenhouse gas with maximum radiative forcing in the tropopause region [*Lacis et al.*, 1990]. Since increased concentrations of nitrogen oxides (NO_x =

NO + NO$_2$) at those altitudes photochemically enhance ozone production, the possible climate effects of anthropogenic NO$_x$ emissions are the topic of many research studies. Special interest exists in the effects of subsonic aviation [e.g. *Schumann*, 1995; *Brasseur et al.*, 1998], because aircraft directly inject NO$_x$ in the tropopause region and because subsonic aviation grows at a rate of 5-6% per year [IATA, 1995]. Other sources of NO$_x$ in the tropopause region are various surface sources that are transported upwards by convection, downward transport from the stratosphere, and production by lightning.

Production by lightning is the worst quantified atmospheric NO$_x$ source, which implies a major constraint on the quality of global chemistry-transport models. Although the production of NO$_x$ by lightning contributes to the natural composition of the atmosphere, a good description of this source is crucial for studying possible climate effects by human activities. Studies on the impact of aircraft NO$_x$ emissions are especially sensitive to the chosen total annual lightning NO$_x$ production [*Brasseur et al.*, 1996; *Berntsen and Isaksen*, 1999]. In a previous study, NO and O$_3$ observations from the POLINAT 2 (Pollution from Aircraft Emissions in the North Atlantic flight corridor) and SONEX (Subsonic Assessment Ozone and Nitrogen Oxide Experiment) 1997 campaigns were compared with results of the three-dimensional chemistry transport model TM3 [*Meijer et al.*, 2000]. This study indicated that the TM3 model fails to reproduce lightning influenced situations.

During the field campaign of the EULINOX (European Lightning Nitrogen Oxides) project [*Höller and Schumann*, 2000], an LPATS (Lightning Position and Tracking System) network [*Bent and Lyon*, 1984] and airborne measurements of NO provided an opportunity to test and improve the model with respect to the parameterisation of lightning. Various meteorological fields from the European Centre for Medium Range Weather Forecasts (ECMWF) were correlated with data from the LPATS network to find a model parameter that can be used to describe the horizontal and temporal distribution and the intensity of lightning. We defined two new lightning parameterisations with different vertical distributions of NO$_x$ from lightning. Both parameterisations are based on a linear relationship between lightning and convective precipitation. The in situ measurements of NO from this campaign, as well as selected cases from POLINAT 2 and SONEX, were used to validate the new and original lightning parameterisations.

3.2   Correlation of ECMWF fields with LPATS lightning observations

The EULINOX field campaign took place in the summer of 1998 and consisted of ground-based measurements of lightning and airborne sampling of trace gases in and around thunderstorms over central Europe. During the EULINOX campaign LPATS data were collected in the period June 22 - August 31, 1998. These data (gridded at a 0.5°×0.5° resolution for the area between 0°-20°E, 45°-55°N and accumulated over 6-hr time intervals) were correlated with ECMWF parameters (at the same resolution) to find model parameters that could be used as a proxy to specify the horizontal distribution of lightning and the intensity of lightning.

Lightning activity occurs in deep convective clouds with a net negative charge in

Figure 3.1: The gridded LPATS data for July 21, 1998, 18-24 UTC, together with the accumulated convective precipitation (mm) and the cloud top heights (km) and the total cloud ice content (g/m2).

the lower part of the cloud and a net positive charge in the upper part [e.g. *Williams*, 1985]. Although the details of cloud electrification are still not fully understood, ice particles, supercooled droplets, and graupel are generally believed to play a major role in the process of charge separation. In this study we analysed the correlation of LPATS data with various ECMWF model parameters: convective precipitation, cloud top heights, and the total cloud ice content. We chose convective precipitation because of its direct link to convection, cloud top heights because these are already linked to lightning according to *Price and Rind* [1992], and the total cloud ice content, which is representative for the total ice particle and graupel content. Unfortunately, the graupel content and maximum updraft velocities are not available. Cloud top heights are calculated from the 3-d cloud cover. Since the ECMWF cloud parameters do not distinguish between different types of clouds, it was assumed that all clouds with a base below the 700 hPa level and thicker than 5 km are convective.

Figure 3.1 shows an example of the gridded LPATS data for the severe thunderstorm of July 21, 1998, together with the ECWMF parameters: convective precipita-
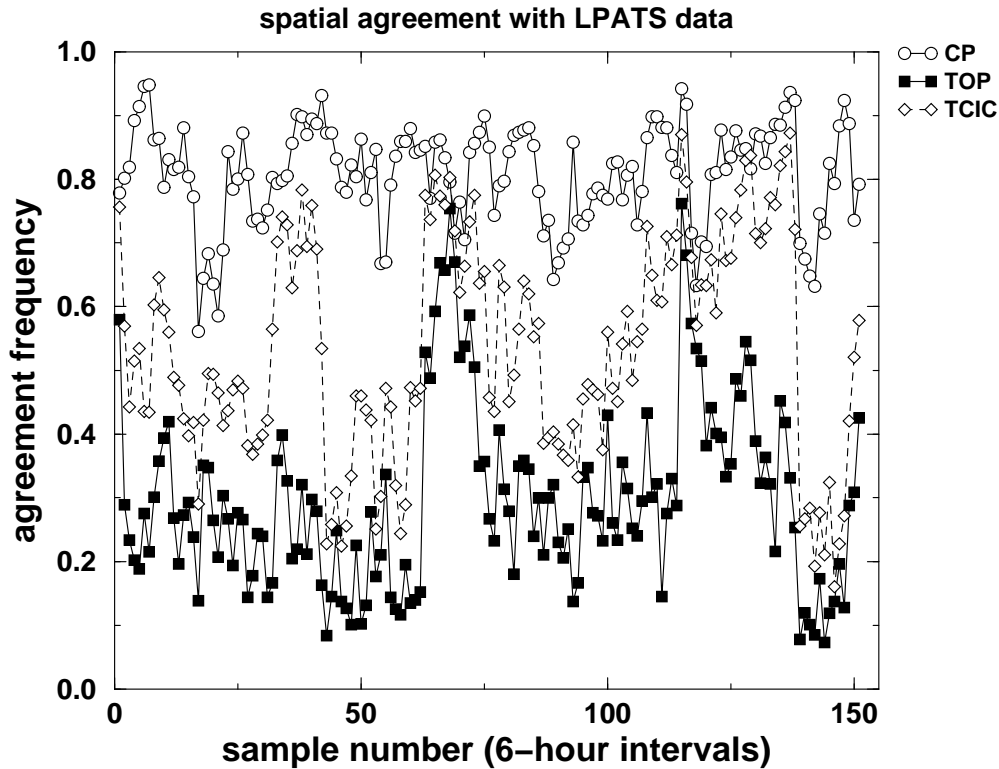
Figure 3.2: The match frequencies of the gridded LPATS data with convective precipitation (CP), cloud top heights (TOP) and total cloud ice content (TCIC).

tion, cloud top height, and total cloud ice content. It is clear that the distributions of all three ECMWF parameters show resemblance with the LPATS data, but that notable differences exist, both in positioning and intensity. Such differences were found to vary from day to day and complicated a quantitative analysis.

In order to quantify the spatial and temporal agreement between the ECMWF parameters and the LPATS data, we adopted a method from *Price and Rind* [1992]: a 1 was assigned for non-zero values and a 0 otherwise. If both the LPATS observation and the ECMWF parameter show either 1 or 0, then they are in spatial agreement. Only days with significant lightning activity (lightning in more than 5% of the grid boxes) were considered. The match frequency is simply the number of boxes in which two parameters are in spatial agreement, divided by the total number of boxes. Figure 3.2 shows the match frequency per 6-hour time interval. All distributions of the meteorological fields deviate significantly from a random distribution. Convective precipitation has the best spatial agreement with an average match frequency of 0.81 +/- 0.08, whereas cloud top heights and the total cloud ice water content have much worse agreement (0.30 +/- 0.14 and 0.54 +/- 0.17). Hence convective precipitation is the better proxy for specifying the horizontal lightning distribution for central Europe under summer conditions.
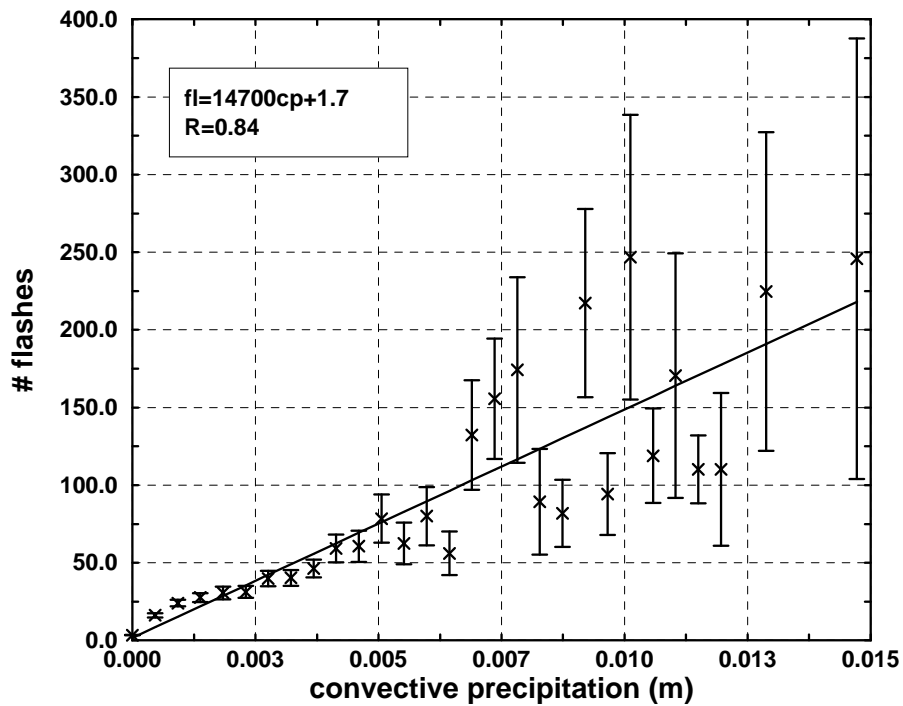
Figure 3.3: The mean number of flashes from the LPATS data as a function of convective precipitation for the entire period. The straight line is a regression with a correlation of 0.84.

Since accumulated convective precipitation has the best horizontal agreement with the flash observations, we derived a relation between lightning intensity and this parameter. This was done by subdividing the range of values of convective precipitation in 50 bins and calculating the mean and standard deviation of all flashes corresponding to each bin. If for a certain bin the number of flash occurrences was too low (< 5) the result for this bin was rejected. This resulted in the rejection of less than 1% of the data. Figure 3.3 gives the result of this analysis. The regression line for convective precipitation has a correlation of 0.84. Hence an average linear relationship of this parameter with lightning is plausible.

3.3 NO$_x$ production by lightning

The original lightning parameterisation in TM3 was according to *Price and Rind* [1992], using convective cloud top heights (defined as the tops of the convective mass fluxes) with a global NO$_x$ production of 5 Tg(N)yr^{-1}. The vertical distribution was based on scaling to the subgrid mass fluxes and air density.
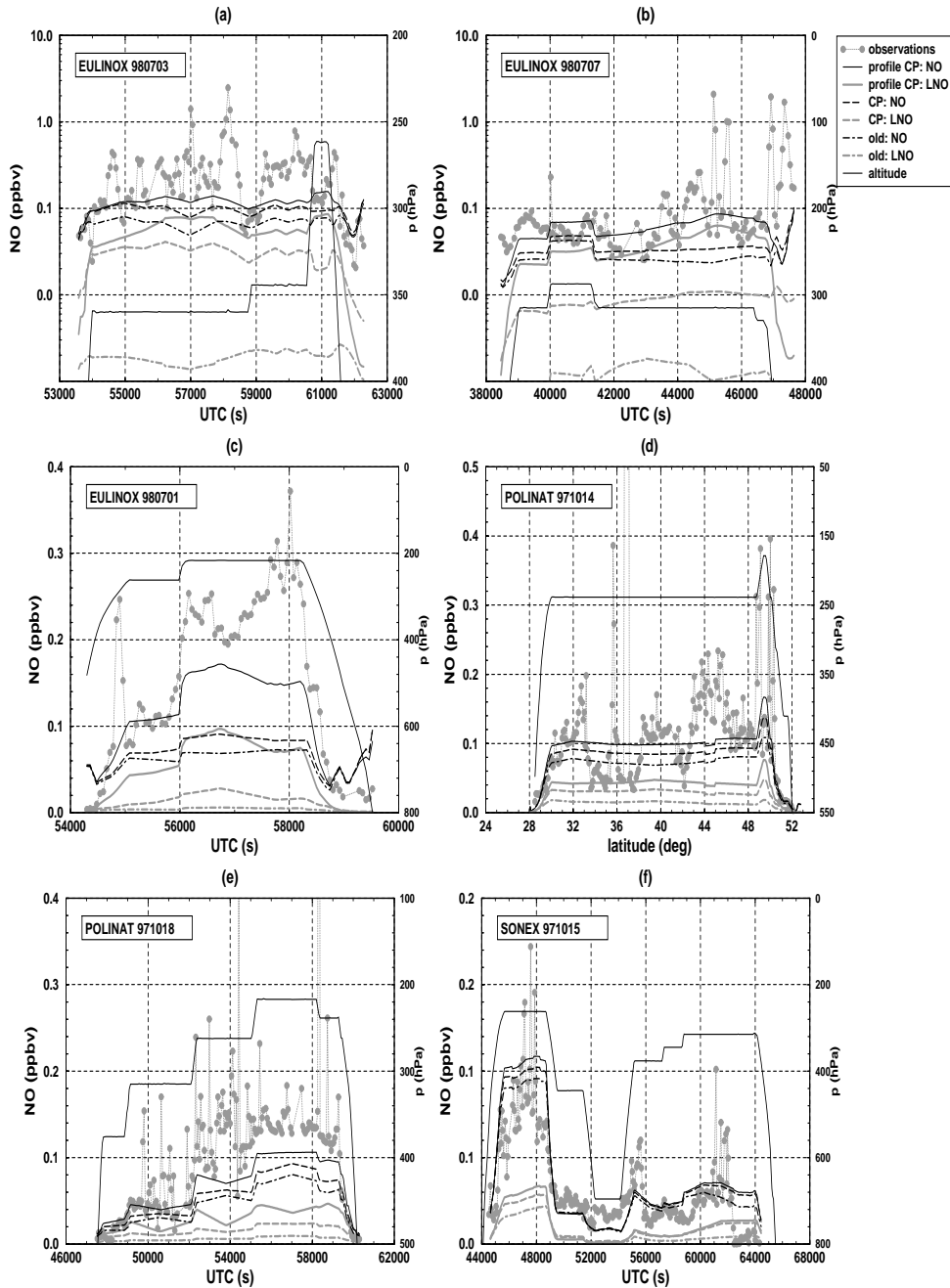
Figure 3.4: Time series of the observed NO concentrations and modelled NO concentrations (NO) with the lightning contributions (LNO) from different lightning parameterisations for the different flights. The flight level is also given, indicated along the right axis. In the legend "orig" denotes the original parameterisation, "CP" the one based on convective precipitation, and "profile" the parameterisation that uses convective precipitation with prescribed NO profiles.
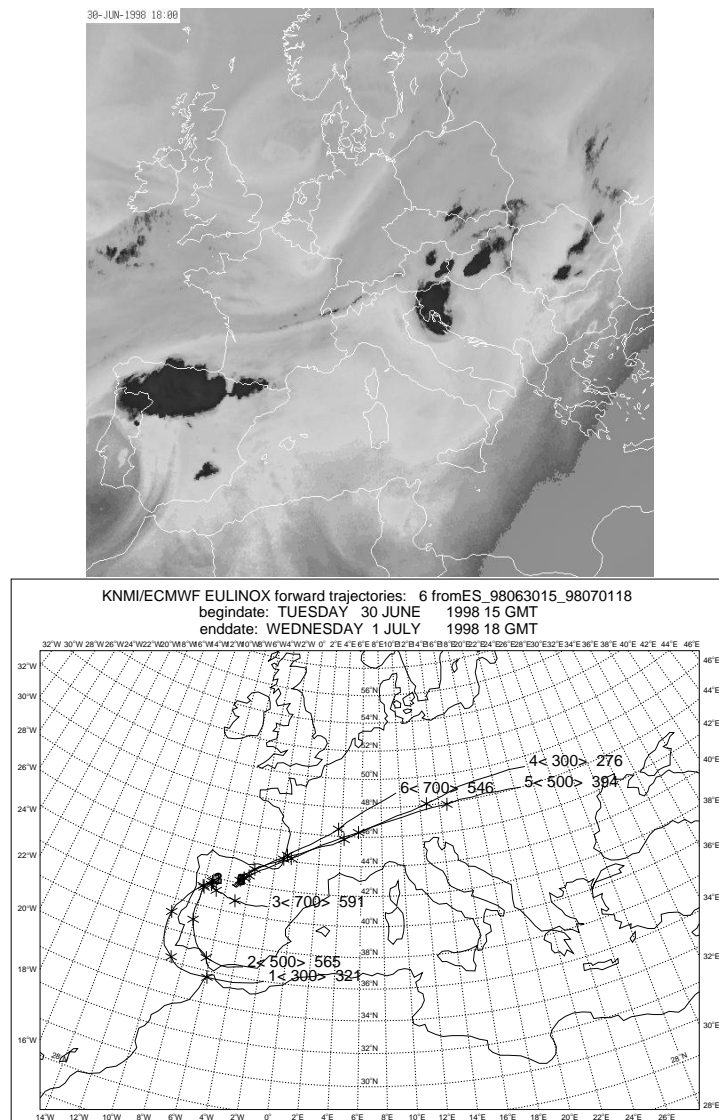
Figure 3.5: The meteorological situation over Spain on June 30, 1998. The left panel shows the Meteosat water vapour channel. The deep dark shades indicate very moist air, often indicative of thunderstorms. The right panel shows the forward trajectories from the moist region.

Our new lightning parameterisation is based on the found linear relation between convective precipitation and lightning intensity. However, the above analysis does not allow deriving the proper vertical distribution of the NO$_x$ production. Furthermore, the analysis only applies to summer conditions over central Europe and does not provide sufficient data to derive a number for the global annual NO$_x$ production from lightning. Therefore, the global source strength is scaled to 5 Tg(N) yr^{-1}, which is

in the range of 2-10 Tg(N)yr^{-1}, as previous reported in several studies [e.g. *Levy and Moxim*, 1996; *Wang et al.*, 1998]. The vertical distribution was defined in two different ways. In the first we follow *Price et al.* [1997]. They assume that NO is produced during the return stroke of a cloud-to-ground (CG) flash and the leader stage of an intra-cloud (IC) flash. The amount of produced NO is related to the energy of a flash, namely 10^{16} molecules NO/J. The average cloud-to-ground return stroke releases 6.7x10^9 J, an intra-cloud flash releases 6.7x10^8 J. The fraction of flashes that are CG can be related to the thickness of the cloud above the freezing level, using a 4th order polynomial fit. The NO produced by CG flashes is distributed from the -15°C level to the surface and the NO from IC flashes from the -15°C level to the cloud top. The clouds in TM3 are defined by the ECWMF 3-d cloud cover. A second vertical distribution is obtained by using prescribed NO profiles that were constructed by *Pickering et al.* [1998], based on 2-D cloud model calculations. These profiles were scaled to the cloud top heights in TM3.

3.4 Comparison of model results with NO observations

The new lightning parameterisations, as well as the original parameterisation were applied in the three-dimensional global chemistry transport model TM3, described in *Meijer et al.* [2000]. The model results were compared with NO observations from the EULINOX campaign 1998, and from the POLINAT 2 and SONEX campaigns that were conducted in October-November 1997 in the vicinity of the North-Atlantic flight corridor (NAFC) [*Schumann et al.*, 2000; *Singh et al.*, 1999; *Thompson et al.*, 2000]. Modelled values were linearly interpolated in space and time to the positions of the 1-minute averaged observations.

Two thunderstorm cases are presented here, namely from July 3 and July 7, 1998. On July 3 the Falcon aircraft penetrated a thunderstorm embedded in a large convective system near Switzerland and NO peaks up to 8 ppbv were measured. On July 7, 1998, the Falcon sampled a band of thunderstorms extending from southern France towards the Alps and two isolated storms over Austria. Figures 3.4a and 3.4b show the observed NO concentrations together with the model results for the different lightning parameterisations. In both cases all model results underestimate the observed lightning peaks, most likely due to the model's coarse spatial and temporal resolution. However, it is interesting to see that in both cases the new parameterisations give substantial lightning contributions, whereas the original parameterisation gives virtually no lightning contribution. The parameterisation with prescribed NO profiles gives the best agreement with the observations.

Since it cannot be expected that a global model reproduces the small-scale peak values occurring in thunderstorm, it is more useful to study cases that have been affected by already dissipated thunderstorms, where the air with enhanced NO$_x$ concentrations from lightning has been dispersed over large areas. One interesting case is July 1, 1998, when the Falcon sampled the outflow of a thunderstorm over Spain from the previous day. The flight took place over southern and western Germany and Switzerland in the absence of thunderstorm activity. Figure 3.5 depicts the meteorological situation on the previous day (June 30, 1998): the Meteosat water vapour

channel reveals a region with very moist air in the north of Spain, corresponding to a thunderstorm complex. Some forward trajectories that started in the thunderstorm area between 300 and 700 hPa, reached the EULINOX sampling area in southern Germany after one day, suggesting that the outflow of this storm has indeed been sampled on July 1, 1998. Figure 3.4c shows the observed NO concentrations with the model results for the different lightning parameterisations. Again the model results for the original TM3 lightning parameterisation have virtually no contributions from lightning to the NO concentrations. The new parameterisation with a vertical profile according to *Price et al.* [1997] produced little NO from lightning. Only the result from the parameterisation with prescribed NO profiles gives a substantial lightning contribution and agrees well with the observations during the first part of the flight, although it still underestimates the highest values acquired during the last part of the flight. Another outflow case is from the POLINAT flight on October 14, 1997 from Tenerife to Shannon, Ireland. Trajectory analysis showed that the sampled air is a mixture of air that had been affected by air traffic in the North Atlantic flight corridor and lightning activity over the Caribbean 3 days earlier [*Schlager et al.*, 1999]. Figure 3.4d shows the NO observations of this flight with the different model results as a function of latitude. All model results show a significant lightning contribution, but the one with prescribed NO profiles gives again the best agreement with a lightning contribution of about 45%. The aircraft contribution, not shown here, was about 35%.

Finally, it is interesting to see how the new parameterisations affect model calculations of situations that have not recently been influenced by lightning. Figure 3.4e shows NO observations with model results of the POLINAT flight on October 18, 1997, in a cut-off low east of Ireland. Trajectory analysis showed that only air traffic had affected the sampled air [*Meijer et al.*, 2000]. Again the new parameterisation with prescribed NO profiles improved the model results, indicating that the calculation of the composition of background air also improves with this new parameterisation. This is furthermore illustrated by comparing the model results of the different parameterisations with the NO observations of the SONEX transatlantic flight of October 15, 1997, in Figure 3.4f. The beginning of the flight over the US east coast has been influenced by lightning, but the remainder of the flight took place in background air. The new parameterisation gives a somewhat higher lightning contribution during the first and last part of the flights, but in this case all parameterisations produce similar results.

Figure 3.6 shows the observed and modelled average NO concentrations with their standard deviations for all flights. Only model results for the new parameterisation with prescribed NO profiles and for the original parameterisation have been included. Averages have been calculated for parts of the flights at (more or less) constant height. The new parameterisation gives a better overall agreement with the observations than the original. The average NO concentrations for the outflow cases (980701a-b, 971014 and 971015a) and the background cases (971018a-d, 971015b) are well reproduced by the new parameterisation. However, the observed averaged NO concentrations for the active thunderstorm cases (980703 and 980707) are still underestimated. The large standard deviations of the NO observations in those two flights confirm the fact that the NO distribution in the sampled air is too inhomogeneous to be reproduced by a large-scale model.
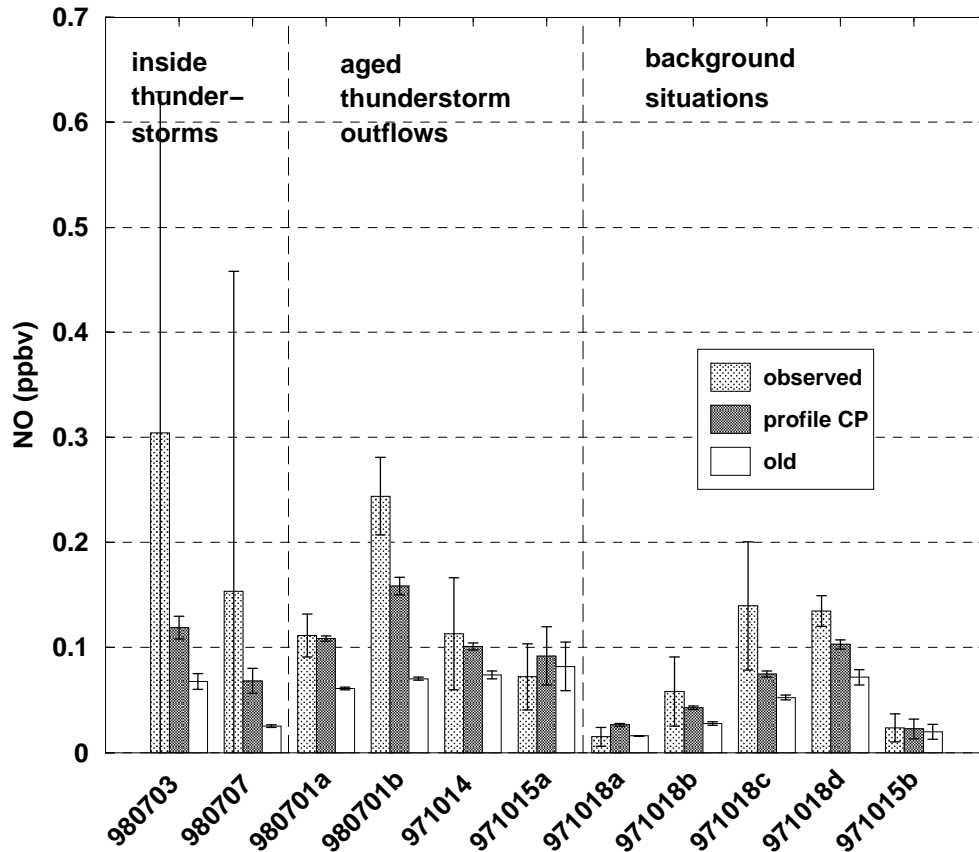
Figure 3.6: The observed and modelled (profile CP and orig) averaged NO concentrations with standard deviations for all flights. The averages have been taken over parts of the flights at constant altitude.

3.5 Discussion

In search for a suitable ECMWF model parameter to describe the horizontal and temporal distribution of lightning, we found high match frequencies between the distributions of the LPATS lightning observations and the ECMWF accumulated convective precipitation. The match frequencies of ECWMF cloud top heights and total ice cloud content with the lightning observations were much lower. The explanation for this is probably that these ECMWF parameters are instantaneous values and consequently sensitive to the sampling frequency. The time resolution of these parameters of 6 hours is clearly too low to properly resolve the short life-times periods of thunderstorm and lightning activity of typically a few hours. Convective precipitation is accumulated over 6 hours in the ECMWF archive and thus much less sensitive to the time sampling interval.

The LPATS lightning observations have been collected for a limited area and period, namely central Europe during summer 1998, so the established linear relation-

ship of convective precipitation with lightning remains to be proven for other regions and periods. However, *Brunner and Velthoven* [1999] have demonstrated the good correlation between ECMWF convective precipitation and lightning for the US continent and the global scale by using other data sets from the National Lightning Detection Network (NLDN) and Optical Transient Detector (OTD) satellite instrument. Furthermore, *Tapia et al.* [1998] found a linear relationship between observed convective precipitation and lightning intensity by analysing 22 thunderstorms over Florida in August 1992 and 1993. By comparing the model results with NO observations from SONEX and POLINAT 2, we demonstrated that the new lightning parameterisation successfully could be applied to other regions of the globe than central Europe only. However, for other important regions such as the tropics, the parameterisation still needs to be evaluated.

Since lightning occurs in the vicinity of thunderstorm updrafts, the majority of the produced NO is efficiently transported upward [*Pickering et al.*, 1998]. This explains why the parameterisation with prescribed NO profiles gives the best agreement, since the model only has grid box averaged updraft velocities, which underestimate the thunderstorm updrafts. The poor performance of the old parameterisation is mainly due to the input data. The cloud top heights in the old parameterisation were defined as the altitudes where the convective motions stop, and were calculated online as a part of the model's convection parameterisation. Although not shown in this study, the agreement with observations increased considerably when cloud top heights were derived from ECMWF 3-d cloud cover (with sufficient restrictions to distinguish between convective and large-scale clouds). So it cannot be concluded that the Price and Rind formulation in which lightning intensity is related to cloud top height, is wrong. However, this formulation is very sensitive to errors in the cloud top height due to the used 4.9-powerlaw relationship between cloud top height and lightning intensity. Furthermore, as demonstrated above, cloud top heights, available at a low time resolution, may be insufficient to simulate lightning activity, considering the intermittent character of thunderstorms.

We scaled the global annual NO_x production by lightning to 5 $Tg(N)yr^{-1}$, which is recommended by *Lee et al.* [1997], and is a commonly applied number in CTM studies. From the EULINOX campaign, Huntrieser et al. (submitted) estimate the annual global lightning source to be 3 $Tg(N)yr^{-1}$ [in *Höller and Schumann*, 2000]. Since this estimation does not include tropical lightning NO_x production, they regard 3 $Tg(N)yr^{-1}$ as a lower limit. Although the model generally underestimates the observed NO concentrations near in active and aged thunderstorms, we do not consider this is an indication that the global annual source should be larger than 5 $Tg(N)yr^{-1}$. Most probably this results from the low temporal and spatial resolution, which hampers the model to reproduce the observed peak concentrations.

3.6 Conclusions

Our comparison of ECMWF parameters with observed flashes by LPATS over the German area, has shown that accumulated convective precipitation is a good parameter to position lightning activity horizontally and in time. Furthermore, an approximate linear relationship between the convective precipitation and the number of lightning

flashes has been found. The lightning parameterisation based on the found linear relationship between lightning intensity and convective precipitation and with prescribed vertical profiles of the lightning produced NO gave the best agreement with observations from EULINOX, POLINAT 2, and SONEX. The new parameterisation gives good results for the background and thunderstorm outflow cases, however it underestimates the NO concentrations in active thunderstorms, which is most likely due to insufficient spatial and temporal model resolution.

4

A model for aircraft exhaust plumes and its application to a global model

abstract

An aircraft exhaust plume chemistry model has been developed, using the Gaussian dispersion plume model. The diffusion of the plume is anisotropic, due to vertical wind shear and stratification of the atmosphere. The model includes an extensive photochemical scheme to study the conversions of emitted NO_x to reservoir nitrogen species, such as HNO_3, and the net production of ozone in the aircraft exhaust plume. It was found that after 15 hours of plume evolution, the chemical state of the plume was in equilibrium with that of the ambient atmosphere. For typical summer conditions in the North Atlantic flight corridor with an emission at 0.00 hrs, $\sim$60% of the emitted NO_x was converted to other nitrogen species, mainly HNO_3 and HO_2NO_2. The net ozone production in the plume amounted to $\sim$ 8 molecules O_3 per emitted NO_x molecule. The amounts converted NO_x and produced O_3 strongly depend on the emission time, month, latitude, and altitude. The conversion numbers of NO_x and the amount of O_3 produced per emitted NO_x molecule were used to replace the engine exit emissions that are normally used in global chemistry models, with modified emissions of NO_x, other nitrogen species, and O_3. Subsequent model calculations indicated that the aircraft-induced NO_x perturbations decreased with 20-30% for January and 20-40% for July. The aircraft plume parameterisation caused for July an enhancement of the ozone perturbation locally in the flight corridor of maximal 8%. Outside the corridor the ozone perturbation decreased with 0-10%, depending on season. Finally, the sensitivity of the plume model to different parameters, such as the dispersion coefficients and the ambient concentrations, was investigated. The plume model appeared to be sensitive to the ambient NO_x and O_3 concentrations, but not to such an extent that the reported changes in the global perturbations would be altered significantly.

4.1   Introduction

Air traffic perturbs the atmosphere by emitting nitrogen oxides (NO_x = NO + NO_2), CO_2, CO, hydrocarbons, water vapour, soot, and sulphur particles. The aircraft emissions of NO_x enhance the ozone production in the tropopause region, where an

ozone perturbation has its largest effect on the radiative forcing [*Lacis et al.*, 1990]. Since transport by aircraft has an average annual growth rate of 5-6% [IATA, 1995], the possible climate effect due to the formation of ozone is an important research topic [i.e. IPCC, 1999]. Global three-dimensional chemistry transport models predict generally an aircraft-induced increase of 20%-70% of the NO_x concentration in the North Atlantic flight corridor, depending on season, with an associated increase in ozone of 2%-10% [e.g. *Schumann*, 1995].

However, global chemistry transport models still have rather coarse spatial resolutions, and are therefore unable to resolve the small-scale processes occurring in aircraft exhaust plumes. In global models the aircraft emissions are injected in large grid boxes, implying instantaneous mixing, which results in efficient ozone production and little formation of nitrogen reservoir species, like nitric acid, HNO_3. In reality such aircraft plumes exist for several hours up to an order of a day. They contain initially very high concentrations of NO_x, yielding a chemical state in which NO_x is efficiently converted into other nitrogen species, such as HNO_3, N_2O_5, HO_2NO_2, NO_3, and PAN. This enhanced formation of nitrogen species will diminish the potential of aircraft emissions to form ozone, once they are mixed with the background. Furthermore, net ozone production or destruction in aircraft exhaust plumes has an impact on the global scale. In an aircraft plume ozone will initially be depleted due to the high NO_x concentrations, but it will be produced in later stages as the plume disperses.

The chemical processes in aircraft plumes can be parameterised by using a plume model to calculate the conversions of nitrogen oxides in aircraft exhaust plumes for different latitudes, altitudes, and season [*Meijer et al.*, 1997]. The original aircraft emissions from the ANCAT inventory [*Gardner et al.*, 1997], which consists of NO_x emissions at the engine exits, were replaced emissions of various nitrogen species that were produced in the plume during 24 hours. This approach diminished the global model's prediction of the aircraft-induced NO_x perturbation with 15%-55% and the ozone perturbation with 15%-25%. *Kraabøl et al.* [2000a] have also addressed the parameterisation of aircraft exhaust plumes. They followed a similar approach and found results that agreed with ours.

After having reported the effects of aircraft plumes on the global scale, we now present the plume model in more detail. We will discuss the parameterisation of the plume processes in a global model. The needed integration time of the plume model for this parameterisation is investigated. Also the parameters that control the plume processes are investigated, as well as other parameters that may influence the plume processes. In this study we included the net ozone production in the plume parameterisation, since this was an important omission in previous studies. Finally we applied the parameterisation of the plume processes to a global model.

4.2 Description of the aircraft exhaust plume model

The model describes the time-evolution of an aircraft emission wake with a cross-section of the exhaust plume, perpendicular to the flight path. The model consists of chemistry in- and outside of the exhaust plume, diffusion of emitted species in the plume, and the expansion of the plume. The expansion causes the dilution of the

emitted species and the entrainment of ambient air.

4.2.1 Gaussian plume model

The expansion of the aircraft exhaust plume is described with the Gaussian plume model. The expansion of an aircraft exhaust plume can be divided into three regimes [*Schumann*, 1994]: the jet, the vortex, and the dispersion regimes. These regimes refer to the flow dynamics that control the structure and growth of the plume. In the jet regime, the plume consists of separate turbulent flows for each exhaust jet. At the end of the jet phase these flows merge and are entrained in the so-called roll-up vortex, which is caused by the airflow around the aircraft. This vortex regime persists for a while, until it becomes unstable and breaks up, after which the dispersion regime starts. In this third regime the mixing of the plume depends on the atmospheric conditions. Typical time intervals are 10 seconds for the jet regime, 2-3 minutes for the vortex regime and several hours up to a day for the dispersion regime. In the first two regimes the plume has a complex dynamical structure, which has been the topic of several studies [i.e. *Kärcher*, 1994; *Louisnard et al.*, 1995; *Kärcher et al.*, 1996]. These studies have shown that less than 2% of the emitted NO_x is converted to other nitrogen species. Therefore, the focus in this study is on the dispersion regime, which can adequately be described by the Gaussian plume dispersion model. Initial conditions for the dispersion will be taken from *Kärcher et al.* [1996].

At cruise altitudes the dispersion of the plume is asymmetric and anisotropic because the atmosphere is usually sheared and stratified. The dispersion is defined by a matrix of variances that follow the Gaussian distribution (σ_h for the horizontal, σ_v for the vertical variance, and σ_s the diagonal term of the matrix, accounting for the deformation and rotation of the plume by vertical wind shear). Analytical solutions for these variances are given by *Konopka* [1995].

$$\sigma_h^2 = \frac{2}{3}s^2 D_v t^3 + (2sD_s + s^2\sigma_{v,0}^2)t^2 + 2D_h t + \sigma_{h,0}^2 \tag{4.1}$$

$$\sigma_s^2 = sD_v t^2 + (s\sigma_{v,0}^2 + 2D_s)t \tag{4.2}$$

$$\sigma_v^2 = 2D_v t + \sigma_{v,0}^2 \tag{4.3}$$

In this equation D_h and D_v are the horizontal and vertical atmospheric diffusion coefficients and D_s is the 'skewed' diffusion coefficient ($D_s^2 < D_h D_v$). The Gaussian distribution variances at the beginning of the dispersions regime are $\sigma_{h,0}$ and $\sigma_{v,0}$. It is assumed here that $\sigma_{s,0} = 0$.

The wind shear s and the skewed diffusion coefficient D_s rotate and deform the cross-section of the plume, but the plume can still conveniently be described in terms of a major and a minor variance of the Gaussian distribution (σ_x and σ_y)

$$\sigma_x^2 = \frac{1}{2}(\sigma_h^2 + \sigma_v^2 + \sqrt{\Delta}) \tag{4.4}$$

$$\sigma_y^2 = \frac{1}{2}(\sigma_h^2 + \sigma_v^2 - \sqrt{\Delta}) \tag{4.5}$$

and

$$\Delta = (\sigma_h^2 - \sigma_s^2)^2 + 4\sigma_s^4 \tag{4.6}$$

The regimes before the dispersion regime are approximated by a single Gaussian plume, representing the (multiple) jet exhausts and vortices. The model starts at a plume age of $t=4$ s, which was the ending time of the model study of the chemical conversions during the jet regime by *Kärcher et al.* [1996]. The cross-section of the plume at $t=4$ s was 900 m^2, according to this study. We start the dispersion regime at $t = 200$ s. The plume variances increase linearly to $\sigma_h = 117$ m and $\sigma_v = 83$ m at $t=200$ s for a Boeing 747-400. These values are adopted from *Dürbeck and Gerz* [1995] and are in agreement with observations of [*Schumann et al.*, 1995b]. In reality, the vortex regime consists of a stable phase with only weak expansion of the plume, and a break-up phase, during which the transition of vortex to dispersion regime occurs. In our approach this distinction is not made, since little is known of this process. For application to other types of aircraft, it is assumed that the horizontal plume variance is proportional to the wingspan. The vertical plume variance is calculated, using the relation of *Hoshizake et al* [1975] for the maximum vertical displacement $h_s \sim \sigma_v$, at a given atmospheric stratification

$$h_s = \frac{8W}{\pi^3 \rho_{\text{air}} N B^2 v} \tag{4.7}$$

with W (kg) the mass of the aircraft, ρ_{air} (kgm^{-3}) the air-density, N (s^{-1}), the Brunt-Väisälä frequency, B (m) the wingspan of the aircraft, and v (ms^{-1}) the velocity. So, given the weight, wingspan, and velocity of the aircraft the initial plume variances can be calculated, relative to the values for the B747-400.

From NO_x and turbulence measurements, *Schumann et al.* [1995b] estimated a vertical diffusion coefficient of 0-0.6 m^2s^{-1} and a horizontal diffusion coefficient of 5-20 m^2s^{-1}. The atmosphere was stably stratified with bulk Richardson number $R_i > 10$ and the vertical wind shear was 0.002 s^{-1}. Results from large-eddy simulations of *Dürbeck and Gerz* [1995, 1996] were in agreement with these observations. They found for typical atmospheric conditions in the North Atlantic flight corridor (with $R_i > 1$) that wind shear had no influence on the horizontal and vertical diffusion coefficients. They found values in the range of $15\ m^2s^{-1} \le D_h \le 23\ m^2s^{-1}$ and $0.15\ m^2s^{-1} \le D_v \le 0.18\ m^2s^{-1}$. The skewed diffusion constant D_s was about $0.4(D_h D_v)^{1/2}$.

4.2.2 Chemistry

The model uses an extensive photochemical mechanism for the troposphere, containing 44 species and 103 reactions, and is adopted from *Strand and Hov* [1994] with only minor changes. The chemistry of nitrous acid (HONO) and the oxidation of sulphur dioxide (SO_2) were included. The chemical reactions with atomic oxygen ($O(^1D)$ and $O(^3P)$)) were made implicit. All gas-phase reaction coefficients are taken from *De More et al.* [1997]. The photolysis rates are calculated with the Tropospheric Ultraviolet-Visible (TUV v4.0) model of *Madronich* [1993], using an 8-stream discrete ordinates method. The calculations were done for a mid-latitude standard atmosphere with clear sky conditions, an ozone column of 325 DU, a ground albedo of 0.02, and a background aerosol concentration (optical thickness of 0.17). The plume model does not take into account rainout of species.

In the aircraft exhaust new particles are formed, that could intensify heterogeneous processes in the exhaust plume with respect to the ambient air. In this study

the heterogeneous formation of HNO_3 from N_2O_5 is considered. The reaction rate constant K_{het} (s^{-1}) of a heterogeneous reactions is calculated with the relationship

$$K_{het} = \frac{1}{4}\gamma \nu S \tag{4.8}$$

with γ the reaction probability or sticking coefficient, S (m^{-1}) the aerosol surface area density, and ν (ms^{-1}) the mean absolute molecular velocity of air particles. This implies that we need to specify the types of aerosol and their surface densities in the plume. Basically three aerosol types are generally present in aircraft plumes: volatile aerosols that most likely consist of H_2SO_4/H_2O droplets, soot particles, and ice particles. Soot and volatile particles are generally considered as identical types, since aircraft soot particles are coated with a layer of H_2SO_4/H_2O [*Kärcher*, 1997]. These two aerosol types will be referred to as sulphate aerosol hereafter. Below the threshold for contrail formation [e.g. *Appleman*, 1953] only sulphate aerosol is present, but when a contrail is formed, ice particles scavenge the sulphate aerosol [*Kärcher et al.*, 1996]. This more or less separates the occurrence of ice particles and sulphate aerosol. We only take into account the reaction on sulphate aerosol, since this type has the larger reaction probability. The reaction probability of N_2O_5 on sulphate aerosol is 0.1 in tropospheric conditions above 200 K, independent of the water content of the aerosols [*DeMore et al.*, 1997]. The reaction probability on ice is not well known, but it is much smaller. It is likely similar to that of the reaction of N_2O_5 on PSC type 2 particles, since these particles are coated with ice. This reaction on PSC-2 particles has a reaction probability of 0.03 [*DeMore et al.*, 1997]. The surface area density of sulphate aerosols for background conditions is set to 0.6×10^{-8} cm^{-1}, adopted from *Danilin et al.* [1994]. We take the sulphate aerosol surface area in the plume from a study of *Kärcher*, 1997] (Figure 5 therein). In that study analytical and numerical calculations of the surface densities were in agreement with measurements by *Fahey et al.* [1995]. At a plume age of 4 s the surface density was $\sim 2\times10^{-4}$ cm^{-1}. As the plume expands the surface density decreases due to dilution, coagulation, and scavenging by soot.

4.2.3 Emissions

The exhaust emissions are treated as concentrations c_{em} (cm^{-3}) in the initial plume cross-section A_{ini} of 900 m^2 (at $t = 4$ s), and depend on the emission indices EI ($g.kg^{-1}$), the speed of the aircraft v (ms^{-1}), and fuel use f (kg/s)

$$c_{em} = \frac{fN_a\text{EI}}{vM_wA_{ini}} \tag{4.9}$$

with M_w the molar weight of the emitted species and N_a Avogadro's number. Table 4.1 gives the emission data of a B747-400 with JT9D-7R4D engines at flight altitude with a speed of 250 m/s and a fuel use of 2.9 kg/s, according to *Schumann* [1994] and *Olivier* [1991].

The NO_x emission is distributed as 89.4% NO, 8,9% NO_2, 1.3% HNO_2, and 0.4% HNO_3. These numbers are based on the model study of *Kärcher et al.* [1996]. The emissions of the different hydrocarbons are based on estimated total emissions and

Table 4.1: Emissions from a B747-400 at cruising altitude with a speed of 250 ms^{-1} and a fuel use of 2.9 kg.s^{-1}

Species	EI (g.kg^{-1})	Emission(g.s^{-1})
CO_2	3150	9135
H_2O	1260	3654
NO_x (as NO2)	16 (7-20)	46.4
CO	1.5 (1.5-10)	4.35
Hydrocarbons	0.6 (0.2-3)	1.73
SO_2	1 (0.02-6)	2.88
soot	0.015 (0.001-0.030)	0.043

Table 4.2: Hydrocarbon fractions of the total emitted hydrocarbons per species per molecule

Hydrocarbon	Emitted fraction
CH_4	0.268248
C_2H_6	0.013750
C_2H_4	0.216896
C_3H_6	0.167908
n-C_4H_{10}	0.013497
HCHO	0.184800
CH_3CHO	0.086150
HCOCHO	0.017129
CH_3COCHO	0.009899
C_8H_{10}	0.021723
total	1.000000

the measured distribution of hydrocarbons [*Shareef et al.*, 1988]. The distribution profile of the hydrocarbon emissions is given in Table 4.2.

The emission data were compared to other data from the aircraft emission model FLEM of the Dutch Civil Aviation Department [*Pulles et al.*, 1995] for a B747-400, a B767-300, and an Airbus 310-200. The latter model gives somewhat lower emission indices. Both data sets are within the uncertainty range given by measurements from *Schumann et al.* [2000].

4.2.4 Numerical approach of the Gaussian plume model with concentric rings

The concentration distribution of the emitted species is Gaussian shaped in the aircraft exhaust, at least by approximation. Since the chemistry responds non-linear to the concentrations of these species, it is necessary to divide the model in concentric rings in order to represent the concentration distributions. Between the rings, fluxes have to be applied to describe the dispersion and the turbulent mixing caused by the chemically induced concentration fluctuations. The mathematical description of this approach was suggested by *Freiberg* [1976] and completed by others [e.g. *Melo et al.*

1978; *Vilà-Guerau de Arellano et al.* 1990]. The mass conservation equation for a species j in ring i of the plume is given by:

$$\frac{dc_i^j(t)}{dt} = \lambda \left(\alpha_i c_{i-1}^j(t) + \beta_i c_i^j(t) + \gamma_i c_{i+1}^j(t) \right) + P_i^j(t, C) - L_i^j(t, C)c_i^j(t) \qquad (4.10)$$

with $c_i^j(t)$ the concentrations of species j in ring i. The terms $P_i^j(t, C)$ and $L_i^j(t, C)$ are the chemical production and loss rates, respectively, with C the concentration vector. The coefficient λ describes the expansion of the plume and depends on the cross-section surface of the plume:

$$\lambda = \frac{d \ln A}{dt} \qquad (4.11)$$

The so-called Lusis coefficients α, β, and γ account for the exchange between neighbouring rings and are constants

$$\alpha_i = \frac{1}{A_i} \frac{A_{i-1}}{A_i - A_{i-1}} \sum_{m=1}^{i-1} A_m \qquad (4.12)$$

$$\gamma_i = \frac{1}{A_i} \frac{A_{i+1}}{A_{i+1} - A_i} \sum_{m=1}^{i} A_m \qquad (4.13)$$

$$\beta_i = -(\alpha_i + \gamma_i) \qquad (4.14)$$

with A_i the surface of ring i, which is given by

$$A_i = 2\pi\sigma_x\sigma_y \ln\left(\frac{N - i + 1}{N - 1}\right) \qquad (4.15)$$

where $i = 1, ..., N$, with N the number of rings, and σ_x and σ_y the plume variances. The area of the outer ring is set equal to twice that of the second outermost ring:

$$A_N = 2A_{N-1} \qquad (4.16)$$

The total surface of the cross-section is:

$$A(t) = \sum_{i=1}^{N} A_i = 2\pi\sigma_y\sigma_x \ln(4N) \qquad (4.17)$$

Note that the number of rings N determines the fraction of the Gaussian plume that is described by the model. We used the model with 10 rings, which means that ~99.6% of the exhaust is incorporated in the model.

The inner- and outermost rings require some special consideration. The innermost ring cannot have fluxes inward, therefore $\alpha_1 = 0$. Likewise, the outermost ring does not have an outward flux, therefore $\gamma_N = 0$ and $\beta = \alpha_N - 1/\alpha_N \sum_{m=1}^{N} A_m$. The entrainment of ambient air into the outermost ring is treated by an additional term $c_a^j \lambda \ln(4N)/\ln(N)$ in equation (4.10), with c_a^j the ambient concentration of species j.

Table 4.3: Ambient concentrations of long-lived species and meteorological parameters in the plume model at 250 hPa and 50° N for January and July

	January	July
T(K)	216	223
$\rho(\text{cm}^{-3})$	8.40×10^{18}	8.12×10^{18}
$H_2O(\text{cm}^{-3})$	1.29×10^{14}	5.51×10^{14}
O_3(ppbv)	108	102
NO_x (pptv)	72.2	93.5
HNO_3 (pptv)	256	415
H_2O_2(pptv)	140	179
CH_4 (ppbv)	1910	1860
CO (ppbv)	97.2	59.4
CH_3OOH (pptv)	42.2	26.6
HCHO (pptv)	29.9	35.6

4.3 Results for an airliner in the North Atlantic flight corridor

Here we present the results of the plume model for the emissions of a B747-400 airliner at 08:00 hrs local time in July at a flight level of 250 hPa ($\sim$10.5 km altitude) at 50° N, which is representative for the North Atlantic flight corridor (NAFC). Temperature, density, and water vapour concentrations are monthly means and averaged over the area 100° E - 20° W, 45° N - 65° N from the European Centre for Medium Range Weather Forecasting (ECMWF) model. This area encompasses the major flight routes over North America, Europe, and the NAFC. Monthly mean concentrations of the three-dimensional chemistry transport model TM3 [*Meijer et al.*, 2000] averaged over the same area provided ambient concentrations for the plume model. Table 4.3 lists these meteorological parameters and the concentrations of the long-lived species. The diffusion coefficients were $D_h = 20$ m^{2}s^{-1}, $D_s = 0.15$ m^{2}s^{-1}, and $D_s = 0.4(D_h D_v)^{1/2}$. A typical shear of 0.002 s^{-1} was imposed. The model was evaluated for 24 hours.

Figure 4.1 shows time series of the concentrations inside the plume and the ambient air of NO, NO_2, HNO_3, HO_2NO_2, HONO, N_2O_5, O_3, and OH for the July case. For the plume only the inner, the middle, and outer ring are shown. Besides the rapid dilution of the plume concentrations, the role of chemistry is evident. Ozone inside the plume is depleted in the early stages due to the very high NO concentrations and is produced again later plume stages. HNO_3 is produced mainly through the reaction of NO_2 with OH, revealing a diurnal variation in the accumulation of HNO_3. N_2O_5 is formed during the night when NO_3 accumulates in the plume. HO_2NO_2 has very different production rates in the different plume rings, illustrating the non-linearity of the chemistry in the plume. Clearly, it is necessary to apply a ring structure to the plume model in order to resolve chemical transformations.

The concentration of the primary emittant NO_x drop slowly to the background values. Only after 20 hours the differences in concentrations become negligible. The secondary nitrogen species HNO_3, HO_2NO_2, and N_2O_5, as well as ozone have signifi-
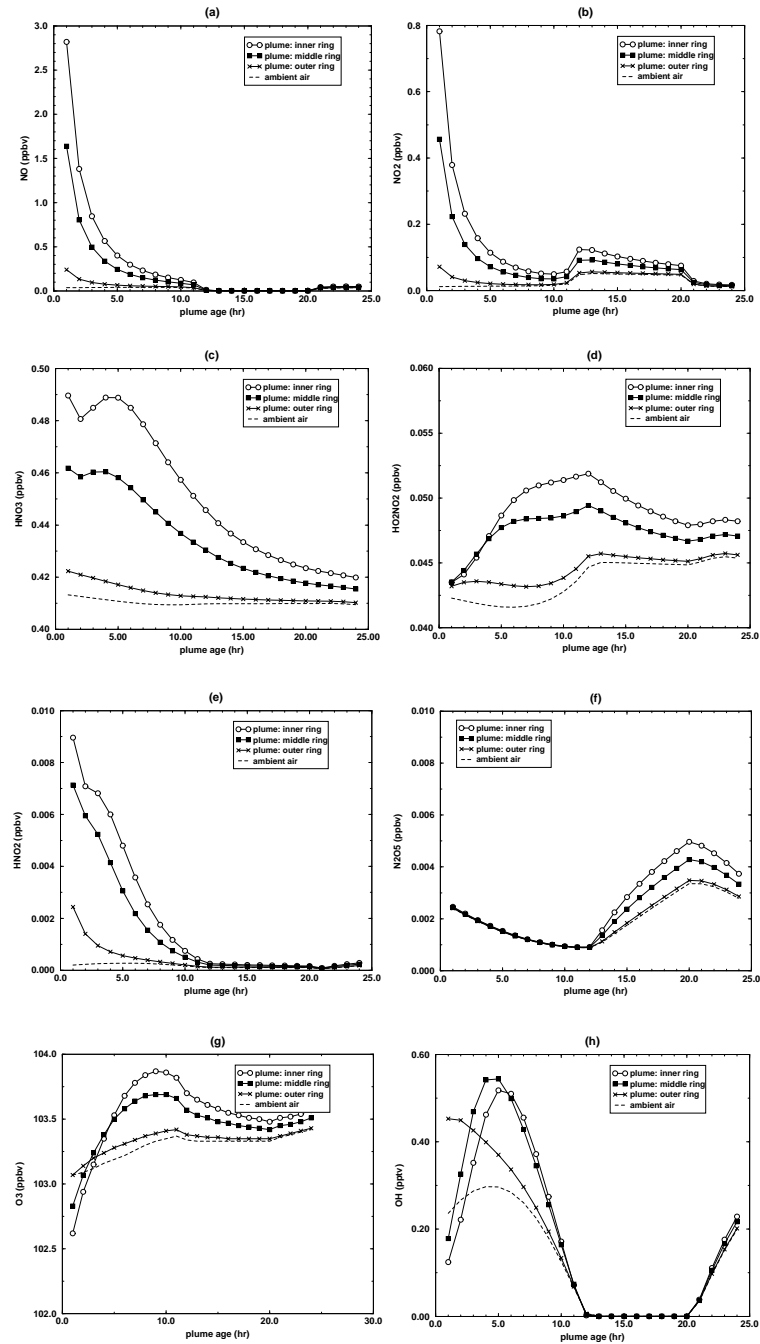
Figure 4.1: Time series of the concentrations inside the plume (inner, middle, and outer ring) and the ambient air of NO, NO_2, HNO_3, N_2O_5, HNO_2, O_3, and OH for an airliner at 250 hPa and 50°N for July. The emission took place at 8 am. local time.

cant deviations from the background concentrations after 24 hours. This demonstrates that the chemical conversions in aircraft plumes constitute a possible important process for the impact on the large-scale.

4.4 Parameterisation of aircraft plumes in a large-scale model

One could imagine that each individual aircraft exhaust is treated by a plume model nested in a large-scale chemistry transport model. There are however almost 100,000 flight movements per day, which make such a nesting of individual plumes computationally not feasible. Instead a parameterisation of the chemical conversions in plumes has to be formulated. To derive such a parameterisation, a Gaussian plume of an aircraft emission in a larger volume of a large-scale grid box is considered. The expanding Gaussian plume with volume $V_p(t)$ contains (of a certain species) the aircraft emissions $N_e(t)$ and the amount of ambient molecules ($N_a(t)$) that is trapped in the plume. The initial concentration $c_p(0)$ in the plume of this species is the total of emitted molecules and ambient molecules in the initial plume volume: $c_p(0) = (N_e + N_a)/V_p(0) = c_e(0) + c_a(0)$, with $c_e(t) = N_e(t)/V_p(t)$ and $c_a(t)$ the concentration in the well-mixed ambient volume $V_a(t)$. Because the chemistry is non-linear the time evolution of the concentration of a reactive species in the plume is not simply a linear superposition of the time evolutions of the concentration of the emitted species and the ambient concentration: $c_p(t) \neq c_a(t) + c_e(t)$ for $t > 0$. The amount of molecules in the plume $c_p(t)V_p(t)$ does not only change due to chemical conversions, but also by the entrainment of ambient air in the expanding plume. At any time instant the aircraft emission can be written as the difference of the number of molecules in the ambient volume with and without this aircraft plume:

$$E(t) = c_a(t)V_a(t) + c(t)V_p(t) - c_a(t)V_a(0) \tag{4.18}$$

The volume of ambient air changes only due to the expansion of the plume, so $V_a(t) = V_a(0) - V_p(t)$ and equation (4.18) can be rewritten as

$$E(t) = V_p(t)\{c_p(t) - c_a(t)\} \tag{4.19}$$

Using this definition of the aircraft emission, we define the emission conversion factor ECF_i as the ratio between the emission of a species i and the emission of all nitrogen oxides (NO_y):

$$ECF_i(t) = \frac{V_p(t)\{c_p^i(t) - c_a^i(t)\}}{V_p(t)\{[NO_y](t) - [NO_y]_a(t)\}} \tag{4.20}$$

NO_y is chemically conserved, so its emission is constant in time. The emission of a non-reactive species is simply $E(t) = V(t)c_p(t) = N_p$. This implies that the new emissions can be calculated from the original aircraft exhaust emission by using these emission conversion factors (EFCs). Hence the emission conversion factors can be used in a large-scale model to calculate effective emissions from the total aircraft emissions at engine exit in each grid box of the model.

We need to take into account the effective emissions of all nitrogen oxides, since the amount of NO_x that is converted to other reservoir nitrogen oxides, such as HNO_3

affects the enhancement of the ozone production in the large-scale model. Since the chemical processes in the plume will either produce or destroy ozone, we also need to include effective ozone emissions in the global model.

Since the ECFs change with time, a choice has to be made regarding the end time of the plume simulation. The emission (and the ECF) of a reactive species changes in time as

$$\frac{dE}{dt} = \frac{\partial V_p}{\partial t}(c_p - c_a) + V_p(\frac{\partial c_p}{\partial t} - \frac{\partial c_a}{\partial t}) \qquad (4.21)$$

The first term on the right-hand side of this equation accounts for the change of the emission due to the entrainment of ambient air, whereas the second term accounts for the change due to the differences between the chemical conversion rates in- and outside the exhaust plume. This demonstrates that the emission will continue to change, even if the plume and the ambient air are in chemical equilibrium. However, if the plume and the ambient air are in equilibrium, it is pointless to prolong the plume simulation. In the next section the net chemical rates of NO_x and O_3 ($(\partial c/\partial t)_{chem}$) for the plume and the ambient air are presented. Those two parameters will sufficiently describe the photochemical state: the net O_3 rate shows whether O_3 is produced or destroyed and the net rate of NO_x is informative about the amount of NO_x that is converted to reservoir species and vice-versa. In the next section we will show that the results are not very sensitive to the choice of end time (if it is taken sufficiently large).

4.5 Emission conversion factors for an airliner in the NAFC

Let us go back to the case of an aircraft emission at 50° N and 250 hPa in July to investigate the net chemical rates of NO_x and ozone for typical flight conditions. Since different seasons and day or night constitute distinctly different chemical regimes, we consider cases with an emission at night (00:00 hrs) and during the day (12:00 hrs) for January and July, respectively. Figures 4.2, 4.3, 4.4, and 4.5 show the time evolution of the net chemical rates of NO_x and O_3 in the plume and in the ambient air, respectively, for each case. The net chemical rates in the ambient air are representative for the rates in a large-scale model grid box, since its meteorological parameters and concentrations are taken from the TM3 model. The net chemical rates of O_3 and NO_x in the ambient air are constant during the night, increase in the morning and decrease in the afternoon. The sudden transitions from daylight to night and vice-versa cause spikes in the net rates. Although the net chemical rates of NO_x and O_3 in the plume are different in each case, they also reveal distinct similar patterns. For all cases the net chemical rate of NO_x in the plume shows a large destruction rate during the first hours, whereafter the net rate slowly converges to the net rate in the ambient air. Also the net chemical rate of O_3 in the plume shows a large initial destruction rate in the plume for all cases, but quickly recovers and does not differ much from the net rate in the ambient air. For both NO_x and O_3 the largest differences between the net chemical rates in the plume and in the ambient air occur during the first hours. There is either slightly more production or slightly more destruction of O_3 in the plume than in the ambient air.
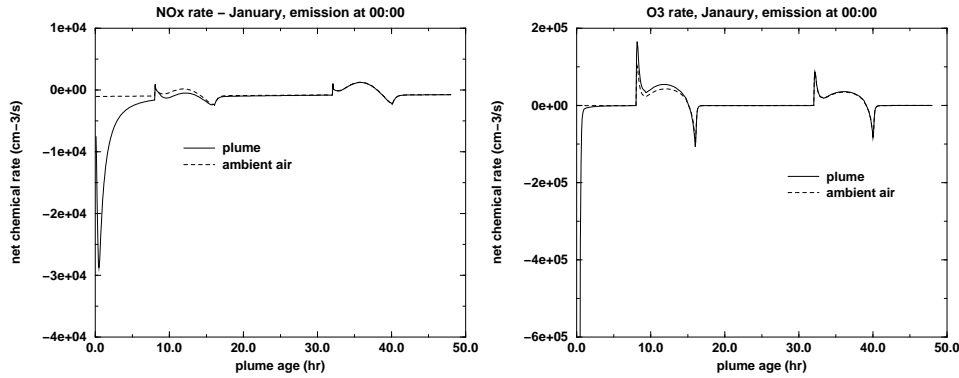
Figure 4.2: Time series of the net chemical conversion rates of NO_x and O_3 in the aircraft plume and the ambient air for an aircraft at 250 hPa and 50° N, with an emission at 00:00 hrs for January.
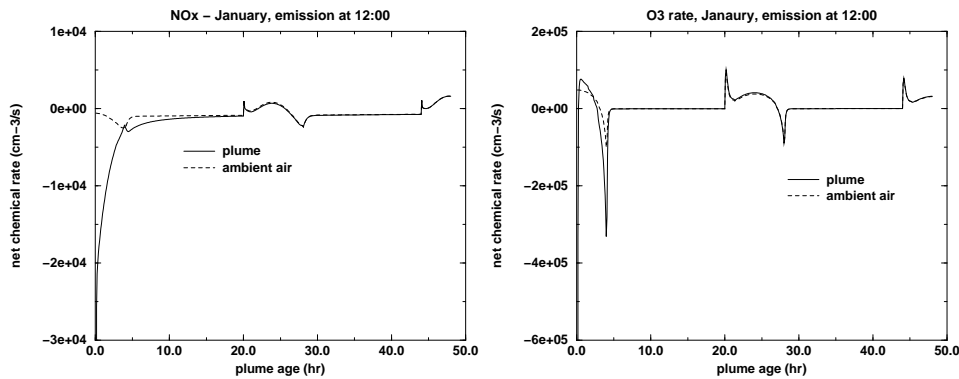
Figure 4.3: As in Figure 4.2, but with an emission at 12:00 hrs for January.

Although it is difficult to obtain a robust stopping criterion from these rates, it is clear that the largest differences between the net chemical rates in the plume and the ambient air occur in the first few hours of the plume evolution. This implies that the results of the large-scale model will not be very sensitive to the precise choice of the end time of the plume simulation, provided it is long enough to allow the net chemical rates in the plume to become close to the rates in the ambient air ($> \sim 10$ hours). When the differences between net chemical rates in the plume and in the ambient air are small, the large-scale model would convert the aircraft NO_x emissions into reservoir species, and form ozone, in the same way as the emission conversion factors would change if the plume simulation would be continued after these 10 hours. From these results it can be concluded that a plume integration time of 15 hours is a suitable choice to calculate the emission conversion factors.
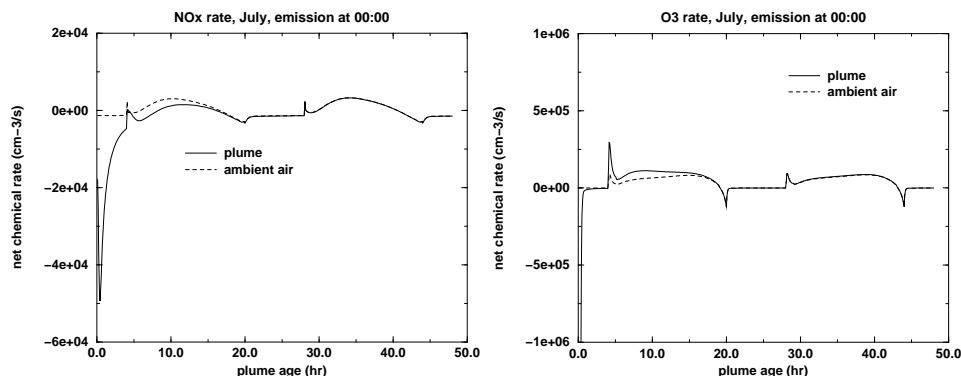
Figure 4.4: As in Figure 4.2, but with an emission at 00:00 hrs for July.
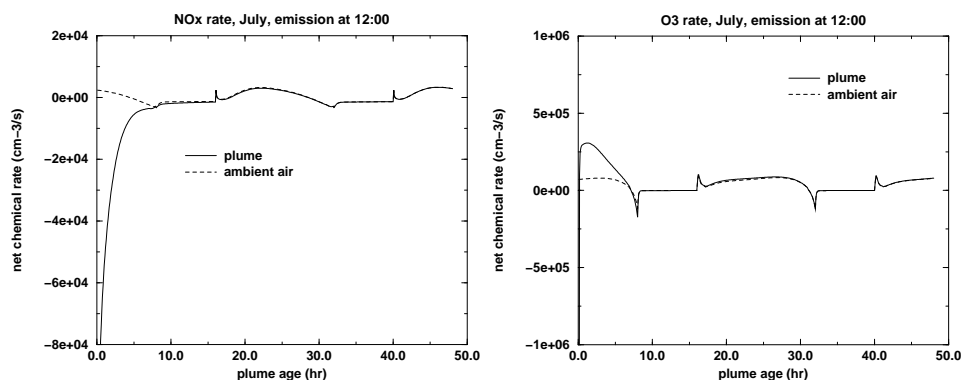
Figure 4.5: As in Figure 4.2, but with an emission at 12:00 hrs for July.

Figure 4.6 shows the time series of the emission conversion factors of NO_x, O_3, HNO_3, HO_2NO_2, N_2O_5, and all other NO_y species for all 4 cases. The ECFs of all species show significant differences between all cases, pointing at the chemical differences that exist due to the different seasons and emission times. Chemical conversion rates are mainly sunlight-driven. The more the plume is exposed to sunlight, the longer it takes for the net chemical rates in the plume and the ambient to reach equilibrium (see Figures 4.2, 4.3, 4.4, and 4.5). For July with an emission at 0:00 hrs the plume is exposed to sunlight during the entire time span in which the chemical states in- and outside the plume reaches equilibrium. Therefore the ECF of NO_x is smallest (0.58) and the ECF of O_3 is largest (0.82) for that case. Of all reservoir nitrogen species the ECFs of HNO_3 and HO_2NO_2 are most significant.

In summary, the emission conversion factors of NO_x, O_3, HNO_3, and HO_2NO_2 have the most significant values, followed by that of N_2O_5. These are the species
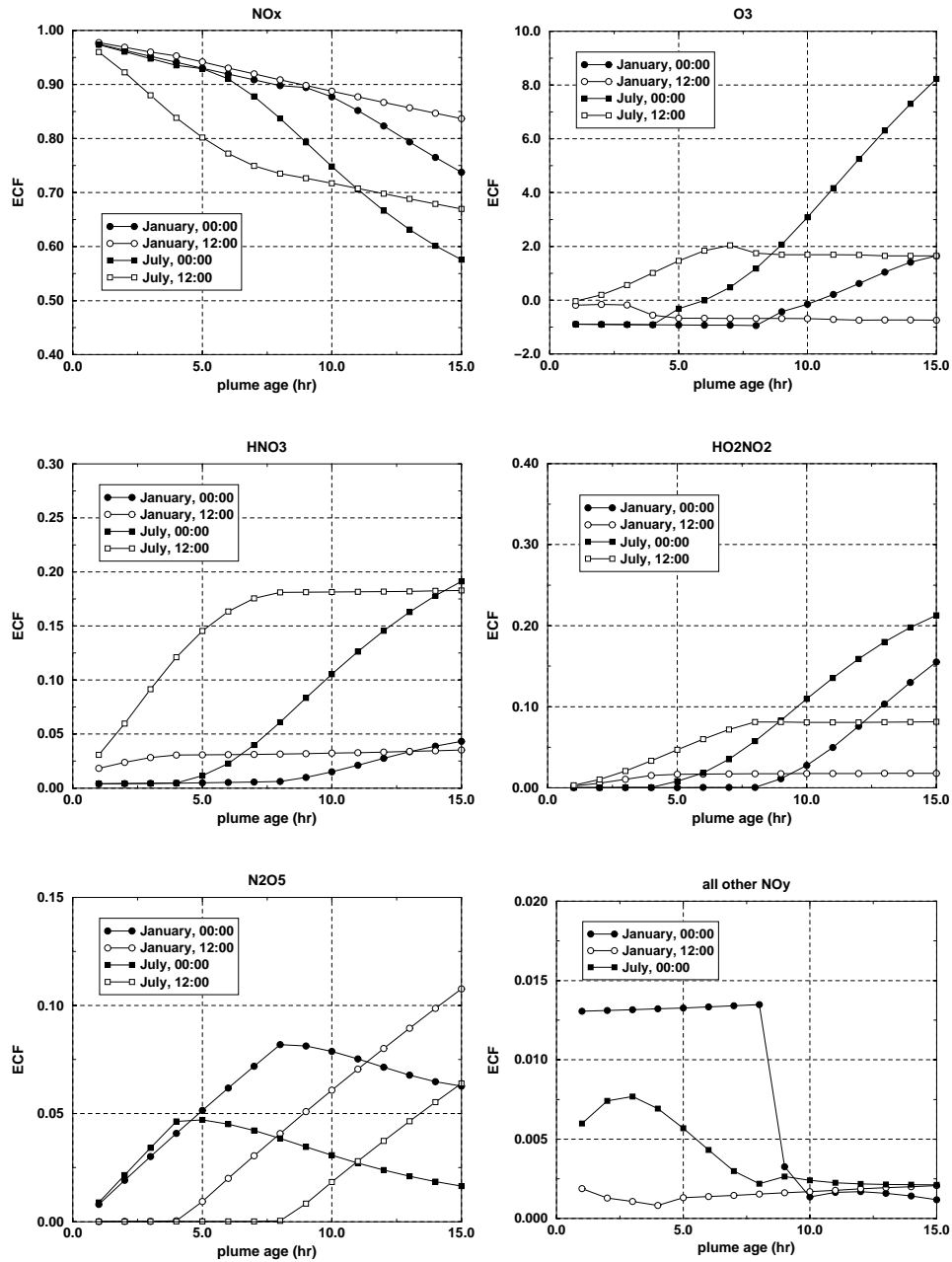
Figure 4.6: Time series of the emissions conversion factors NO_x, O_3, HNO_3, HO_2NO_2, N_2O_5, and all other nitrogen species (NO_y), for an aircraft at 250 hPa and 50°, with emissions at 00:00 and 12:00 hrs for January and July.

that should be included as effective aircraft plume emissions in large-scale models. The other nitrogen oxides are not important in this respect. The exact values of the ECFs are the result of the complex process of the evolution of the chemical regime of the plume towards the regime in the ambient air. Different seasons and times of emission of give already significant variations in the emission conversion factors. Without analysing all the differences found in the emission conversion factors, it can be concluded that the emission conversion factors are determined by the chemical regimes (in the plume and the ambient air) in combination with the emission time. In order to apply this plume parameterisation in a global model, the emission conversion factors must be calculated for different emission times and different chemical regimes.

4.6 Spatial and temporal dependence of the emission conversion factors

We chose to calculate the emission conversion factors per month, latitude, altitude, and emission time. The importance of emission time was already pointed out above. The variation per month, latitude, and altitude, largely governs the chemical state, because these parameters determine the amount of sunlit hours per day and the solar zenith angles. Also ambient concentrations, air density, temperature, and humidity determine the chemical state, so monthly and zonally means of these parameters are used, adopted from the TM3 model. However, the largest gradients of these parameters are usually observed in the vertical, so altitude constitutes an important control parameter of the ECFs. Especially the influence of air density is important, because the reactions of HNO_3 and HO_2NO_2 from NO_2 are termolecular reactions. The rate coefficients of these reactions therefore depend on air density.

Figure 4.7 illustrates these expected dependencies of the ECFs of NO_x, HNO_3, N_2O_5, and O_3 after 15-hours integration time: panel (a) show the results as a function of emission time for an airliner at 250 hPa and 50° N for July, panel (b) as a function of month for an emission at 0:00 hrs at 50° N and 250 hPa, panel (c) as a function latitude for an emission at 0:00 hrs at 250 hPa for July, and panel (d) as a function of pressure for an emission at 0:00 hrs at 50° N for July. The variation with emission time shows the highest NO_x ECF and highest O_3 ECF just before sunrise for nocturnal emissions, since these emission times cause the largest exposure time to sunlight during the transition of chemical state in the plume to that of the ambient air. Similarly, these emission conversion factors are largest for July. Lower in the atmosphere these factors increase, mainly due to the higher air density.

The temporal and spatial variations of the ECFs are clearly of such magnitude that they need to be included in the parameterisation. Especially the pressure dependence appeared to be very large. Note that although these dependencies are mainly due to the amount of sunlit hours and the air density, other plume parameters such as the temperature play also a role in the variation of the ECFs.
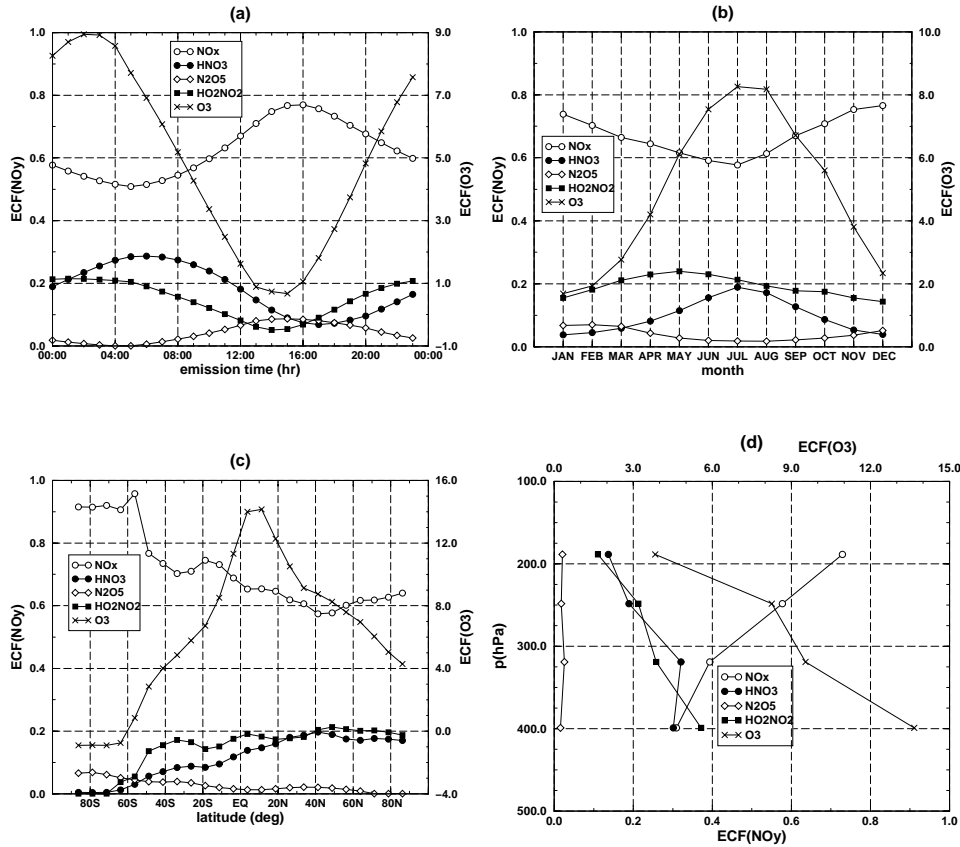
Figure 4.7: The emission conversion factor of NO_x, HNO_3, N_2O_5, and O_3 as a function of: (a) different emission times, (b) month, (c) latitude, and (d) pressure.

4.7 Implementation of the emission conversion factors in a global model

In this section we evaluate the effects of the chemical modifications in aircraft exhaust plumes in a global model. This is done with the three-dimensional global chemistry transport model TM3 at a horizontal resolution of $5°$ in longitudinal and $3.75°$ in latitudinal direction with 19 hybrid σ-levels, extending from the surface up to 10 hPa. The TM3 model has undergone major changes with respect to the version as described in *Meijer et al.*, [2000]. Here we briefly state the major changes. The chemistry scheme has been extended with a parameterisation for the non-methane-hydrocarbons (NMHC) oxidation [*Houweling et al.*, 1998]. The photolysis rates are calculated with a parameterised radiative transfer scheme [*Krol and van Weele*, 1997] instead of being taken as prescribed climatological values. Wet deposition is based on actual ECMWF precipitation fields instead of climatological fields [*Jeuken et al.*,
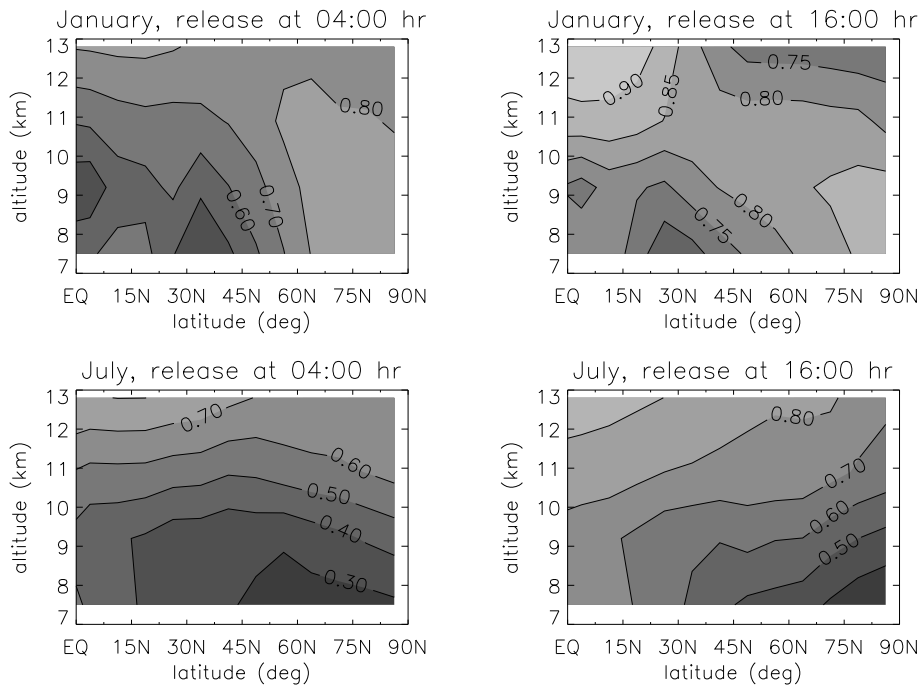
Figure 4.8: The emission conversion factor of NO_x on the Northern-Hemisphere at flight altitudes for January and July at 04:00 and 16:00.

2001]. Finally, a new parameterisation of the NO_x production by lightning, based on accumulated convective precipitation has been developed [*Meijer et al.*, 2001].

In order to calculate the effects of exhaust plume processes, the original engine exit emissions from the DLR/ANCAT 2 NO_x emissions were transformed into aircraft plume emissions by using the ECFs. The ECFs were taken as a function of emission time, latitude, month, and pressure. The aircraft plume emissions contain NO_x, HNO_3, HO_2NO_2, N_2O_5, PAN, and O_3. As an illustration Figures 4.8 and 4.9 show the ECFs of NO_x and O_3 for the Northern Hemisphere at flight-altitudes for the months January and July for an airliner in the morning and afternoon.

Three calculations were performed: one run (A) with the unmodified ANCAT NO_x emissions, one run (B) with the modified aircraft plume emissions, and one run (C) without aircraft emissions. The difference of the results of run (A) and run (C) give the 'traditional' perturbation by air traffic. The difference of the results of run (A) and run (B) show how this perturbation was changed by using modified aircraft plume emissions. Figures 4.10 and 4.11 show for January and July the monthly mean aircraft NO_x and O_3 perturbations at 250 hPa (run A - run C), and the reductions of these perturbations due to the chemical conversions in aircraft plumes in absolute (run A - run B) and relative numbers (100% × [run A - run B]/[run A - run C]).

The largest NO_x increases due to air traffic coincide with the main aircraft routes, i.e. the North Atlantic flight corridor, and the U.S. and European mainland. In
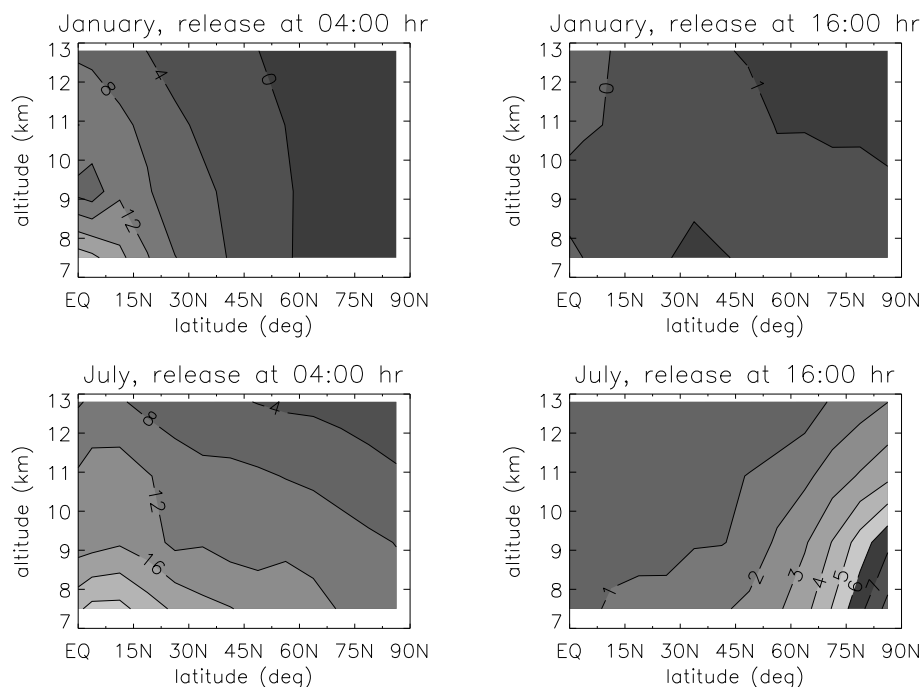
Figure 4.9: The emission conversion factor of O_3 on the Northern-Hemisphere at flight altitudes for January and July at 04:00 and 16:00.

those regions the monthly mean NO_x perturbations are in the range of 50 - 110 pptv for January and 50 - 90 pptv for July. The NO_x perturbations in January are generally larger than in July, due to a longer lifetime of NO_x during wintertime. The O_3 perturbations around and in the main flight corridors are in the range of 1.8 - 2.1 ppbv for January and 2.-3.8 ppbv for July. In July the ozone perturbation attains maximum values at high latitudes. The values and spatial features of these perturbations are in agreement with other CTM calculations [e.g. *Brasseur et al*, 1996; *Wauben et al.*, 1997; *Meijer et al.*, 2001].

    The inclusion of the aircraft plume effects reduced the NO_x perturbations for January and July. The locations of the largest reductions coincide with the main flight routes. For January these reductions are in the range of 15-30 pptv, for July in the range of 10-35 pptv. In relative numbers these reductions in the NAFC amount approximately 20%-30% for January and 20%-40% for July. The reductions of ozone amount to 0.0-0.10 ppbv (0%-5%) for January and -0.1 ppbv to 0.2 ppbv (-5% to 10%) for July. Generally the ozone perturbation is reduced due to the efficient conversion of NO_x in the aircraft exhaust plumes, leading to a diminished O_3 production on the global scale. On the other hand, in most conditions the photochemistry in the aircraft exhaust plumes produce additional ozone emissions. If photochemical activity is sufficiently high, net ozone production in the aircraft plumes can be large enough to enhance the aircraft-induced ozone perturbation. This explains the increase (negative
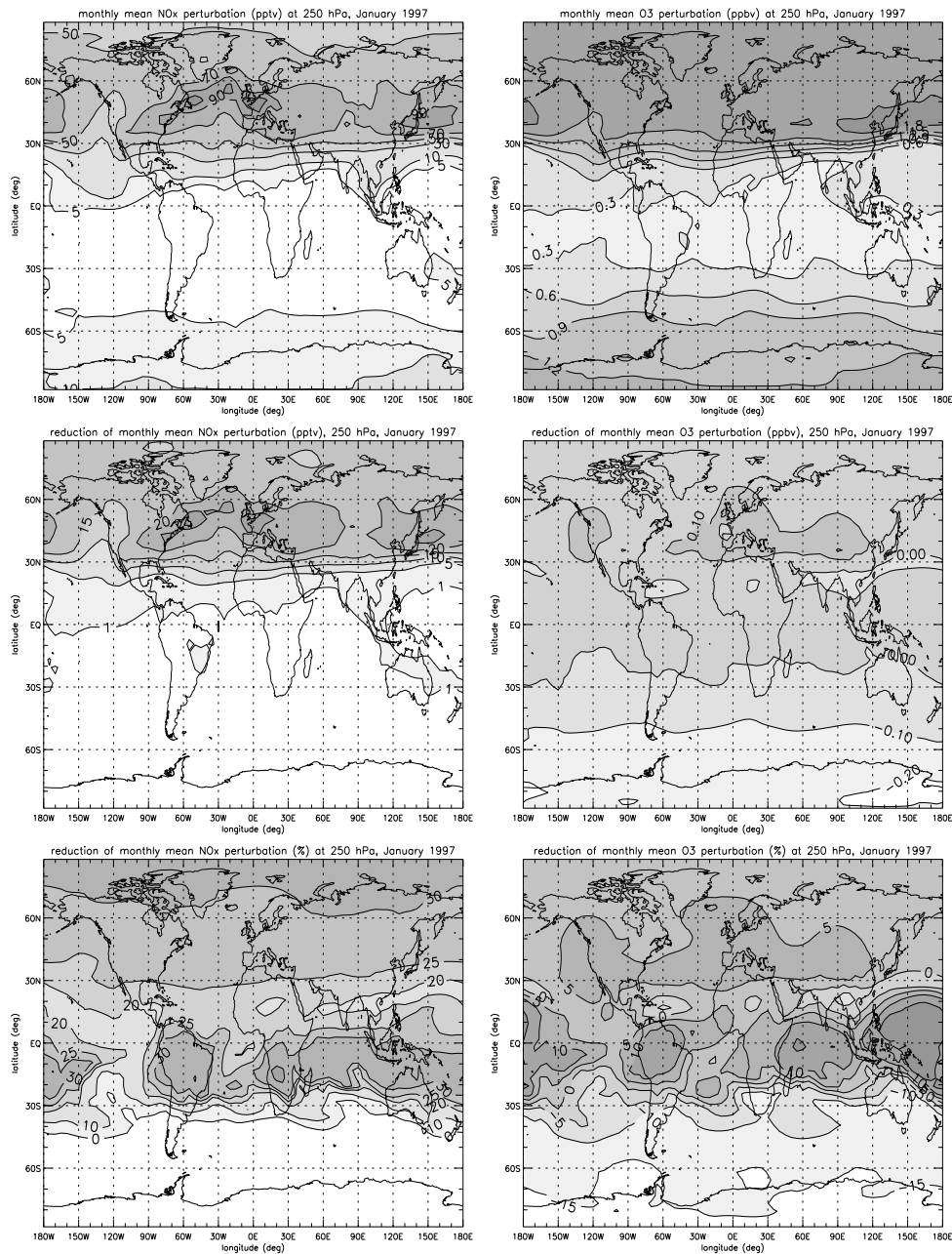
Figure 4.10: The impact of aircraft NO_x emissions on the monthly mean concentrations of NO_x and O_3 at 250 hPa for January: the top two panels show the aircraft perturbations as calculated by TM3 with unmodified ANCAT emissions, the middle two panels show how these perturbations are reduced by replacing the ANCAT emissions with modified aircraft plume emissions, and the lower two panels show these changes in percentages. Positive numbers in the lower four panels indicate a reduction due to the inclusion of aircraft plume emissions.
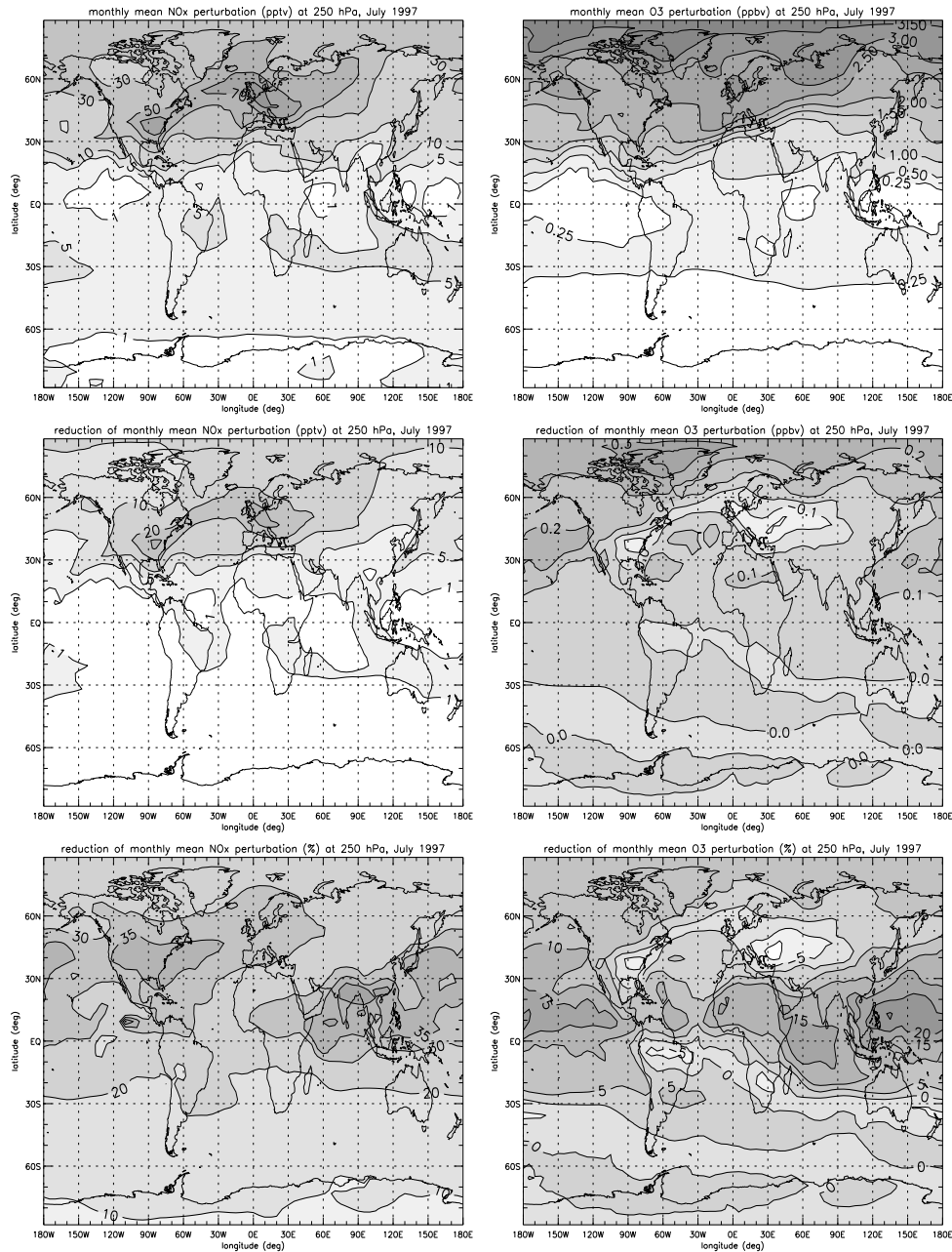
Figure 4.11: The impact of aircraft NO_x emissions on the monthly mean concentrations of NO_x and O_3 at 250 hPa for July: the top two panels show the aircraft perturbations as calculated by TM3 with unmodified ANCAT emissions, the middle two panels show how these perturbations are reduced by replacing the ANCAT emissions with modified aircraft plume emissions, and the lower two panels show these changes in percentages. Positive numbers in the lower four panels indicate a reduction due to the inclusion of aircraft plume emissions.

reduction) of the ozone perturbation locally in the NAFC for July. The maximal enhancement was 8%.

Kraabøl et al., [2000b] performed similar calculations with normal and modified aircraft emissions in a three-dimensional regional chemistry transport model covering Europe, North America, and the North Atlantic. They report maximum NO_x perturbations of 70 pptv and maximum O_3 perturbations of 2.7 ppbv for July 1998 from the calculation with unmodified aircraft emissions. In their study the NO_x perturbations were reduced with maximally 20 pptv ($\sim$40%) and the O_3 perturbations with maximally 0.5 ppbv ($\sim$30%). The reductions of the NO_x perturbation are very similar to those presented in this study. However, they did not include aircraft plume emissions of ozone, which explains the large reduction of aircraft-induced ozone in their study, contrary to ours.

Previously, we reported reductions of the NO_x and O_3 perturbations in *Meijer et al.*, [1997] (15%-25% less NO_x and 15%-20% less O_3 for January and 15%-55% less NO_x and 15%-25% O_3 for July). Also in this study the net ozone production was not taken into account, which explains the larger reductions of the ozone perturbations. The reductions for NO_x are very similar to the numbers in this study, albeit somewhat larger. As our previous study did not take into account the time of emission in the plume parameterisation, some differences are to be expected.

4.8   Sensitivity studies: Other dependencies of the emission conversion factors

The control parameters (emission time, latitude, month, and pressure) determine largely the emission conversion factors, mainly by describing the amount of sunlight, but also by prescribing zonal and monthly mean values of other important parameters, such as the ambient concentrations, temperature, and humidity. The variations in these zonal and monthly mean values could have an effect on the calculated ECFs. Other model parameters are not prescribed by the control parameters, but could also have some effect on the ECFs. These parameters are the diffusion coefficients, vertical wind shear, total ozone column, cloud optical thickness, aerosol surface density, and type of aircraft.

To investigate the importance of these parameters, the sensitivity of the ECFs for some further parameters was investigated for typical flight conditions , i.e. an aircraft at 50° N and 250 hPa with the emission time at 00:00 hrs for July. This case represents a typical situation with strongest plume effects, as can been seen in Figure 4.6. This case, simulated with default parameters, gives the reference case. The emission conversion factors after 15 hours for the reference case were 0.58 for NO_x, 0.19 for HNO_3, 0.21 for HO_2NO_2, 0.02 for N_2O_5, and 8.2 for O_3. For almost all parameters it appeared that there was no significant influence on the distribution among the reservoir species. Therefore only the emission conversion factors of O_3 and NO_x were considered, except the case for different aerosol surface densities in the plume.

Table 4.4: ECFs of NO_x and O_3 for different dispersion parameters

R_i	$s(\text{s}^{-1})$	$D_h \ (\text{m}^2\text{s}^{-1})$	$D_v \ (\text{m}^2\text{s}^{-1})$	$f(NO_x)$	$f(O_3)$
90.25	0.002	15	0.15	0.576	8.19
90.25	0.002	23	0.15	0.576	8.26
90.25	0.002	20	0.15	0.576	8.23
90.25	0.002	20	0.18	0.575	8.52
361	0.001	20	0.15	0.581	7.32
22.56	0.004	20	0.15	0.572	9.19
5.64	0.008	20	0.15	0.570	9.95

Table 4.5: ECFs of NO_x and O_3 for different temperatures

T(K)	$f(NO_x)$	$f(O_3)$
216	0.640	8.15
223	0.576	8.23
230	0.544	8.19

4.8.1 Diffusion coefficients and vertical wind shear

The diffusion coefficients control the dilution rate of the plume and thus the time needed for the plume to evolve to the same chemical regime as for the ambient air. Only typical atmospheric conditions with bulk-Richardson numbers $R_i > 1$ were presented here. All used values are based on the work of *Dürbeck and Gerz* [1995; 1996]. The atmospheric stratification in all cases was 0.019 s^{-1}. The vertical wind shear and diffusion coefficients can be varied independently, since these were independent when $R_i > 1$. Table 4.4 shows the emission conversion factors of NO_x and O_3 for the cases. The sensitivity to the diffusion coefficients appeared to be negligible. Variation of the vertical wind shear had most influence on the emission conversion factors, due to the fact that it controls the expansion of the plume on longer time-scales. For typical vertical wind shear (0.001 s^{-1} - 0.004 s^{-1}) the ECF varies by ~10% relative to the reference case. For a vertical wind shear of 0.008 s^{-1}, which rarely occurs, the ECF for O_3 increases with 20%. Vertical wind shear has a negligible influence on the ECF of NO_x.

4.8.2 Temperature, humidity, and photolysis rates

Temperature, humidity (water vapour concentration), and the photolysis rates are key parameters that control the photochemistry. Temperature and humidity are largely prescribed by the control parameters, but deviations of the zonal and monthly mean values could have an effect on the ECFs. Therefore minimum and maximum values of the temperature and water vapour concentration were obtained by calculating the 2-σ values of these parameters in the NAFC (the above defined area at 250 hPa) for July. Table 4.5 shows the dependence of the emission conversion on temperature and Table 4.6 on water vapour concentration. The temperature dependence of the conversion factors of NO_x was modest. The ECF increased with maximally 11% for the low

Table 4.6: ECFs of NO_x and O_3 for different water vapour concentrations

$H_2O(cm^{-3})$	$f(NO_x)$	$f(O_3)$
0.3×10^{14}	0.675	6.03
5.5×10^{14}	0.576	8.23
10.7×10^{14}	0.548	8.84

Table 4.7: ECFs of NO_x and O_3 for clouded situations and different ozone columns

O_3 (DU)	cloud cover(%)	$f(NO_x)$	$f(O_3)$
325	100	0.646	10.24
325	0	0.576	8.23
225	0	0.520	9.49
425	0	0.612	7.32

temperature case. There was no significant effect on the ECF of O_3. Increasing the water vapour concentration did not have a large effect, but for very dry air the ECF of NO_x increased with 17% and decreased the emission conversion factor of O_3 with 27%. The low water vapour concentration implies low OH concentrations in the plume, resulting in low production rates of HNO_3 and O_3.

The control parameters prescribe the photolysis rates for a typical ozone column of 325 DU and clear sky conditions. Variation of the ozone column and cloudiness, which form the most important parameters for the photolysis rates, are not covered by the control parameters. The total O_3 column determines predominantly the tropospheric photolysis rate of O_3 and consequently the formation rate of OH. Typical mid-latitude values of the O_3 column range from 225 to 425 DU. Backscattering of solar radiation at cloud tops enhances the photolysis rates of all species in the air above. The enhancements for the different species have a strong zenith angle dependence, so the net effect of clouds cannot be given beforehand. We investigated the effects of a stratiform cloud layer at an altitude of 2 km with an optical thickness of 20. Such a cloud deck constitutes a realistic 'worst' case for the midlatitude Atlantic. Table 4.7 depicts the emission conversion factors for the clear-sky cases with a O_3 column of 225, 325, and 425 DU, and the stratiform cloud case with an O_3 column of 325 DU. The presence of stratiform clouds enhances the photolysis rates and consequently increases the ratio of NO of NO_2, which results in an increase of 12% of the ECF of NO_x. The ECF of O_3 increases with 24%. Variation of the ozone column gave only modest variations of about 10%.

4.8.3 Heterogeneous chemistry

The conversions of NO_x to the stable reservoir species HNO_3 could substantially be enhanced by the heterogeneous conversion of N_2O_5. The characteristics of aerosol produced by aircraft are, however, quite uncertain. The reference case contains only sulphate aerosol with surface area densities, estimated from *Kärcher*, [1997]. This case represents a realistic scenario with a high, but realistic abundance of sulphate aerosol. In order to obtain the importance of heterogeneous chemistry, we compared
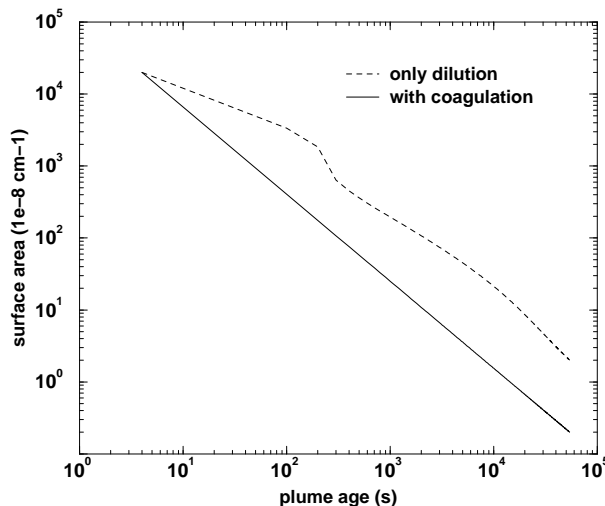
Figure 4.12: The time evolution of the surface area of aircraft produced aerosol. The straight line represents the case with coagulation and is approximated from Figure 5 in *Kärcher* [1997]. The other case start with the same initial surface area but neglects the processes of coagulation and scavenging.

this case with fictitious cases without sulphate aerosol, and without coagulation or scavenging of aerosol. In the later case the surface area density only diminishes due to the dilution of the plume, which represents a kind of worst case scenario. In order to make a crude estimation of the influence of contrails, this 'worst case' scenario is also applied to ice particles (without bothering about atmospheric conditions). Figure 4.12 shows the time evolution of the surface aerosol density for the reference case (with coagulation and scavenging) and for the case with only dilution of the plume. Since N_2O_5 is more stable in winter conditions, the effects of heterogeneous chemistry are also considered for January. Table 4.8 shows the ECFs for January and July for these aerosol cases. In all cases the impact on the ECFs was negligible, even for the case that neglected the coagulation and scavenging of aerosol. Generally an enhanced ECF for HNO_3 was observed at the cost of N_2O_5, as expected. For the 'only dilution' case for January the ECF of HNO_3 increased with 42%, but this change is not significant due the small absolute value of the ECF of HNO_3 (0.061).

4.8.4   Ambient NO_x and O_3 concentrations

The entrainment of ambient air in the plume directly affects the chemical state of the aircraft pollutants. The ambient concentrations are largely prescribed by the control parameters, but large possible variations could still have an important effect. The entrainment of the key species NO_x and O_3 were considered here. For NO_x a free tropospheric background situation of 0.02 ppbv and a polluted situation of 0.5 ppbv, as can occur during convection over polluted areas, were considered. For O_3 we distinguished between a free tropospheric background situation of 40 ppbv and a stratospheric situation of 160 ppbv. Table 4.9 shows the emission conversion factors

Table 4.8: ECFs of NO_x, HNO_3, N_2O_5, and O_3 for different aerosol

aerosol type	$f(NO_x)$	$f(HNO_3)$	$f(N_2O_5)$	$f(O_3)$
		January		
none	0.738	0.038	0.067	1.69
sulphate	0.738	0.043	0.063	1.65
dilution	0.735	0.061	0.048	1.48
ice	0.737	0.046	0.061	1.51
		July		
aerosol type	$f(NO_x)$	$f(HNO_3)$	$f(N_2O_5)$	$f(O_3)$
none	0.577	0.189	0.018	8.26
sulphate	0.576	0.191	0.017	8.23
dilution	0.571	0.201	0.012	7.92
ice	0.574	0.193	0.016	7.95

Table 4.9: ECFs of NO_x and O_3 for different ambient concentrations

O_3(ppbv)	NO_x(ppbv)	$f(NO_x)$	$f(O_3)$
40	0.10	0.800	5.43
100	0.10	0.647	5.62
160	0.10	0.514	5.70
100	0.02	0.607	7.75
100	0.25	0.672	3.33
100	0.50	0.704	1.20

for these ambient concentrations. A smaller ambient concentration of ozone resulted in a larger ECF of NO_x (increased with 38% to 0.80). The entrainment of air with lower ozone concentrations resulted in less OH in the plume, hence in lower conversion rates of NO_x to HNO_3. The ECF of O_3 dropped with 34% to 5.43 relative to the reference case. The opposite situation with ozone-rich air entraining the plume resulted in slightly less changes in the ECFs. A low ambient NO_x concentration changed slightly the conversion of NO_x (5% smaller ECF) and the O_3 production (5% larger ECF). However, very high ambient NO_x concentrations had a relative strong effect of NO_x (maximal increase of 20%), and completely reduced the ozone production (reduction of 85%).

4.8.5   Type of aircraft

Different aircraft have different emission indices and fuel usage, resulting in different emissions or, equivalently, different initial NO_x concentrations in the plume. Different aircraft also have different plume cross-sections, but that appeared not to be an important parameter. Table 4.10 shows these differences caused by using the data of an Airbus 310 and a Boeing 737, compared with the base case of a B747. Lower emissions corresponded with lower initial NO_x concentrations, resulting in less ozone depletion and enhanced conversion of NO_x to HNO_3. It has an effect on the ECF of O_3 for a B767-300 (smallest emission), which increases with 19% to 9.90. The effect

Table 4.10: ECFs of NO_x and O_3 for different aircraft

aircraft	NO_x emission (g.s^{-1})	f(NO_x)	f(O_3)
B747-400	46.0	0.576	8.23
B747-400	25.0	0.572	9.20
B767-300	13.0	0.570	9.90
A310-200	14.0	0.570	9.84

on the ECF of NO_x was negligible for these cases.

4.8.6 Summary of the sensitivity study

The ECF of NO_x has appeared not to be very sensitive to most parameters from this study. For most parameters the variation was less than 10%, which can be regarded as small, considering the involved uncertainties. The only exception to this was the case with a low ambient ozone concentration with an increase of the NO_x emission conversion factor of 40%. The ECF of ozone was more sensitive with typical variations of 25%, with the remarkable exception for the case of a high ambient NO_x concentration of 0.5 ppbv, which gave an 85% reduction of the ozone emission conversion factor. The impact of events of high NO_x concentrations or low O_3 concentrations at cruising altitude will have a large impact locally, but the frequency of such events is likely too small to have a significant impact on the monthly mean, large-scale perturbations. The variations of the ECFs for the other parameters are small enough to expect a linear response of the chemistry on the global scale. This implies that an uncertainty of roughly 10% and 25% could be attributed to the calculated reductions of the aircraft-induced NO_x and O_3 perturbations, respectively.

4.9 Discussion

The aircraft exhaust plume model is a rather complex model containing many assumptions on dispersion and chemistry. Clearly testing the plume model with observations would be highly desirable. Unfortunately no suitable observations are available to evaluate the plume model calculations of the chemical conversions. There are only some observations, made in young plumes with ages less than 100 s, from the 1994 and 1995 POLINAT campaigns [*Schlager et al.*, 1997; *Klemm et al.*, 1998]. *Kraabøl et al.* [2000b] compared these observation with results of their plume model. They found a 'broad' agreement, meaning that the observed concentrations fell within the concentration profile of the plume. After repeating this comparison with our plume model, we found a similar agreement with these observations. Such a comparison can be regarded as a test for the initial plume model conditions. Furthermore, the dynamical parameters of the plume model have been compared with observations. The dispersion parameters, calculated by *Dürbeck and Gerz* [1996], are in agreement with observed dilution factors [*Schumann et al.*, 1995b]. Also the computed NO_x emission indices are in agreement with observed emission indices [*Schumann et al.*, 2000]. So, although it was not possible to compare the plume model results with observations,

there is evidence for a good description of the dispersion of the plume, the emission indices, and the initial conditions of the plume model. These facts, combined with a fair understanding of tropospheric chemistry, give some confidence in the obtained plume results. Furthermore, the sensitivity studies show that the computed ECFs vary only mildly over a very large range for different (typical) conditions and parameter settings. Of course, one must be careful, since there may be processes missing. For instance, little is known of the uptake of HNO_3 by contrail ice particles.

The ECFs depend on the assumed lifetime of the aircraft exhaust plume in the plume model. The differences in net chemical NO_x production and net chemical O_3 production between the exhaust plume and the ambient air are largest in the first few hours after the emission. By setting the lifetime of the aircraft exhaust plumes to 15 hours, the first hours with largest differences in net rates are always within this lifetime. The smaller differences between the net rates at older plume ages are negligible with respect to the uncertainties involved: the net rates of the ambient air should be representative for the rates that are calculated by the global model. In this study we assumed that it was sufficient to meet with this demand by differentiating the emission conversion factors per month, hourly emission, latitude, and altitude. The sensitivity studies showed that is a valid assumption, although other parameters impose roughly an uncertainty of $\sim 10 - 20$ % on the ECFs. Of course this could be further refined, for instance by differentiating the ECFs per ambient ozone and NO_x concentrations. These are probably the missing parameters to which the plume model is most sensitive. We feel that such refinements are not very useful at the moment. Such refinements could prove to be useful after the current model results have been tested against observations.

Others have also addressed the chemical processes in aircraft exhaust plumes. We already have compared our results with the work of *Kraabøl et al.* [2000a; 2000b]. Many aspects of their work are based on the same assumptions we made. Hence most of our findings are in agreement. The major difference is their lack of including an ozone aircraft plume emission in their large-scale model, which resulted in much larger reductions of the O_3 perturbation, compared to our findings. Others [*Danilin et al.*, 1994; *Karol et. al.*, 1997; *Moulik and Milford*, 1999; and *Möllhoff et al.*, 1996] have developed aircraft plume models as well, but they did not investigate the implications for the global scale. *Petry et al.* [1998] has also developed a plume model, but they applied it in a different way. They took a box model as a representation of a grid box of a large-scale model and compared the chemical conversions in that box model with the conversions of their plume model (both one- and multi-layered). They adjusted the aircraft emissions (into emissions of NO_x, O_3, and nitrogen reservoir species) in de grid box model, until chemical conversions of NO_x and the net ozone production were equal to that in the plume model. They found the grid box needs small positive adjustments of the NO_x emission (maximum $\sim$10 %), that correspond with an emission conversion factor of 1.1. Hence, they found negative emissions for the total other nitrogen species. Also, the effective O_3 emission was generally negative ($\sim$-150 %). These numbers are clearly different, but we feel that these numbers should be interpreted differently: we defined ECFs that could be applied to a global model, but the effective emissions, calculated by *Petry et al.* [1998] are the changes needed to force the chemical state of their box model to that of their plume model. We therefore believe that their numbers are not applicable to a global CTM, because their effective

emissions would force the chemistry of each CTM grid box with aircraft emissions into a state that corresponds to aircraft plumes. This would lead to false results, since the amount of NO_x in that grid box also has other sources than aircraft emissions alone.

4.10 Conclusions

Up to now large-scale models have been using aircraft emissions that are based on the composition of the exhaust gases directly at the nozzle exits of the aircraft engines. Furthermore, these models apply these data by assuming instantaneous mixing of the NO_x aircraft emissions, hence neglecting the chemical conversions occurring during the dispersion of the exhaust plumes to larger scales. We have developed a plume model to study these chemical conversions during dispersion of the exhaust. With this plume model we have demonstrated distinctly different behaviour between the chemistry in the plume and the background. The chemistry in the plume results generally in faster conversion of NO_x to reservoir nitrogen species with HNO_3 and HO_2NO_2 as the main constituents. O_3 is initially depleted, but at later stages it is efficiently produced. Generally it results in net ozone production, but it can also result in small net ozone destruction.

We have formulated a parameterisation to include these plume processes in a large-scale model by means of emission conversion factors that modify the engine exit emissions into exhaust plume emissions. Having applied this parameterisation to the three-dimensional chemistry transport model TM3, we found reductions of the aircraft-induced NO_x perturbations of 20-30% for January and 20-40% for July due to chemical plume processes. Similarly the aircraft-induced ozone perturbations reduced by 0%-10%, but for July in the NAFC the ozone perturbation was locally enhanced with maximally 8%.

Due to the current lack of observations in aged plumes, the numbers should be regarded as preliminary estimates of a possible large-scale effect of chemical conversions in aircraft exhaust plumes. Nevertheless we have narrowed down this estimate as much as possible by using validated input parameters for the plume model, wherever possible and by taking the emission conversions as a function of time of emission, month, latitude, and altitude. Furthermore, by means of sensitivity studies we have demonstrated that other plume parameters, not covered by these control parameters, will probably not have a big impact on the emission conversion factors.

4.11 Appendix: The Effects of the Conversion of Nitrogen Oxides in Aircraft Exhaust Plumes in global Models

This Appendix contains a publication that describes briefly some of the work presented in this Chapter: E. W. Meijer, J. P. Beck, G. J. M. Velders, P. F. J. van Velthoven, and W. M. F. Wauben, Geophys. Res. Lett., 24, 3013-3016, 1997

abstract
A parameterisation is needed in global models to account for the sub-grid chemical processes taking place in the plume of an aircraft, since these processes can cause the conversion of a considerable amount of the emitted NO_x to reservoir species, such as HNO_3. For this purpose, the chemical conversions of nitrogen oxides in the plume of an aircraft were investigated with a newly developed model. The calculated fractions of different nitrogen compounds formed within 24 hours in the exhaust plumes, differentiated for the global domain and season, were used to modify the original aircraft NO_x emissions from the ANCAT emission inventory to emissions of various nitrogen compounds and we applied these to the global Chemistry Transport Model KNMI (CTMK). The results obtained imply that neglect of aircraft plume processes in global modelling leads to an overestimation of the NO_x and O_3 perturbations. Compared with a CTMK calculation with unmodified aircraft NO_x emissions, the NO_x perturbations in the North Atlantic flight corridor (NAFC) decreased by 15%-55%, due to conversions in the plumes. The resulting O_3 perturbation decreased by 15%-25%.

Introduction

Global chemistry transport models are required to evaluate atmospheric effects and possible climatic consequences of subsonic aviation [*Friedl et al*, 1997;*Schumann*, 1995]. In the AERONOX project [*Schumann*, 1995] calculations with different 3D global chemistry transport models (CTMK, MEDIANTE, STOCHEM and GISS 3-D), predicted a NO_x perturbation in the North Atlantic flight corridor of 20%-70%, depending on the season, causing a photochemically generated increase in O_3 of 2%-9%. Using the IMAGES model, *Brasseur et al.*, [1996] found similar results, only spread over a larger altitude and latitude range.

However, since global 3D models have relatively coarse grids, these models cannot account for the processes in aircraft exhaust plumes. Such plumes contain high concentrations of NO_x (NO + NO_2), putting the chemistry in a state in which NO_x is efficiently converted to other nitrogen compounds (HNO_3 + N_2O_5 + HO_2NO_2 + NO_3 + PAN + organic nitrates), diminishing the potential of aircraft emissions to form O_3.

To account for the chemical processes in aircraft plumes in global models, we use a plume model to calculate the conversions of nitrogen oxides in aircraft exhaust plumes for different altitudes, latitudes and season. The concentrations of NO_x and the other nitrogen compounds can be expressed as fractions of the total emitted nitrogen compounds, starting with only NO_x. The calculated fractions, differentiated for the global domain and season, were used in the 3D global chemistry transport model CTMK to modify the NO_x aircraft emissions, from the ANCAT emission inventory [*Gardner et al.*, 1997] For this, we used fractions after 24 hours, since by then all concentrations in the plume are within a 10% range of the concentrations in the ambient air. By comparing CTMK simulations with unmodified and modified aircraft emissions, we estimated the influence of chemical processes in aircraft exhaust plumes for the global scale.

Plume model description

The model describes the chemical processes and dispersion of the exhaust plume of an aircraft at cruising altitude for different conditions by varying the time of emission, season, latitude and altitude [*Meijer et al.*, 1996]. The dynamics of the plume are described by the Gaussian plume theory. Although the Gaussian plume theory is strictly speaking only valid for the dispersion regime, it is also applied to the earlier stages of the exhaust gas dynamics. The diffusion of the plume is asymmetric and anisotropic in a sheared and stratified atmosphere. The dispersion coefficients σ_h, σ_v and σ_s are given by analytical expressions for the variances of a Gaussian plume [*Konopka*, 1995]:

$$\sigma_h^2 = \frac{2}{3}s^2 D_v t^3 + (2sD_s + s^2\sigma_{v,0}^2)t^2 + 2D_h t + \sigma_{h,o}^2$$
$$\sigma_s^2 = sD_v t^2 + (s\sigma_{v,0}^2 + 2D_s)t$$
$$\sigma_v^2 = 2D_v t + \sigma_{v,0}^2$$

The dispersion regime starts after 100 s with initial dispersion coefficients $\sigma_{h,0} = 117$ m and $\sigma_{v,0} = 83$ m and a horizontal diffusivity $D_h = 20$ m^{2}s^{-1}, a vertical diffusivity $D_v = 0.15$ m^{2}s^{-1}, and a skewed diffusion constant $D_s = 0.4(D_h D_v)^{1/2}$. These values were adopted from *Dürbeck and Gerz* [1995],[1996] and are in good agreement with experimental results from POLINAT-I [*Schumann et al.*, 1995b]. A typical shear of $s = 0.005$ s^{-1} was imposed. Before the dispersion regime, the diffusivities are estimated from an initial total cross-section of the plume of 50 m^2 with equal vertical and horizontal initial dispersion coefficients and zero skewed diffusivity. Further, the Gaussian plume is divided into 10 elliptical rings to account for the non-linearity of the chemical equations. Besides entrainment of ambient air through the outermost ring, fluxes between the rings are applied to describe the dispersion and the turbulent mixing caused by the chemically induced concentration fluctuations. The mathematical description of this approach was suggested by *Freiberg* [1976] and completed by *Melo et al.* [1978].

The model uses an extensive photochemical mechanism, containing 44 species and 103 reactions, and is adopted from *Strand and Hov* [1994]. All gas-phase reaction

rates are taken from *DeMore et al.* [1994]. The photolysis rates are derived from calculations by *Weele and Duynkerke* [1993]. For the heterogeneous reaction of N_2O_5 to HNO_3 an initial surface area of sulphate aerosol of $8x10^{-8}$ cm^{-1} is assumed, based on model calculations by *Fahey et al.* [1995]. The surface area drops to a background value of $0.6x10^{-8}$ cm^{-1}, due to the dispersion of the plume. Rainout of species is not taken into account.

The emissions of a B747-400 airliner with JT9D-7R4D engines have been derived from studies of *Schumann* [1994] and *Olivier* [1991]. The emissions of the hydrocarbons are based on measured hydrocarbon emission distributions by *Shareef et al.* [1988].

Results of the plume model

The concentrations of the nitrogen compounds, averaged over all 10 rings, are presented as the fractions of the total emitted amount of nitrogen compounds. Figure 4.13 shows these fractions as a function of plume age for January and July, at a latitude of 50°N and an altitude of 10 km, with emission at noon. The fractions of NO_x, HNO_3, HO_2NO_2, N_2O_5 and PAN, have been included in the Figure. The large differences between results for January and July reveal the large temperature and photolysis dependence of the conversion processes of nitrogen oxides. In summer (July) the conversion of NO_x is much faster than in winter (January). In January the formed nitrogen compounds consists primarily of N_2O_5 and HNO_3, whereas in July mainly HNO_3 is formed. The formation of HNO_3 from N_2O_5 and NO_2 depends apparently strongly on the temperature. The main processes in the conversion of NO_x starts with the formation of N_2O_5 from NO_2 and NO_3. In July the formation of HNO_3 from the reaction of NO_2 and OH is important, but is suppressed in January by the lower temperature.

To illustrate the uncertainties in these results, the NO_x fractions for 10 times faster and smaller dilution are given in Figure 4.13. Also, the effect of heterogeneous reactions is given in this Figure and reveals small impact. In Figure 4.14 the fractions of NO_x remaining after 24 hours are represented for latitudes from 90°S to 90°N and for altitudes from 5 to 12 km for the month July. The presented fractions are an average over 4 simulations emission times at 0.00, 6.00, 12.00 and 18.00. At fixed latitude, the NO_x fractions decrease with increasing altitude, due to the temperature and pressure dependency of the formation of HNO_3 from OH and NO_2. The small increase in photolysis rates with altitude cannot compensate this. High temperatures and high photochemical activity result in low NO_x fractions.

Global modelling with modified aircraft emissions

The results of the plume model simulations were used to modify the aircraft emissions in the 3-D global Chemistry Transport Model KNMI (CTMK) [*Velders et al.*, 1994; *Wauben et al.*, 1997]. CTMK calculates the horizontal and vertical transport of tracers on the basis of 12-hourly output from the European Centre for Medium-Range Weather Forecasts (ECMWF) model. The chemistry scheme contains the daytime chemistry of 13 trace gases with photolytical and anorganic reactions of NO_x,
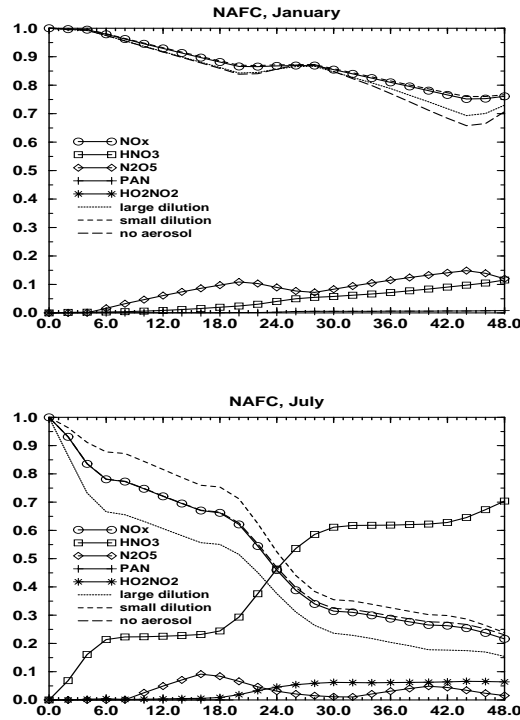
Figure 4.13: The fractions of various nitrogen compounds as a function of plume age at $50°$ N and 10 km for July and January. The emissions took place at noon. The fractions are an average over all 10 rings of the plume model cross-section.

O_3, HO_x and CO, and it contains methane oxidation. Nighttime chemistry consists of an off-line parameterised heterogeneous reaction, which converts NO_2 and O_3 into HNO_3 [*Dentener and Crutzen*, 1993].

In this study the calculations with CTMK were performed with a horizontal resolution of $8°$ in longitude and $10°$ in latitude. The modification of the aircraft emissions has been done in the following way: the results of plume simulations after a 24 hours period, averaged over emission times of 0.00, 6.00, 12.00 and 18.00, for latitudes from $90°$S to $90°$N and for 5 to 12 km for the month January, April, July and October were interpolated to the CTMK model grid. The included nitrogen compounds were NO_x, HNO_3 and N_2O_5. Since CTMK does not include N_2O_5 explicitly, the N_2O_5 emissions were injected as NO_x during daytime and as HNO_3 during nighttime. The results of the CTMK simulation with modified aircraft emissions are compared with a simulation with unmodified aircraft NO_x emissions to estimate the effect of the chemical processes in aircraft plumes on the global NO_x and O_3 perturbations. The differences between the NO_x and O_3 perturbations at 200 hPa of the run with modified and un-
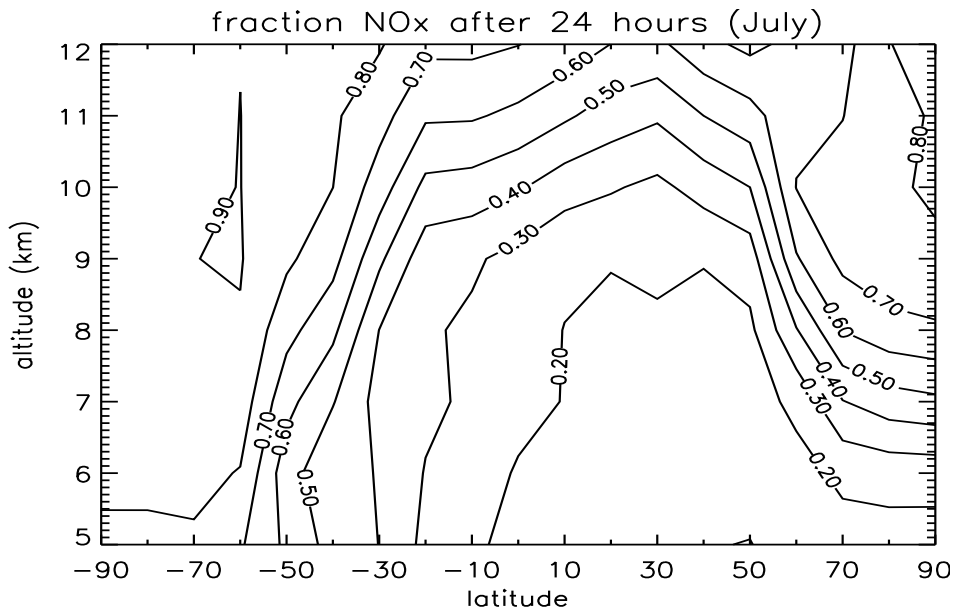
Figure 4.14: The fraction of NO_x remaining after 24 hour for July. The presented fraction is an average over 4 simulations with emission times at 0.00, 6.00, 12.00 and 18.00.

modified aircraft emissions are given in Figure 4.15 for the months January and July. Here, positive numbers indicate that the use of modified aircraft emissions lead to a reduction of the perturbations. The simulation with the modified aircraft emission predicts 4-12 pptv lower NO_x and 0.7-0.8 ppbv lower O_3 in the NAFC for January. For July it gives 10-40 pptv lower NO_x and 1.0-2.2 ppbv lower O_3. Calculations with modified emissions predict a perturbation of NO_x of 20-70 pptv in the NAFC in January and 10-35 pptv in July. The resulting O_3 perturbation varies from 1 to 3 ppbv in January and from 3 to 8 ppbv in July.

Discussion and conclusions

We made an attempt to parameterise the effects of aircraft plume processes on the global ozone response to subsonic aircraft emissions. The results imply that neglect of aircraft plumes in global modelling leads to an overestimation of the NO_x and O_3 perturbations. They indicate that the NO_x perturbation is overestimated by 15%-25% for January and 15%-50% for July and the O_3 perturbation with 15%-20% for January and about 15%-25 % for July.

However, these reductions should be regarded as a first indication, since many uncertainties are present in this approach. The sensitivity to the dispersion rates, the type of aircraft and the role of heterogeneous reactions have been discussed in *Meijer et al.*, [1997]. The results seem to be most sensitive to the dispersion rates. Global model calculations with upper and lower limits of the fractions after 24 hours, reveal a 5 pptv variation of the reduction of NO_x perturbations and for ozone a 0.4

reduction of NOx perturbation (pptv), 200 hPa, January

reduction of O3 perturbation (ppbv), 200 hPa, January

reduction of NOx perturbation (pptv), 200 hPa, July

reduction of O3 perturbation (ppbv), 200 hPa, July
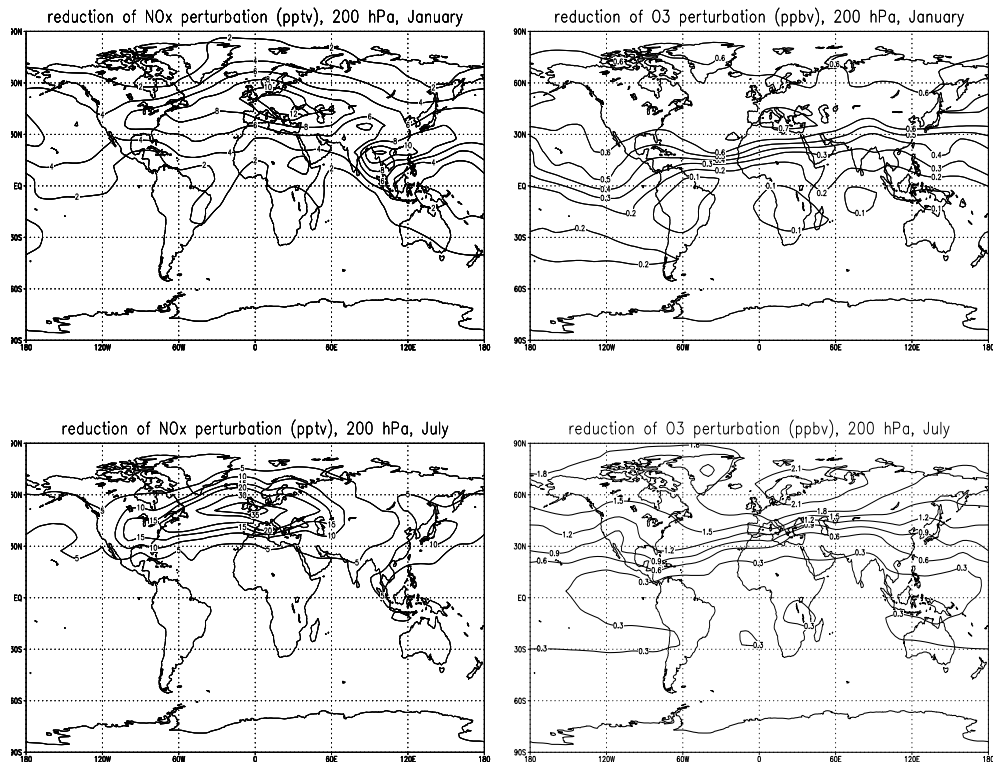
Figure 4.15: The difference between the perturbations of NO_x (pptv) and O_3 (ppbv), due to modified and unmodified aircraft emissions, at 200 hPa for the months January and July. Positive numbers indicate that the use of modified aircraft emissions lead to a reduction of the perturbations.

ppbv variation. Another important parameter is the assumed lifetime of the plume, which is especially important under summer conditions. Under winter conditions, the fractions of the nitrogen compounds are far less dependent on the plume age. Future work will discuss these uncertainties in more detail.

5

Summary, conclusions, and outlook

5.1 Overview and aim of this thesis

Subsonic aircraft increase the ozone concentration in the tropopause region at northern midlatitudes by the emission of nitrogen oxides. Different model calculations indicate that aircraft emissions cause an increase of the NO_x concentration in the range of 20-70% in North Atlantic flight corridor: the 8-12 km layer at northern midlatitudes, between the US and the European continents. According to these models, the NO_x perturbations induce by photochemical processes an increase of ozone in the range of 2-10%. Assessments of the possible climate impact of these calculated ozone increases cause an estimated radiative forcing of about 0.015-0.05 W/m^2 for 1992. However, the calculated increases of the NO_x and O_3 concentrations stem from different chemistry transport models that are insufficiently validated with observations. Furthermore, the uncertainties involved in chemistry transport modelling are numerous and impose a constraint on the reliability of such calculations.

In this thesis the impact of aircraft emissions of NO_x was calculated with the three-dimensional global chemistry transport model TM3. These model results were compared to observations of NO_x and O_3. This comparison aimed to obtain confidence in the earlier performed impact studies, but also to reveal model weaknesses in order to improve the model. Not long ago suitable measurements were not available to test the model with respect to aircraft emission studies, so the work presented in this study forms an important contribution to the reliability of the reported effects of subsonic aviation. Obviously the process of testing and improving of a model is an iterative and ongoing process. This work constitutes also a first step in that process.

5.2 Summary and conclusions

Here a short overview is given of the work with the main conclusions. The conclusions are presented as answers to the scientific questions that guided the investigations in this thesis:

1. How well do the model calculations of the NO and O_3 concentrations in the main flight corridors agree with observations?

2. Can observations support model estimates of the calculated aircraft-induced perturbations of the NO and O_3 concentrations?

3. How much do the other NO_x sources contribute to the atmospheric composition of the main flight corridors?

4. Can the uncertainties in the spatial and temporal distributions of lightning, as well as in the global total of the lightning NO_x production, be reduced?

5. Do the small-scale processes, associated with single aircraft exhaust plumes, that cannot be resolved by a chemistry-transport model, have an effect on the global distributions of NO_x and O_3?

The first three questions relate to the work presented in Chapter 2, the fourth question to Chapter 3, and the last question to Chapter 4.

1. The lack of measurements and the high amount of uncertainties involved in global chemistry transport modelling, motivated the European POLINAT (Pollution from Aircraft Emissions in the North Atlantic Flight Corridor) project, which included extensive observations in the North American flight corridor. The 1997 campaign was conducted in close collaboration with the NASA project SONEX (Subsonic Assessment Ozone and Nitrogen Oxide Experiment). These observations provided excellent data to test the model. How well the model results agree with the observations is a simple question with a far from trivial answer. Observations can be considered as snapshots in space and time. Furthermore, they generally produce very rather irregular time series that may consist of large concentration gradients in time and space, which cannot be reproduced by a large-scale chemistry transport model. This is because global chemistry transport models still have coarse spatial and temporal resolutions, imposed by computational limitations. In this thesis the TM3 model had a horizontal resolution of 5° in longitude and 3.75° in latitude, and 19 vertical hybrid σ-pressure levels, extending from the surface to 10 hPa. Near the tropopause at mid-latitudes, this corresponds to model grid boxes of $\sim 400 \times 400$ km, which are ~ 1.5 km thick. Bearing in mind this coarseness of the model, the NO_x and O_3 concentrations, observed during the POLINAT 2 and SONEX 1997 campaigns, compared reasonably well with the model calculations. For these campaigns we found correlation coefficients between model results and observations of 0.66 for NO_x and 0.67 for O_3, respectively. Differences between calculated and observed ozone concentrations were mainly caused by small-scale features related to the position of the tropopause. This implied that stratospheric observations of the ozone concentration were generally a bit underestimated by the model. For the NO_x concentration, the agreement between observations and calculations was best when observations were in the range of 0-150 pptv. Most observations were in that range. Higher values, however, were generally not well reproduced by the model. This is partly understandable, since these high concentrations are likely the cause of small scale features, such as plumes of recently produced NO_x by lightning, or of the exhaust of recently passed aircraft. Features that clearly cannot be reproduced by the model. On the other hand, the model never produced values that exceeded 200 pptv, which is clearly a too low upper limit. This suggested that some processes be not well reproduced by the model. Either NO_x production by lightning or upward transport of boundary layer NO_x are likely to be

underestimated in cases where high NO concentrations were observed in larger air volumes. This is the subject of ongoing research.

2. Of course, observations of concentrations cannot directly confirm the reported average perturbations, but by analysing selected cases, the observed concentrations could confirm the calculated aircraft contributions for these cases. In order to calculate the aircraft contributions the total concentrations, a labelling technique was developed. This labelling technique distributed the contributions from the different NO_x sources to the concentrations of O_3 and the nitrogen species. The calculated distributions were interpreted with the help of trajectory analyses. For several flights the observations revealed distinct gradients in the NO concentration, that coincided with the position of the North Atlantic flight corridor. There was a clear north-south gradient during flights from Ireland to the Canary Islands and vertical profiles revealed a maximum in the NO concentrations at flight altitudes. Model calculations reproduced fairly well these observed gradients in the NO concentrations. Furthermore, the aircraft contributions to the calculated total NO concentrations were dominant in the flight corridor and had similar gradients as the total NO concentration, whereas the other sources revealed different gradients or none at all. The trajectory analyses supported the model calculations. The model predicted that aircraft contributed with 50% to the NO concentration in the North Atlantic flight corridor, but could be as high as 75%. Overall this implies that it is very likely that the model could not reproduce these observations of the NO concentration, or, stated differently, the observed NO concentrations support the calculated aircraft-induced NO perturbations. Unfortunately, such gradients were not observed in the O_3 concentration. Gradients in the O_3 concentrations were determined by other factors. The location of the observations relative to the tropopause was probably the most important parameter. The model predicted an average aircraft contribution of about 10% to the ozone concentration, but this could not be supported by the observations, due to the strong natural variability of the ozone concentration.

3. The labelling technique, introduced in Chapter 2, could readily give these numbers. The NO_x sources were divided in the categories aircraft, stratospheric input, lightning NO_x production, and surface sources. The last category is the total of all fossil fuel emissions, minus those of aviation, biomass burning emissions, NO_x production by ammonia oxidation, and microbial production. Model calculations for the POLINAT 2/SONEX campaign in October 1997 indicated that both lightning NO_x production and surface sources gave contributions of 15-25% to the total NO concentration. Lightning NO_x production contributed 20% to the ozone concentrations and surface sources 30%, and were more important contributors than aircraft. Stratospheric input gave only minor contributions to the NO and O_3 concentrations. Inflow of ozone from the stratosphere was the main source of O_3, although ozone production from surface NO_x sources could be equally large in some cases. However, the contributions of the other sources could not be supported by observations, due to a lack of cases where these sources were dominant. Furthermore, the model results did not agree well with observations of large NO concentrations (>500 pptv). Such high concentrations are probably the result of recent events of lightning or convection, hence the model treatment of these processes could be insufficient. This could either be a result of a too coarse model resolution, or a shortcoming in the representation of these processes. Either way, the model calculated contributions of the other NO_x

sources should therefore be regarded as tentative.

4. This question, which logically appeared after the conclusions from the comparison with the observations from the POLINAT 2 and SONEX campaign, was the topic of Chapter 3. The possibility to improve the model in this respect was provided by the EULINOX (European Lightning Nitrogen Oxides) project that included observations of trace gases and lightning flashes in regions affected by thunderstorms. This observation campaign took place in Europe during the summer of 1998. First, a comparison of the observations of the NO concentration with model results, confirmed the suspicion that the model description of the lightning NO_x production was unsatisfactory. Moreover, the model was never capable to reproduce the measurements or to give substantial lightning contributions. In order to improve the parameterisation of lightning NO_x production, lightning observations were compared with various meteorological quantities of the ECWMF (European Centre for Medium range Weather Forecasting) model. A good correlation between a meteorological quantity and observed lightning would imply that this quantity could be used as a proxy for lightning. This comparison showed that accumulated convective precipitation was the best suited quantity with an approximate linear relationship with the observed lightning flashes, implying that accumulated convective precipitation could be used to describe the horizontal and temporal distribution of lightning, as well as its intensity. The found relationship with convective precipitation was the basis of a new parameterisation, which was tested against observations with different choices for the vertical distribution of the lightning produced NO_x. It appeared that the use of this parameterisation with a vertical profile that accounts for the strong convective redistribution of NO_x gave the best agreement with observations. Since the EULINOX campaign was conducted for a relative short period (summer 1998) and only comprised observations over western Europe, it was not possible to convincingly reduce the large uncertainty in the number for the global NO_x production (2-20 Tg[N]/yr). Instead, the global annual NO_x production by lightning was set to the 'best' estimate of 5 Tg(N)/yr. Others from the EULINOX team (Huntrieser et al.), estimated a lower limit of 3 Tg[N]/yr. Nevertheless, the new parameterisation implied a significant model improvement with respect to the temporal and spatial distribution of lightning. The model was now capable to produce substantial contributions from lightning NO_x production, which improved the agreement with observations inside or near thunderstorm clouds, as well as observations in the outflows of already dissipated thunderstorms.

5. This last question has been the subject of much debate in the past. An aircraft exhaust exists as a separate plumes that slowly mixes with the ambient air, and can persist for as long as one day. During the mixing the NO_x concentrations in such plumes are much higher than in the ambient air, which leads to photochemical conversion rates that differ from those in the environment, since the photochemistry responds non-linearly to the NO_x concentration. To quantify these differences an aircraft exhaust plume model was developed. It was found that after 15 hours of plume evolution, the chemical state of the plume was in equilibrium with that of the ambient atmosphere. For typical summer conditions in the North Atlantic flight corridor with an emission at 0.00 hrs, ~60% of the emitted NO_x, was converted after 15 hours to other nitrogen species, mainly to HNO_3 and HO_2NO_2. Although ozone was depleted during the early stages of the plume, the faster ozone production afterwards, resulted in an overall production of ~ 8 molecules O_3 per emitted NO_x molecule. The amount

of converted NO_x and the net production of O_3 depend strongly on the emission time, the month, the latitude, and the altitude. These parameters govern to a large the extent the differences in photochemical state in- and outside the aircraft exhaust plume. The conversion numbers of NO_x to other nitrogen species, and the O_3 produced per NO_x were used to replace the engine exist emissions that are normally used in global chemistry transport models with modified aircraft emissions of NO_x, other nitrogen species, and O_3. The conversion numbers were given as a function of emission time, month, latitude, and altitude. The global model calculations with modified aircraft emissions indicated that the aircraft-induced NO_x perturbations in the North Atlantic flight corridor decreased with $\sim 25 - 40\%$, depending on season. The aircraft plume parameterisation caused for July an enhancement of the ozone perturbation locally in the flight corridor of 0-8%. Outside the corridor the ozone perturbation decreased with 0-10%, depending on season. However, suitable observations to test these results are not yet available.

Significant progress has been made with the studies presented in this thesis with respect to the impact of subsonic aviation on the atmospheric composition. It was found that the TM3 model was capable of reproducing the observed NO_x and O_3 concentrations. Furthermore, for selected cases the observations of the NO_x concentrations confirmed the calculated aircraft contributions to the total NO_x concentration. Furthermore, the model's description of NO_x production by lightning has considerably improved, which is also beneficial for further studies of the impact of subsonic aviation (or other air pollution problems). Finally, the possible effects of aircraft exhaust plumes have now been quantified.

5.3 Outlook

As mentioned earlier, the process of model evaluation and improvement, is an ongoing and iterative process. Furthermore, the amount of available data has increased considerably over the last years. Not only from dedicated research campaigns, such as POLINAT, SONEX, and EULINOX, but also from observations on instruments on board of commercial airliners (NOXAR, MOZAIC, and CARIBIC). The dedicated research campaigns are extremely useful to validate well-defined aspects of the models, since they provide a comprehensive collection of observations. On the other hand the measurements from instrumented commercial aircraft provide observations over large areas and long time periods, which is especially useful for testing the climatology and overall performance of a global chemistry transport model. In the framework of the TRADEOFF project an extensive data set has been compiled that includes most measurement campaigns for the period 1995-1998 with fairly good coverage of the North Atlantic flight corridor, as well as other regions of the globe. The TM3 model is participating in this project, which is already ongoing. These new calculations are now being performed at a higher resolution, namely $2.5° \times 2.5°$ and 31 layers.

The model parameterisation of the NO_x production by lightning has been improved by the work in this thesis, but has only been tested for the European continent under summer conditions. Others have also found good correlation between convective precipitation and lightning flashes for the US continent, but the model itself has not been tested for other regions with respect to lightning. It must be noted that

the regions of most intense lightning are situated in the tropics. Clearly lightning research campaigns in tropical areas are necessary for further testing of the new lightning parameterisation in TM3. Another important issue is the global annual number of NO_x production in lightning, which is still quite uncertain. The currently given range of 2-20 Tg(N)/yr stems from different methods, that try to extrapolate the NO_x production in a single thunderstorm or flash to the globe. Only good coverage of NO observations of air recently exposed to lightning, could reduce the uncertainty range from these extrapolation methods, which by themselves would benefit mostly from observation campaigns in the tropics.

The model simulations of upward transport of NO_x from the boundary layer requires further testing. The comparison to the NO observations of POLINAT 2 and SONEX suggests that the TM3 model does not always reproduce the convective redistribution of trace gases. It is often difficult to attribute high NO concentrations to either lightning or convection, since these two are closely linked. Over polluted areas it is very unlikely that lightning alone enhances the NO concentrations. Even with a possible underestimation of the convective redistribution of trace gases, the model results indicate that the ozone perturbation in the North Atlantic flight corridor due to surface NO_x sources is much larger than the aircraft-induced perturbation. It is therefore very important to direct further research into the model treatment of convective transport. First steps have already been taken into that direction. The ECMWF that provides the meteorological fields for the TM3 model, has started a new re-analysis for 40 years (ERA-40 project). The new meteorological fields will be archived at a higher resolution and subgrid mass fluxes will now be included in the archival. The ECMWF convective mass fluxes can replace the fluxes that were calculated by the TM3 model. This could imply an improvement since these new subgrid mass fluxes have been calculated at a much higher resolution ($0.5° \times 0.5°$ and 61 layers instead of $2.5° \times 2.5°$ and 31 layers).

The effects of chemical conversions in single aircraft exhaust plumes are likely to have an impact on the global scale. However, these estimates are completely model-based and lack substantial validation. Obviously, sophisticated measurements of single aircraft plumes would be needed to test the calculated chemical conversions in aircraft plumes. Such measurements are perhaps too demanding for present day observational techniques that have already undergone tremendous progresses. The aircraft plume model approach has two important assumptions that need to be validated. The first is the assumed lifetime of 15 hours, which could be too long. Perhaps the mixing of most plumes is enhanced by intermittent fair weather turbulence. Secondly, it is assumed that single plumes do not overlap. Overlapping of aircraft plumes would significantly alter the chemical conversions and the mixing in the plumes. Whether overlapping occurs frequently is not yet known.

A still unanswered question is the removal of active nitrogen from the atmosphere. Removal of nitrogen oxides occurs predominantly through the formation of HNO_3 and subsequent wet deposition (solution in cloud water droplets, followed by precipitation). Since this removal process directly determines the atmospheric residence times of NO_x and consequently the ozone production efficiency, it constitutes an important outstanding problem.

The focus of this thesis was on the aircraft emissions of nitrogen oxides and the subsequent ozone production. However, as mentioned in the introduction, aviation

has also other possible climate effects. An effect that is directly linked to nitrogen oxides is the decrease of the lifetime of atmospheric methane, which has a cooling effect with a similar magnitude as the warming effect of the estimated ozone increase. This effect is the result of an increased hydroxy radical budget. Our understanding of the hydroxy radical budget is not complete, and is another important research question. From all possible climate effects the net warming due to contrail formation and the possible enhancement of cirrus formation are clearly the worst quantified effects, which need much more study.

As pointed out above, the model results of the impact of surface NO_x sources indicate large O_3 perturbations that exceed the impact of aviation. It would therefore be interesting to assess the effects of other NO_x sources in the same way as those from aircraft emissions. In fact, the IPCC 1999 special report on aviation was requested by the ICAO (International Civil Aviation Organisation), which is a quite unique example of an economic sector that takes interest in the possible climate effects of its activities. It would be a logical follow-up to study the effects of other sectors. For example, NO_x emissions by ships are, just like aviation, occurring in a relatively unperturbed atmosphere, where ozone production is efficient and the residence times of pollutants are relatively long. Also, the impact of different economic regions is relatively easy to address. These kinds of studies are not only interesting from a scientific point of view, but from the point of view of policy makers.

References

Appleman, H., The formation of exhaust condensation trails by jet aircraft, *Bull Am. Meteorol. Soc.*, 34, 14-20, 1953.

Baughcum, S. L., M. Metwally, R. K. Seals, and D. J. Wuebbles, Subsonic aircraft emission inventories, *NASA Ref. Publ.*, *1385*, 15-29, 1996.

Beck, J. P., C. E. Reeves, F. A. A. M., de Leeuw, and S. A. Penkett, The effect of air traffic emissions on tropospheric ozone in the northern hemisphere, *Atmos. Environ.* 26A, 17-29, 1992.

Bent, R. B. and W. A. Lyons, Theoretical evaluations and initial operational experiences of LPATS (lightning position and tracking system) to monitor lightning ground strikes using a time-of-arrival (TOA) technique. In *VII Intern. Conf. on Atmospheric Electricity*, 317-328, Albany, N.Y., 1984.

Berntsen, T. K. and I. S. A. Isaksen, Effects of lightning and convection on changes in tropospheric ozone due to NO_x emissions from aircraft, *Tellus 51B*, 766-788, 1999.

Brasseur, G. P., J.-F. Müller, and C. Granier, Atmospheric impact of NO_x by subsonic aircraft: A three-dimensional model study, *J. Geophys. Res.*, 101, 1423-1428, 1996.

Brasseur, G. P., R. A. Cox, D., Hauglustaine, I. S. A. Isaksen, J. Lelieveld, D. H. Lister, R. Sausen, U. Schumann, A. Wahner, and P. Wiesen, *Atmos. Environ.*, 32, 2329-2418, 1998.

Bregman, A., J. Lelieveld, M. M. P. van den Broek, P. C. Siegmund, H. Fischer, and O. Bujok, The N_2O and O_3 relationship in the lowermost stratosphere: a diagnostic for mixing processes as represented by a three dimensional chemistry-transport model., *J. Geophys. Res.* 105, 17,279-17,290, 2000.

Brühl, C., and P. J. Crutzen, On the disproportionate role of tropospheric ozone as a filter against solar UV-B radiation, *Geophys. Res. Lett.*, *16*, 703-706, 1989.

Brunner, D., J. Staehelin, and D. Jeker, Large-scale nitrogen oxide plumes in the tropopause region and implications for ozone, *Science, 282*, 1305-1309, 1998.

Brunner, D. W. and P. F. J. van Velthoven, Evaluation of parameterizations of the lightning producion of nitrogen oxides in a global CTM against measurements. Paper presented at the AGU 1999 fall meeting, *EOS Transactions 80-46, F174*, 1999.

Carlson, T. N., Airflow through midlatitude cyclones and the comma cloud pattern, *Mon. Wea. Rev.*, 108, 1498-1509, 1980.

Chapman, A theory of upper-atmospheric ozone, *Memoirs Roy. Meteorol. Soc.*, III, 103, 1930.

Chatfield, R. B. and P. J. Crutzen, Sulfur dioxide in remote oceanic air: cloud transport of reactive precursors, *J. Geophys. Res.*, 89, 7112-7132, 1984.

CIAP, Climatic Impact Assessment Program, Department of Transportation, *Publ. DOT-TST-75-51 and ff. (8 vols.)*, 1975.

Crutzen, P. J., The influence of nitrogen oxides on atmospheric ozone content, *Q. J. R. Meteorol. Soc.*, 97, 320-325, 1970.

Crutzen, P. J., SSTs - a threat to the earth's ozone shield, *Ambio*, 41-51, 1972.

Danilin, M. Y., A. Ebel, H. Elbern, and H. Petry, Evolution of the concentrations of trace species in an aircraft plume: Trajectory study, *J. Geophys. Res.*, 99, 18,951-18972, 1994.

DeMore, W. B., S. P. Sander, D. M. Golden, R. F. Hampson, M. J. Kurylo, C. J. Howard, A. R. Ravishankara, C. E. Kolb, M. J. Molina, Chemical kinetics and photochemical data for use in stratospheric modeling, 1994, Evaluation number 11., *JPL-Publ 94-26*, Jet Propulsion Laboratory, Pasadena, California, 1994.

DeMore, W. B., S. P., Sander, D. M. Golden, M. J. Molina, R. F. Hampson, M. J. Kurylo, C. J. Howard, A. R. Ravishankara, and C. E. Kolb, Chemical kinetics and photochemical data for use in stratospheric modeling, Evaluation number 12, *JPL-Publ. 97-4*, JPL, California, 1997.

Dentener, F. J., and P. J. Crutzen, Reaction of N_2O_5 on tropospheric aerosols: Impact on the global distributions of NO_x, O_3, and OH, *J. Geophys. Res.*, *98*, 7149-7163, 1993.

Dickerson, R. R., G. J. Huffman, W. T. Luke, L. J. Nunnermacker, K. E. Pickering, A. C. D. Leslie, C. G. Linsey, W. G. N. Slin, T. J. Kelly, A. C. Delany, J. P. Greenberg, P. R. Zimmerman, J. F. Boatman, J. D. Ray and D. H. Stedman, Thunderstorms: An Important Mechanism in the Transport of Air Pollutants, *Science*, 235, 460-465, 1987.

Dürbeck, T. and T. Gerz, Large-eddy simulation of aircraft exhaust plumes in the free atmosphere: effective diffusion constants and cross-sections. *Geophys. Res. Lett.*, 22, 3203-3206, 1995.

Dürbeck, T. and T. Gerz, Dispersion of aircraft exhausts in the free atmosphere. *J. Geophys. Res.*, 101, 26,007-26,015, 1996.

Ehhalt, D. H., F. Rohrer, and A. Wahner, Sources and distribution of NO_x in the upper troposphere at northern midlatitudes, *J. Geophys. Res.*, *97*, 3725-3738, 1992.

Ehhalt, D. H. and F. Rohrer, The impact of commercial aircraft on tropospheric ozone, in: The chemistry of the atmosphere - Oxidants & Oxidation in the Earth's atmosphere, 7th BOC Priestley Conf., 1994, *The Roy. Soc. of Chem.*, Spec. Publ. 170, 105-120, 1995.

EPA (Environmental Protection Agency), Air quality criteria for ozone and other photochemical oxidant research, *EPA 600/8-84-020A*, 1984.

Fahey, D. W., E. R. Keim, K. A. Boering, C. A. Brock, J. C. Wilson, H. H. Jonsson, S. Anthony, T. F. Hanisco, P. O. Wennberg, R. C. Miake-Lye, R. J. Salawitch, N. Louisnard, E. L. Woodbridge, R. S. Gao, S. G. Donelly, R. C. Wamsley, L. A. Del Negro, S. Solomon, B. C. Daube, S. C. Wofsy, C. R. Webster, R. D. May, K. K. Kelly, M. Loewenstein, J. R. Podolske, and K. R. Chan, Emission Measurements of the Concorde Supersonic Aircraft in the Lower Stratosphere, *Science*, 270, 70-74, 1995.

Finlayson-Pitts, B. J., J. N. Pitts, Atmospheric chemistry: fundamentals and experimental techniques, Wiley, New York, 1986.

Fortuin, J. P. F., and U. Langematz, An update on the global ozone climatology and on concurrent ozone and temperature trends, *Proc. Int. Soc. Opt. Eng.*, *2311*, 207-216, 1995.

Friedl, R. R., B. E. Anderson, K. Liou, D. H. Rind, H. B. Singh, D. J. Wuebbles, S. L. Baughcum, J. Hallet, K. Sassen, L. R. Williams, Atmospheric effects of subsonic aircraft: Interim assessment report if the advanced subsonic technology program, *NASA Ref. Publ. 1400*, 1997.

Freiberg, J., The iron catalyzed oxidation of SO_2 to acid sulfate in dispersing plumes, *Atmos. Environ.*, 10, 121-130, 1976.

Fung, I., J. John, J. Lerner, E. Matthews, M. Prather, L. P. Steele, and P. F. Fraser, Three-dimensional model synthesis of the global methane cycle. *J. Geophys. Res.*, *97*, 13,003-13,065, 1991.

Gallardo, L., and V. Cooray, Could cloud-to-cloud discharges be as effective as cloud-to-ground discharges in producing NO_x?, *Tellus 48B*, 641-647, 1996.

Galloway, J. N., H. Levy II, and P. S. Kasibhatla, Year 2020: consequences of polution growth and development on deposition of oxidized nitrogen, *Ambio*, 23, 120-123, 1984.

Gardner, R. M., K. Adams, T. Cook, F. Deidewig, S. Erndedal, R. Falk, E. Fleuti, E. Herms, C. E. Johnson, M. Lecht, D. S. Lee, M. Leech, D. Lister, B. Massé, M. Metcalfe, P. Newton, A. Schmitt, C. Vandenberh, and R. van Drimmelen, The ANCAT/EC global inventory of NO$_x$ emissions from aircraft, *Atmos. Environ.*, 12, 1751-1766, 1997.

Haagen-Smit, A. J. and M. M. Fox, Photochemical ozone formation with hydrocarbons and automobile exhaust, *J. Air. Pollut. Control Assoc.*, 4, 105, 1954.

Hauglustaine, D. A., Granier, C., Brasseur, G. P., and Mégie, G., Impact of present aircraft emissions of nitrogen oxides on tropospheric ozone and climate forcing, *Geophys. Res. Lett.*, 21, 2031-2034, 1994.

Heijboer, L. C., H. M. Kelder, M. J. M. Saraber, and P. F. J. van Velthoven, An analytical model describing the basic structure and development of mature extratropical cyclones, *Mon. Wea. Rev.*, 124, 571-582, 1996.

Heimann, M., The global atmospheric tracer model TM2: DKRZ TM2 model documentation, *Techn. Rep.*, 10, Max-Planck-Inst. für Meteorol., Hamburg, Germany, 1995.

Hidalgo, H. and P. J. Crutzen, The tropospheric and stratospheric composition perturbed by NO$_x$ emissions of high-altitude aircraft, *J. Geophys. Res.*, 82, 5833-5866, 1977.

Höller H. and U. Schumann, EULINOX - The European lightning nitrogen oxides projects, DLR, *Forschungsbericht 2000-28*, Oberpfaffenhofen, Germany, 2000.

Holton, J. R., P. H. Haynes, M. E. McIntyre, A. R. Douglas, R. B. Rood, and L. Pfister, Stratosphere-troposphere exchange, *Rev of Geophysisc*, 33, 403-439, 1995.

Hoshizake, H., L. B. Anderson, R. J. Conti, N. Farlow, J. W. Meyer, T. Overcamp, K. O. Redler, and V. Watson, Aircraft wake microscale phenomena. The stratosphere perturbed by propulsion effluents, Chapter 2, *CIAP DOT-TST-75-35*, Natl. Tech. Inf. Serv., Springfield, VA, 1975.

Houweling, S. M., F. Dentener, and J. Lelieveld, The impact of nonmethane hydrocarbon compounds on tropospheric chemistry, *J. Geophys. Res.*, 103, 10,673-10.696, 1998.

IATA, Environmental review - 1995, published by International Air Transport Association, 1995.

IPCC (Intergovernmental Panel on Climate Change), Aviation and the global atmosphere, Ed. J. E. Penner et al., Cambridge University Press, New York, 1999.

IPCC (Intergovernmental Panel on Climate Change), IPCC Third assessment report – Climate Change 2001, Cambridge University Press, New York, 2001.

Isaksen, I. S. A., The tropospheric ozone budget and possible man made effects, in *Proc. Quadrennial Ozone Symposium*, WMO, Boulder, Colo., 845-852, 1980.

Jacob, D. J. , B. G. Heikes, S.-M. Fan, J. A. Logan, D. L. Mauzerall, J. D. Bradshaw, H. B. Singh, G. L. Gregory, R. W. Talbot, D. R. Blake, and G. W. Sachse, Origin of ozone and NO$_x$ in the tropical troposphere: a photochemical analysis of aircraft observations over the South Atlantic Basin, *J. Geophys. Res.*, 101, 24,235-24,350, 1996.

Jaeglé, L., D. J. Jacob, W. H. Brune, I. C. Faloona, D. Tan, Y. Kondo, G. W. Sachse, B. Anderson, G. L. Gregory, S. Vay, H. B. Singh, D. R. Blake, and R. Shetter, Ozone production in the upper troposphere and the influence of aircraft during SONEX: Approach of NO$_x$-saturated conditions, *Geophys. Res. Lett.*, 26, 3081-3084, 1999.

Jeuken, A. B. M., H. J. Eskes, P. F. J. van Velthoven, H. M. Kelder, and E. V. Hólm, Assimilation of total ozone satellite measurements in a three-dimensional tracer transport model. *J. Geophys. Res.*, *104*, 5551-5563, 1999.

Jeuken A. B. M., J. P. Veefkind, F. Dentener, S. Metzger, C. Robles-Gonzalez. Simulation of the aerosol optical depth over Europe for August 1997 and a comparison with observations. *J. Geoph. Res.*, In press, 2001.

Johnston, H. S., Reduction of stratospheric ozone by nitrogen oxide catalysts from supersonic aircraft exhaust, *Science*, 173, 517-522, 1971.

Kärcher, B., Transport of exhaust products in the near trail of a jet engine under atmospheric conditions, . *J. Geophys. Res.*, 99, 14,509-14,517, 1994.

Kärcher, B., M. M. Hirschberg, and P. Fabian, Small-scale chemical evolutions of aircraft exgaust species at cruising altitudes, *J. Geophys. Res.*, 15,169-15,190, 1996.

Kärcher, B., Heterogeneous chemistry in aircraft wakes: Constraints for uptake coefficients, *J. Geophys. Res.*, 102, 19,119-19,135, 1997.

Karol I. L., Y. E. Ozolin, and E. V. Rozanov, Box and gaussian plume models of the exhaust composition evolution of subsonic tranport aircraft in and out the flight corridor, *Ann. Geophys.*, 15, 88-96, 1997.

Klemm, O., W. R. Stockwell, H. Schlager, and H. Ziereis, Measurements of nitrogen oxides from aircraft in the northeast Atlantic flight corridor, *J. Geohpys. Res.*, 103, 31,217-31,229, 1998.

Köhler, I., R. Sausen, and R. Reinberger, Contributions of the aircraft emissions to the atmospheric NO_x content, *Atmos. Environ. 31*, 1801-1818, 1997.

Kondo, Y., S. Kawakami, M. Koike, D. W. Fahey, H. Nakajima, Y. Zhao, N. Toriyama, M. Kanada, G. W. Sachse, and G. L. Gregory, Performance of an aircraft instrument for the measurement of NO_y, *J. Geophys. Res. 102*, 28,663-28,671, 1997.

Konopka, P., Analytical Gaussian solutions for anisotropic diffusion in a linear shear flow, *J. Non-Equilib. Thermodyn.*, 20, 78-91, 1995.

Kraabøl, A. G., F. Flatøy, and F. Stordal, Impact of NO_x emissions from subsonic aircraft: Inclusion of plume processes in a three dimensional model covering Europe, North America and the North Atlantic, *J. Geophys. Res.*, 105, 3573-3582, 2000a.

Kraabøl, A. G., Konopka, P., and H. Schlager, Modelling chemistry in aircraft plumes 1: comparison with observations and evaluation of a layered approach, *Atmos. Environ.*, 34, 3939-3950, 2000b.

Krol, M. C. and M. van Weele, Implications of variations in photodissociation rates for global tropospheric chemistry, *Atmos. Environ.*, 31, 1257-1273, 1997.

Lacis, A. A., D. J. Wuebbles, and J. A. A. Logan, Radiative forcing o climate by changes in the vertical distributions of ozone, *J. Geophys. Res.*, 95, 9971-9981, 1990.

Law, K. S., and J. A. Pyle, Modeling trace gas budgets in the troposphere, 1, Ozone and odd nitrogen, *J. Geophys. Res.*, 98, 18,377-18,400, 1993.

Lee, D. S., I. Köhler, E. Grobler, F. Rohrer, R. Sausen, L. Gallardo-Klenner, J. G. J. Olivier, F. J. Dentener, and A. F. Bouwman, Estimations of global NO_x emissions and their uncertainties, *Atmos Environ.*, 31, 1735-1749, 1997.

Levy, H., II., and W. J. Moxim, A global three-dimensional time-dependent lightning source of tropospheric NO_x, *J. Geophys. Res.*, 101, 22,911-22,922, 1996.

Louis, J. F., A parametric model of vertical eddy fluxes in the atmosphere, *Boundary Layer Meteorol.*, 17, 187-202, 1979.

Louisnard, N., C. Baudoin, G. Billet, F. Garnier, D. Hills, T. Mentel, P. Mirabel, J. C. Petit, J. L. Schultz, D. Taleb, J. Thlibi, A. Wahnmer, and P. Woods, Sub-Project 2: Physics and chemistry in the aircraft wake, in: AERONEX report, U. Schumann (Ed.), *Publ. EUR 16209 EN*, Off. for Off. Publ. of the Eur. Comm., Brussels, 1995.

Madronich, S., The atmosphere and UV-B radiation at ground level, in *Environmental UV Photobiology*, A. Young *et al.* (eds.), Plenum Press, New York, 1993.

Meijer, E. W., J. P. Beck and G. J. M. Velders, Modelling the gas-phase and heterogeneous conversions of nitrogen oxides in the exhaust plume of an aircraft, *RIVM report 722201010*, Bilthoven, Netherlands, 1996.

Meijer, E. W., P. F. J. van Velthoven, W. M. F. Wauben, J. P. Beck, and G. J. M. Velders, The effect of the conversion of nitrogen oxides in aircraft exhaust plumes in global models, *Geophys. Res. Lett.*, 24, 3013-3016, 1997.

Meijer, E. W., P. F. J. van Velthoven, A. M. Thompson, L. Pfister, H. Schlager, P. Schulte, and H. Kelder, Model calculations of the impact of NO_x from air traffic, lightning, and surface emissions, compared with measurements, *J. Geophys. Res. 105*, 3833-3850, 2000.

Meijer, E. W., P. F. J. van Velthoven, D. W. Brunner, H. Huntrieser, and H. Kelder, Improvement and evaluation of the parameterisation of nitrogen oxide production by lightning, *Phys. Chem. Earth*, 26, 577-583, 2001.

Melo, O. T., M. A. Lusis, R. D. S. Stevens, Mathematical modelling of dispersion and chemical reactions in a plume - oxidation of NO to NO_2 in the plume of a power plant, *Atmos. Environ.*, 12, 1231-1234, 1978.

Möllhoff, M., J. Hendricks, E. Lippert, H. Petry, and R. Sausen, Model analyses of the chemical conversions of exhaust species in the expanding plumes of subsonic aircraft, *In: Proc. of an Intern. Coll. on the Impact of Aircraft Emissions upon the Atmosphere*, 521-526, Paris, 1996.

Moulik M. D. and J. B. Milford, Factors influencing ozone chemistry in subsonic aircraft plumes, *Atmos. Environ.*, 33, 869-880, 1999.

Müller, J. F., Geographical distribution and seasonal variation of surface emissions and deposition velocities of atmospheric trace gases, *J. Geophys. Res.*, 97, 3787-3804, 1992.

Müller J.-F. and G. P. Brasseur, Sources of upper tropospheric HO_x: a three-dimensional model study, *J. Geophys. Res.*, 104, 1705-1715, 1999.

Murphy, D. M., D. W. Fahey, M. H. Profitt, S. C. Liu, K. R. Chan, C. S. Eubank, S. R. Kawa, and K. K. Kelly, Reactive nitrogen and its correlation with ozone in the lower stratosphere and upper troposphere, *J. Geophys. Res.*, 98, 8751-8773, 1993.

Nüsser, H. G. and A. Schmitt, Schlussbericht zum Forschungsvorhaben Berechnung der Emissionsverteilung und deren Trends, *BMBF-Förderzeichen*, 01 LL 9212/7, 1996.

Olivier, J. G. J., Inventory of aircraft emissions: a review of recent literature, *RIVM report 736301008*, Bilthoven, Netherlands, 1991.

Peixoto, J. P. and A. H. Oort, Physics of Climate, *Am. Inst. of Physics*, New York, 1992.

Peters, L. K., C. M. Berkowitz, and T. T. Tsang, The current state and future direction of Eulerian models in simulating the tropospheric chemistry and transport of trace species: A review, *Atmos. Environ.*, 29, 189-222, 1995.

Petry, H., J. Hendricks, M. Möllhoff, E. Lippert, A. Meier, A. Ebel, and R. Sausen, Chemical conversion of subsonic aircraft emissions in the dispersing plume: Calculation of effective emission indices, *J. Geophys. Res.*, 103, 5759-5772, 1998.

Pickering, K. E., A. M. Thompson, J. R. Scala, W.- K. Tao, R. R. Dickerson, and J. Simpson, Free tropospheric ozone production following entrainment of urban plumes into deep convection , *J. Geophys. Res.*, 97, 17,985-18,000, 1992.

Pickering, K. E., Y. Wang, W.-K. Tao, C. Price, and J.-F. Muller, Vertical distributions of lightning NO_x for use in regional and global chemical transport models, *J. Geophys. Res.* 103, 31,203-31,216, 1998.

Price, C., and D. Rind, A simple lightning parameterization for calculating global lightning distributions, *J. Geophys. Res.*, 97, 9919-9933, 1992.

Price, C., J. Penner, and M. Prather, NO_x from lightning. 1. Global distribution based on lightning physics, *J. Geophys. Res.* 102, 5929-5941, 1997.

Pulles, J. W., S. Lowe, R. van Drimmelen, G. Baarse, and P. McMahon, The AERO-project: model description and status, Dutch Civil Aviation Department (NRL) Report, The Hague, Netherlands, 1995.

Russell, G. L., and J. A. Lerner, A new finite-differencing scheme for the tracer transport equation, *J. Appl. Meteorol.*, 20, 1483-1498, 1981.

Saunders, C. P. R., Thunderstorm electrification laboratory experiments and charging mechanisms, *J. Geophys. Res.*, 99, 10,773-10,779, 1994.

Schlager, H., P. Konopka, P. Schulte, U. Schumann, H. Ziereis, F. Arnold, M. Klemm, D. E. Hagen, P. Whitefield, and J. Ovarlez, In situ observations of air traffic emission signatures in the North Atlantic flight corridor, *J. Geophys. Res.*, *102*, 10,739-10,750, 1997.

Schlager, H., P. Schulte, F. Flatøy, F. Slemr, P. van Velthoven, H. Ziereis, and U. Schumann, Regional nitric oxides enhancements in the North Atlantic flight corridor observed and modelled during POLINAT 2, a case study, *Geophys. Res. Lett. 26*, 3061-3064, 1999.

Schumann, U., On the effect of emissions from aircraft engines on the state of the atmosphere, *Ann. Geophys.*, 12, 365-384, 1994.

Schumann, U. (ed.), AERONOX – The impact of NO_x emissions from aircraft upon the atmosphere at flight altitudes 8-15 km, *Publ. EUR 16209 EN*, Off. for Off. Publ. of the Eur. Comm., Brussels, 1995.

Schumann, U., P. Konopka, R. Baumann, R. Busen, T. Gerz, H. Schlager, P. Schulte, and H. Volkert, Estimates of diffusion parameters of aircraft exhaust plumes near the tropopause from nitric oxide measurements and turbulence measurements, *J. Geophys. Res.*, 100, 14,147-14,162, 1995b.

Schumann, U., The impact of nitrogen oxide emssions from aircraft upon the atmosphere at flight altitudes – results from the AERONOX project, *Atmos. Environ.*, 31, 1723-1734, 1997.

Schumann, U., H. Schlager, F. Arnold, J. Ovarlez, H. Kelder, Ø. Hov, G. Hayman, I. S. A. Isaksen, J. Staehelin, and P. D. Whitefield, Pollution from aircraft emissions in the North Atlantic flight corridor: Overview on the POLINAT projects, *J. Geophys. Res.*, 105, 3605-3631, 2000.

Seinfeld, H., S. N. Pandis, Atmospheric chemistry and physics. From air pollution to climate change, Wiley, New York, 1998.

Shareef, G. S., W. A. Butler, L. A. Bravo, and M. B. Stockton, Air emissions species manual, Vol. I. Volatile Organic Compound (VOC) Species Profiles, *EPA-450/2-88-003a*, 1988.

Siegmund, P. C., P. F. J. van Velthoven, and H. Kelder, Cross-tropopause transport in the extratropical northern winter hemisphere, diagnosed from ECMWF data, *Quarterly J. Royal Meteorol. Soc.*, 122, 1921-1942, 1996.

Singh, H. B., M. Kanakidou, P. Crutzen and D. Jacob, High concentrations and photochemistry of carbonyls and alcohols in the global troposphere, *Nature*, 378, 50-54, 1995.

Singh H. B., A. M. Thompson, and H. Schlager, SONEX airborne mission and coordinated POLINAT-2 activity: overview and accomplishments, *Geophys. Res. Lett.*, 26, 3053-3056, 1999.

Sparling, L. C., M. R. Schoeberl, A. R. Douglas, C. J. Weaver, P. A. Newman, and L. R. Lait, Trajectory modeling of emissions from lower stratospheric aircraft, *J. Geophys. Res.*, *100*, 1427-1438, 1995.

Stevenson, D. S., W. J. Collins, C. E. Johnson, and R. G. Derwent, The impact of aircraft nitrogen oxide emissions on tropospheric ozone studied with a 3D Lagrangian model including fully diurnal chemistry, *Atmos. Environ.*, 31, 1837-1850, 1997.

Strand, A. and Hov, Ø., A two-dimensional global study of tropospheric ozone production. *J. Geophys. Res.*, 99, 22,877-22,895, 1994.

Tapia, A., J. A. Smith, and M. Dixon, Estimation of convective rainfall from lightning observations, *J. Appl. Meterol.*, 37, 1497-1509, 1998.

Thompson, A. M., H. B. Singh, and H. Schlager, Introduction to special section: Subsonic Assesment and Nitrogen Oxide Experiment (SONEX) and Pollution from Aircraft Emissions in the North Atlantic Flight Corridor (POLINAT 2), *Geophys. Res. 105*, 3595-3603, 2000.

Tiedtke, M., A comprehensive mass flux scheme for cumulus parameterization in large-scale models, *Mon. Weather Rev.*, *117*, 1779-1800, 1989.

Velders, G. J. M., L. C. Heijboer, and H. Kelder, The simulation of the transport of aircraft emissions by a three-dimensional global model, *Ann. Geophys.*, *12*, 385-393, 1994.

Velders, G. J. M., Scenario study of the effects of CFC, HCFC and HFC emissions on stratospheric ozone, *RIVM Rep.*, *722201006*, Nat. Inst. of Public Health and the Environment, Bilthoven, Netherlands, 1995.

Velthoven, P. F. J. van, R. Sausen, C. E. Johnson, H. Kelder, I. Köhler, A. B. Kraus, R. Ramarson, F. Rohrer, D. Stevenson, A. Strand, and W. M. F. Wauben, The passive transport of NO_x emissions from aircraft studied with a hierarchy of models, *Atmos. Environ.*, 31, 1783-1800, 1997.

Vilà-Guerau de Arellano, J., A. M. Talmon, and P. H. J. Builtjes, A chemically reactive plume model for the NO-NO_2-O_3 system, *Atmos. Environ.*, 24, 2237-2246, 1990.

Wang, Y., A. W. DeSilva, and G. C. Goldenbaum, Nitric oxide production by simulated lightning: Dependence on current, energy, and pressure, *J. Geophys. Res.*, *103*, 19,149-19,159, 1998.

Warneck P., Chemistry of the natural atmosphere, *Int. Geophysics Series*, 41,334-339, Academic Press, New York, 1988.

Wauben, W. M. F., P. F. J. van Velthoven, and H. Kelder, A 3D chemistry transport model study of changes in atmospheric ozone due to aircraft NO_x emissions, *Atmos. Environ.*, *31*, 1819-1836, 1997.

Weele, M. van, P. G. Duynkerke, Effects of clouds on the photodissociation of NO_2: Observation and modelling, *J. Atmos. Chem.*, 16, 231-255, 1993.

Wennberg, P. O., T. F. Hanisco, L. Jaeglé, D. Jacob, E. J. Hintsa, E. L. Lanzendorf, J. G. Anderson, R. S. Gao, E. R. Keim, S. Donnelly, L. Del Negro, D. W. Fahey, S. A. McKeen, R. J. Salawitch, C. R. Webster, R. D. May, R. Herman, M. H. Proffitt, E. Atlas, S. Schauffler, F. Flocke, T. E. McElroy, P. Bui, Hydrogen Radicals, Nitrogen Radicals, and the production of ozone in the upper troposphere, *Science*, 279, 49-53, 1998.

WHO (World Health Organization), Air quality guidelines, Regional European Office, Copenhagen, 1984.

Williams, E. R., Large-scale charge separation in thunderclouds, *J. Geophys. Res. 90*, 6013-6025, 1985.

Ziereis, H., H. Schlager, P. Schulte, P. F. J. van Velthoven, and F. Slemr, Distributions of NO, NO_x, and NO_y in the upper troposphere and lower stratosphere between 28° and 61°N during POLINAT 2, *J. Geophys. Res.*, 105, 3653-3664, 2000.

Curriculum Vitae

Ernst Meijer werd geboren op 4 oktober 1967 in Rotterdam. In 1985 behaalde hij het VWO diploma aan de Christelijke scholengemeenschap Blaise Pascal, waarna hij technische natuurkunde ging studeren aan de TU Delft. Hoewel de opleiding een duidelijke technische kant heeft, bleek de interesse voor de meer theoretische natuurkunde groter. Hij studeerde dan ook af op het driedimensionale Ising-model. Enigszins verzadigd van de theoretische natuurkunde ging hij hierna op zoek naar andere interessegebieden. Door zelf actief te zoeken naar een plek waar hij zijn vervangende dienstplicht kon vervullen, kwam hij terecht bij TNO Milieuwetenschappen, waar hij in aanraking kwam met atmosferische chemie. Dit bleek een goede keuze en het veld van atmosferische chemie en meteorologie bleek goed in zijn interessegebied te passen. Het werk bij TNO werd een half jaar voortgezet, waarna hij de overstap maakte naar het RIVM om daar te werken aan de effecten van vliegverkeer. Na ongeveer een jaar kwam er een positie vrij bij het KNMI om daar vergelijkbaar werk te doen met de mogelijkheid om van dit werk een promotieonderzoek te maken. Na een succesvolle sollicitatie en enkele jaren werk is deze belofte inderdaad ingelost, getuige dit proefschrift.